Slovak Biophysical Society

Book of Contributions

9th Slovak Biophysical Symposium

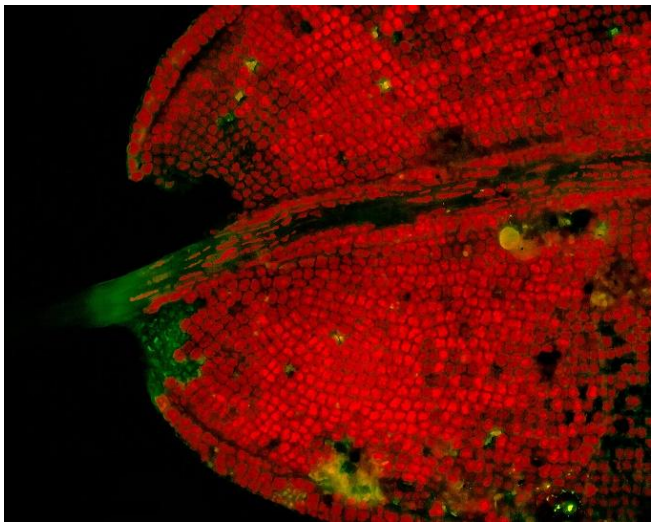

September 16 – 18, 2020
Holiday Inn, Trnava

ISBN: 978-80-973719-0-6

Book of Contributions. 9th Slovak Biophysical Symposium
September 16 - 18, 2020, Trnava, Slovakia

Editors: Alžbeta Marček Chorvátová, Miroslav Michalka

Reviewers: Diana Fedunová, Ľubica Lacinová, Gabriel Žoldák

ISBN: 978-80-973719-0-6
EAN: 9788097371906

Organized by:

Slovenská biofyzikálna spoločnosť

International Laser Centre Bratislava

FAKULTA PRÍRODNÝCH VIED / UCM TRNAVA

Supported by:

ORGANIZATION

CONFERENCE VENUE

Holiday Inn, Hornopotočná 5, 91701 Trnava, Slovakia

In the case of changes due to COVID situation, the conference will be held in the Conference hall (Aula Jozefa Matúša) at the University of Ss. Cyril and Methodius, Bučianska 4/A, Trnava.

SCIENTIFIC COMMITTEE

Alžbeta Marček Chorvátová (ILC Bratislava a FPV UCM Trnava)
Erik Sedlák (TIP UPJŠ Košice)
Dušan Chorvát (ILC Bratislava)
Ľubica Lacinová (BC SAV Bratislava a FPV UCM Trnava)
Pavol Miškovský (TIP UPJŠ Košice)

ORGANIZING COMMITTEE

from International Laser Center, Bratislava and Department of Biophysics, Faculty of Natural Sciences, University of Ss. Cyril and Methodius in Trnava

Alžbeta Marček Chorvátová
Ignác Bugár
Dušan Chorvát
Štefan Húšťava
Ľubica Lacinová
Anton Mateašík
Miroslav Michalka

from Department of Biophysics and Center for Interdisciplinary Biosciences, P. J. Šafárik University in Košice

Erik Sedlák
Veronika Huntošová

REVIEWERS

Diana Fedunová,
Ľubica Lacinová
Gabriel Žoldák

EDITORS

Alžbeta Marček Chorvátová
Miroslav Michalka

Table of Contents

Program

WEDNESDAY, September 16, 2020

12:00 – 13:30 **Registration**
13:30 – 13:40 **Opening ceremony**

13:40 – 15:40 **Session I**
Chair: L. Lacinová

13:40 – 14:30
PL1 J. Kubacková, A. Hovan, A. Strejčková, D. Horváth, Z. Tomori and **G. Bánó**
Viscoelastic photopolymers for micron-scale biomedical applications

14:30 – 14:50
SC1 **A. Antošová**, M. Gančár, E. Bystrenová, Z. Lučkayová, M. Baťková, Z. Bednáriková, Z. Gažová
α- Lactalbumin amyloid fibrillization in acidic pH - dependence on Hofmeister cations

14:50 – 15:20
SC2 **A. Marček Chorvátová** and D. Chorvát
Spectrally- and time-resolved microscopy study of the interaction of microplastics with Chlorella sp. algae

15:20 – 15:40
SC3 **S. Dulanská**, I. Coha, M. Nodillo and Ž. Grahek
Sequential determination of 90Sr and 210Pb in bone samples using molecular recognition technology product AnaLig® Sr-01

15:40 – 16:00 **Coffee break**

16:00 – 17:15 **Session II**
Chair: A. Zahradníková

16:00 – 16:20
SC4 **M. Gaburjáková**, J. Gaburjáková and J. Almassy
Luminal Eu^{3+} interferes with luminal Ca^{2+} regulation of the cardiac ryanodine receptor

16:20 – 16:40
SC5 **L. Lacinová**, R.T. Mallmann, L. Moravčíková, B. Jurkovičová-Tarabová, N. Klugbauer
Regulation of the $Ca_V2.2$ channel by Grina/TMBIM3 protein resembles that by G-protein-coupled receptors

16:40 – 17:00
SC6 **B. Iaparov**, I. Zahradník, A. Zahradníková
Modelling calcium spark at different cardiac ryanodine receptor distributions

17:00 – 17:15
CP1 **P. Krist:**
Presentation of ZEISS company

17:15 – 18:15 **Welcome drink with buffet**
17:15 – 18:15 **Poster session I (PO01-PO15)**
18:15 – 18:45 **Meeting of Slovak BioImaging section**

THURSDAY, September 17, 2020

8:30 – 10:20 **Session III**

Chair: J. Jakuš

8:30 – 9:20

PL2 **J. Míšek**, J. Jakuš, M. Veterník, I. Tonhajzerová, M. Kopáni, V. Jakušová, N. Višňovcová, K. Sládičeková, D. Parízek, L. Janoušek and J. Vojtek
Our experience in risk assessment related to electromagnetic fields

9:20 – 9:40

SC7 **O. Boško**, M. Šimera, I. Poliaček
Príručka elektromyografických techník EMG atlas vodivostných štúdií

9:40 – 10:00

SC8 **M. Kopáni**, J. Pánik, B. Filová, J. Míšek, M. Kohan, J. Jakuš, P. Povinec, Š. Polák
Analysis of iron in rabbit cerebellum after exposure to generated and mobile GSM electromagnetic fields

10:00 – 10:20

SC9 **L. Martvoň**, I. Poliaček
Simulations of unilateral vagal cooling effect on cough reflex

10:20 – 10:50 **Coffee break**

10:50 – 12:10 **Session IV**

Chair: D. Chorvát

10:50 – 11:10

SC10 **I. Zahradník**, B. Iaparov, A. Zahradníková
Modeling of calcium sparks in cardiac myocytes

11:10 – 11:30

SC11 **A. Hovan**, M. Petrenčáková, T. Kožár, D. Jancura, P. Miškovský, G. Bánó & E. Sedlák
Enhanced singlet oxygen production by photo-damaged AsLOV2 domain: experiments and modeling

11:30 – 11:50

SC12 **M. Veterník**, L. Martvoň, J. Míšek, J. Jakuš, I. Poliaček
Microinjection of neuroactive modulator into the ventral respiratory group – computer simulations

11:50 – 12:10

SC13 **A. Zahradníková**, B. Iaparov, and I. Zahradník
Accuracy of open probability and open time estimation from single-channel records

12:10 – 14:00 **Lunch Break**

14:00 – 15:30 **Session V**

Chair: E. Sedlák

14:00 – 14:50

PL3 **T. Hianik**
DNA aptamers in biosensors and in targeted drug delivery

14:50 – 15:10

SC14 **V. Subjaková**, M. Beltrán-Gastélum, B. Esteban-Fernández de Ávila, H. Gong, Z. Garaiova, M. Ionov, P. Lekshmy Venugopalan, T. Hianik and J. Wang
Ultrasound-propelled nanomotors modified with fluorescein-labeled aptamers and dendrimers as potential treatment for breast cancer

15:10 – 15:30

SC15 **K. Štroffeková**, A. Doroshenko, S. Tomková, and T. Kozar
Hypericin hydrophobic interactions with anti-apoptotic members of Bcl2 family

15:30 – 16:30 **Coffee break**

15:30 – 16:30 **Poster session II** (PO16-PO29)

16:30 – 16:40

SC16 **Š. Húšťava and A. Marček Chorvátová**
Education of Biophotonics in Slovakia: from past activities to future concepts

16:40 – 17:15 **SKBS prizes (ceremony)**

17:15 – 18:10 **General Assembly of the Slovak Biophysical Society**

18:30 departure for **Conference dinner**

19:00 – 22:00 **Conference dinner**

FRIDAY, September 18, 2020

9:00 – 11:00 **Session VI**

Chair: K. Štroffeková

9:00 – 9:50

PL4 **M. Cagalinec**, A. Zahradníková Jr, J. Pavelková, S. Kureková, M. Hoťka and A. Zahradníková
Calcium signaling and contractility in cardiomyocyte of Wolframin invalidated rats

9:50 – 10:10

SC17 **A. Zahradníková jr.**, M. Novotová, Jasna Marinovic, and I. Zahradník
2D spectral analysis of highly autofluorescent samples

10:10 – 10:30

SC18 **N. Tomášková**, G. Yassaghi, T. Kožár, R. Varhač, A. Musatov, P. Man, P. Novák, and E. Sedlák
Pseudo-peroxidase activity of cytochrome c and its structural consequences

10:30 – 10:50

SC19 **A. Singh**, M. Rief, G. Žoldák
Observing Hsp70 mechanics during the hydrolysis of a single ATP molecule

10:50 -11:00 **Concluding remarks**

WEDNESDAY, September 16, 2020

17:15 – 18:15 **Poster session I**

PO01 I. Baglaeva, I. Zahradník, B. Iaparov and A. Zahradníková
A guide on calcium signalling in cardiac myocytes

PO02 Z. Bednariková, B. N. Ratha, R. K. Kar, S. A. Kotler, S. Raha, S. De, N. C. Maiti, A. Bhunia, Z. Gažová
The role of salt-bridge stability in the initial steps of insulin fibrillation

PO03 F. Belén Fuenzalida, D. Jancura, S. Sanchez-Cortes, P. Miškovský, Z. Jurašeková
Glyphosate SERS detection: looking for the detection limits

PO04 O. Cehlár, L. Horňáková, J. Šinský, J. Hanes and R. Škrabana
The reactivity of the C-terminal anti-tau antibody shows differences possibly due to the changes in the global folds of tau isoforms

PO05 D. Džubinská, M. Zvarík, Z. Garaiová, L. Šikurová, I. Waczulíková
Ultrafiltration and size-exclusion chromatography for the isolation of exosomes

PO06 V. Džupponová, G. Žoldák
Recombinant expression, purification and biophysical characterization of the λ-type IgG light chain

PO07 V. Dzurillová, E. Sedlák
Ribosome display as a tool for directed evolution of haloalkane dehalogenases

PO08 A. Espina, S. Sanchez-Cortes, Z. Jurašeková
Polyphenols and metal (iron, copper) ion complexation characterized by optical (UV-Vis and Raman) spectroscopy

PO09 J. Gaburjaková and M. Gaburjaková
The cardiac ryanodine receptor provides an effective pathway for Zn2+ transport in cardiomyocytes

PO10 M. Gala, P. Pristáš and G. Žoldák
Sequence-structure analysis of bacterial heat shock proteins 70

PO11 M. Gancar, E. Kurin, Z. Bednaríková, J. Marek, P. Mucaji, M. Nagy, Z. Gažová
Amyloid aggregation of insulin: An interaction study of selected green tea constituents

PO12 Z. Garaiová, V. Šubjaková, J. Magiera, M. Holota, Š. Šutý, M. Ionov, S. Michlewska, I. Waczulikova, N. Sanz-del Olmo, F. Javier de la Mata, M. Bryszewska, T. Hianik
Liposomal locked-in dendrimers for development of cytostatic drugs

PO13 I. Garčárová, K. Šipošová, V. Huntošová, A. Musatov
The polyphenol rottlerin: assessment of disassembly activity of protein aggregates and cytotoxicity

PO14 N. Gašparíik, A. Kozeleková, P. Louša, J. Hritz
^{19}F labelling of 14-3-3ζ recombinant protein for ^{19}F NMR spectroscopy

PO15 V. Huntošová, R. Seliga and D. Horváth
Time-resolved measurements of oxygenation and oxidative stress level in cancer spheroids

THURSDAY, September 17, 2020

15:30 – 16:30 **Poster session II**

PO16 D. Chorvát, A. Biathová and A. Marček Chorvátová
Estimation of activation energy of nonradiative processes in nicotinamide adenine dinucleotide in vitro

PO17 L. Ilavská, M. Morvová Jr., J. Trebatická, Z. Ďuračková and L. Šikurová
Determination of metabolites in the urine of youths with depression

PO18 J. Jacko, M. Morvová Jr., A. Benčová, L. Šikurová, Y. Gbelská
The effect of PDR16 gene deletion on membrane potential in Candida albicans

PO19 A. Jutková, S. Datta, D. Chorvát, P. Miškovský, D. Jancura and J. Kronek
Polymeric micelles and endogenous lipoprotein nanoparticles as delivery systems of anticancer drug curcumin and photosensitizer hypericin

PO20 I. Klbik, I. Maťko, O. Šauša, K. Čechová and M. Melicherčík
Effect of dimethyl sulfoxide on phase behaviour of liposomes as a model for cryopreservation of biological cells studied by calorimetry, positron annihilation and molecular dynamics simulations

PO21 J. Kubačková, G.T. Iványi, V. Kažiková, A. Strejčková, A. Hovan, G. Žoldák, G. Vizsnyicza, L. Kelemen, G. Bánó
Viscosity measurements using elastic polymer micro-cantilevers

PO22 J. Marek, Z. Gažová
Decomposition of AFM topographic surfaces: Modelling of growth curves.

PO23 M. Morvová Jr., L. Šikurová
Human skin autofluorescence in health and eczema

PO24 B. Spodniaková, Z. Bednáriková, M. Gančár, A. Antošová, S. Hamuľáková, Z. Gažová
Effects of bis-coumarin homodimers on preformed amyloid fibrils of globular and intrinsically disordered proteins

PO25 A. Strejčková, J. Kubacková, A. Hovan, Z. Tomori and G. Bánó
Passive rheology using elastic micro-structures

PO26 K. Šipošová, V. Hovhannisyan, D. Sedláková, A. Musatov, Sh.-J. Chen
Fabrication and examination of magnetic zeolite nano/micro-particles for controlled drug release and modulation of amyloidogenesis

PO27 Šutý Š., Garaiová Z., Magiera J., Ionov M., Bryszewska M., Shcharbin D., Majoral J. P., Hianik T., Waczulíková I.
Modeling of the effect of amphiphilic phosphorus dendrons on erythrocyte membrane fluidity measured in terms of fluorescence anisotropy

PO28 V. Talafová, M. Humenik, G. Žoldák, T. Scheibel, and E.Sedlák
The fibril formation study of recombinant spider silk protein eADF4(C16) in different pH environments

PO29 N. Tomášková, R. Varhač, E. Sedlák
Dynamics of heme region is main effector of cytochrome c peroxidase-like activity

PO30 V. Vaník, Z. Bednáriková, G. Fabriciová, A. Antošová, Z. Gažová and D. Fedunová
The ionic liquids as modulators of insulin amyloid aggregation

PO31 M. Berta, V. Dzurillová, E. Sedlák
Increasing of GPCR solubility by directed protein evolution approach

List of Plenary Lectures

PL1 J. Kubacková, A. Hovan, A. Strejčková, D. Horváth, Z. Tomori and **G. Bánó**
Viscoelastic photopolymers for micron-scale biomedical applications

PL2 **J. Míšek**, J. Jakuš, M. Veterník, I. Tonhajzerová, M. Kopáni, V. Jakušová, N. Višňovcová, K. Sládičeková, D. Parízek, L. Janoušek and J. Vojtek
Our experience in risk assessment related to electromagnetic fields

PL3 **T. Hianik**
DNA aptamers in biosensors and in targeted drug delivery

PL4 **M. Cagalinec**, A. Zahradníková Jr, J. Pavelková, S. Kureková, M. Hoťka and A. Zahradníková
Calcium signaling and contractility in cardiomyocyte of Wolframin invalidated rats

List of Short Communications

SC1 **A. Antošová**, M. Gančár, E. Bystrenová, Z. Lučkayová, M. Baťková, Z. Bednáriková, Z. Gažová
α- Lactalbumin amyloid fibrillization in acidic pH - dependence on Hofmeister cations

SC2 **A. Marček Chorvátová** and D. Chorvát
Spectrally- and time-resolved microscopy study of the interaction of microplastics with Chlorella sp. algae

SC3 **S. Dulanská**, I. Coha, M. Nodillo and Ž. Grahek
Sequential determination of 90Sr and 210Pb in bone samples using molecular recognition technology product AnaLig® Sr-01

SC4 **M. Gaburjáková**, J. Gaburjáková and J. Almassy
Luminal Eu^{3+} interferes with luminal Ca^{2+} regulation of the cardiac ryanodine receptor

SC5 **L. Lacinová**, R.T. Mallmann, L. Moravčíková, B. Jurkovičová-Tarabová, N. Klugbauer
Regulation of the $Ca_V2.2$ channel by Grina/TMBIM3 protein resembles that by G-protein-coupled receptors

SC6 **B. Iaparov**, I. Zahradník, A. Zahradníková
Modelling calcium spark at different cardiac ryanodine receptor distributions

CP1 **P. Krist**
Presentation of ZEISS company

SC7 **O. Boško**, M. Šimera, I. Poliaček
Príručka elektromyografických techník EMG atlas vodivostných štúdií

SC8 **M. Kopáni**, J. Pánik, B. Filová, J. Míšek, M. Kohan, J. Jakuš, P. Povinec, Š. Polák
Analysis of iron in rabbit cerebellum after exposure to generated and mobile GSM electromagnetic fields

SC9 **L. Martvoň**, I. Poliaček
Simulations of unilateral vagal cooling effect on cough reflex

SC10 **I. Zahradník**, B. Iaparov, A. Zahradníková
Modeling of calcium sparks in cardiac myocytes

SC11 **A. Hovan**, M. Petrenčáková, T. Kožár, D. Jancura, P. Miškovský, G. Bánó & E. Sedlák
Enhanced singlet oxygen production by photo-damaged AsLOV2 domain: experiments and modeling

SC12 **M. Veterník**, L. Martvoň, J. Míšek, J. Jakuš, I. Poliaček
Microinjection of neuroactive modulator into the ventral respiratory group – computer simulations

SC13 **A. Zahradníková**, B. Iaparov, and I. Zahradník
Accuracy of open probability and open time estimation from single-channel records

SC14 **V. Subjaková**, M. Beltrán-Gastélum, B. Esteban-Fernández de Ávila, H. Gong, Z. Garaiova, M. Ionov, P. Lekshmy Venugopalan, T. Hianik and J. Wang
Ultrasound-propelled nanomotors modified with fluorescein-labeled aptamers and dendrimers as potential treatment for breast cancer

SC15 **K. Štroffeková**, A. Doroshenko, S. Tomková, and T. Kozar
Hypericin hydrophobic interactions with anti-apoptotic members of Bcl2 family

SC16 **Š. Húšťava and A. Marček Chorvátová**
Education of Biophotonics in Slovakia: from past activities to future concepts

SC17 **A. Zahradníková jr.**, M. Novotová, Jasna Marinovic, and I. Zahradník
2D spectral analysis of highly autofluorescent samples

SC18 **N. Tomášková**, G. Yassaghi, T. Kožár, R. Varhač, A. Musatov, P. Man, P. Novák, and E. Sedlák
Pseudo-peroxidase activity of cytochrome c and its structural consequences

SC19 **A. Singh**, M. Rief, G. Žoldák
Observing Hsp70 mechanics during the hydrolysis of a single ATP molecule

List of Posters

PO01 I. Baglaeva, I. Zahradník, B. Iaparov and A. Zahradníková
A guide on calcium signalling in cardiac myocytes

PO02 Z. Bednariková, B. N. Ratha, R. K. Kar, S. A. Kotler, S. Raha, S. De, N. C. Maiti, A. Bhunia, Z. Gažová
The role of salt-bridge stability in the initial steps of insulin fibrillation

PO03 F. Belén Fuenzalida, D. Jancura, S. Sanchez-Cortes, P. Miškovský, Z. Jurašeková
Glyphosate SERS detection: looking for the detection limits

PO04 O. Cehlár, L. Horňáková, J. Šinský, J. Hanes and R. Škrabana
The reactivity of the C-terminal anti-tau antibody shows differences possibly due to the changes in the global folds of tau isoforms

PO05 D. Džubinská, M. Zvarík, Z. Garaiová, L. Šikurová, I. Waczulíková
Ultrafiltration and size-exclusion chromatography for the isolation of exosomes

PO06 V. Džupponová, G. Žoldák
Recombinant expression, purification and biophysical characterization of the λ-type IgG light chain

PO07 V. Dzurillová, E. Sedlák
Ribosome display as a tool for directed evolution of haloalkane dehalogenases

PO08 A. Espina, S. Sanchez-Cortes, Z. Jurašeková
Polyphenols and metal (iron, copper) ion complexation characterized by optical (UV-Vis and Raman) spectroscopy

PO09 J. Gaburjaková and M. Gaburjaková
The cardiac ryanodine receptor provides an effective pathway for Zn^{2+} transport in cardiomyocytes

PO10 M. Gala, P. Pristáš and G. Žoldák
Sequence-structure analysis of bacterial heat shock proteins 70

PO11 M. Gancar, E. Kurin, Z. Bednaríková, J. Marek, P. Mucaji, M. Nagy, Z. Gažová
Amyloid aggregation of insulin: An interaction study of selected green tea constituents

PO12 Z. Garaiová, V. Šubjaková, J. Magiera, M. Holota, Š. Šutý, M. Ionov, S. Michlewska, I. Waczulikova, N. Sanz-del Olmo, F. Javier de la Mata, M. Bryszewska, T. Hianik
Liposomal locked-in dendrimers for development of cytostatic drugs

PO13 I. Garčárová, K. Šipošová, V. Huntošová, A. Musatov
The polyphenol rottlerin: assessment of disassembly activity of protein aggregates and cytotoxicity

PO14 N. Gašparíik, A. Kozeleková, P. Louša, J. Hritz
^{19}F labelling of 14-3-3ζ recombinant protein for ^{19}F NMR spectroscopy

PO15 V. Huntošová, R. Seliga and D. Horváth
Time-resolved measurements of oxygenation and oxidative stress level in cancer spheroids

PO16 D. Chorvát, A. Biathová and A. Marček Chorvátová
Estimation of activation energy of nonradiative processes in nicotinamide adenine dinucleotide in vitro

PO17 L. Ilavská, M. Morvová Jr., J. Trebatická, Z. Ďuračková and L. Šikurová
Determination of metabolites in the urine of youths with depression

PO18 J. Jacko, M. Morvová Jr., A. Benčová, L. Šikurová, Y. Gbelská
The effect of PDR16 gene deletion on membrane potential in Candida albicans

PO19 A. Jutková, S. Datta, D. Chorvát, P. Miškovský, D. Jancura and J. Kronek
Polymeric micelles and endogenous lipoprotein nanoparticles as delivery systems of anticancer drug curcumin and photosensitizer hypericin

PO20 I. Klbik, I. Maťko, O. Šauša, K. Čechová and M. Melicherčík
Effect of dimethyl sulfoxide on phase behaviour of liposomes as a model for cryopreservation of biological cells studied by calorimetry, positron annihilation and molecular dynamics simulations

PO21 J. Kubačková, G.T. Iványi, V. Kažiková, A. Strejčková, A. Hovan, G. Žoldák, G. Vizsnyicza, L. Kelemen, G. Bánó
Viscosity measurements using elastic polymer micro-cantilevers

PO22 J.Marek, Z.Gažová
Decomposition of AFM topographic surfaces: Modelling of growth curves.

PO23 M. Morvová Jr., L. Šikurová
Human skin autofluorescence in health and eczema

PO24 B. Spodniaková, Z. Bednáriková, M. Gančár, A. Antošová, S. Hamuľáková, Z. Gažová
Effects of bis-coumarin homodimers on preformed amyloid fibrils of globular and intrinsically disordered proteins

PO25 A. Strejčková, J. Kubacková, A. Hovan, Z. Tomori and G. Bánó
Passive rheology using elastic micro-structures

PO26 K. Šipošová, V. Hovhannisyan, D. Sedláková, A. Musatov, Sh.-J. Chen
Fabrication and examination of magnetic zeolite nano/micro-particles for controlled drug release and modulation of amyloidogenesis

PO27 Šutý Š., Garaiová Z., Magiera J., Ionov M., Bryszewska M., Shcharbin D., Majoral J.P., Hianik T., Waczulíková I.
Modeling of the effect of amphiphilic phosphorus dendrons on erythrocyte membrane fluidity measured in terms of fluorescence anisotropy

PO28 V. Talafová, M. Humenik, G. Žoldák, T. Scheibel, and E.Sedlák
The fibril formation study of recombinant spider silk protein eADF4(C16) in different pH environments

PO29 N. Tomášková, R. Varhač, E. Sedlák
Dynamics of heme region is main effector of cytochrome c peroxidase-like activity

PO30 V. Vaník, Z. Bednáriková, G. Fabriciová, A. Antošová, Z. Gažová and D. Fedunová
The ionic liquids as modulators of insulin amyloid aggregation

PO31 M. Berta, V. Dzurillová, E. Sedlák
Increasing of GPCR solubility by directed protein evolution approach

Viscoelastic photopolymers for micron-scale biomedical applications

J. Kubacková[1], A. Hovan[2], A. Strejčková[3], D. Horváth[4], Z. Tomori[1] and G. Bánó[2]

[1]Slovak Academy of Sciences, Institute of Experimental Physics, Department of Biophysics, Watsonova 47,040 01 Košice, Slovakia
[2]Department of Biophysics, Faculty of Science, P.J.Šafárik University, Jesenná 5, 041 54 Košice, Slovakia
[3]Department of chemistry, biochemistry and biophysics, Institute of Biophysics, The University of Veterinary Medicine and Pharmacy in Košice, Komenského 73, 041 81 Košice, Slovakia
[4]Center for Interdisciplinary Biosciences,P.J.Šafárik University, Jesenná 5, 041 54 Košice, Slovakia

e-mail: gregor.bano@upjs.sk

The development boom of biomedical lab-on-chip (LOC) applications during the last two decades brought the need for the miniaturization of conventional mechanical actuators and manipulators. Laser-beam-driven mechanical micro-structures, trapped and moved by optical tweezers, can be easily integrated into the micro-fluidic LOC environment. The vast majority of light-driven micro-structures is prepared by two-photon polymerization direct laser writing (TPP-DLW) using different photoresist materials.

To facilitate the micro-structure development and optimization, the material properties of thephoto-polymers need to be determined experimentally. Although prior research has identified several methods that could be used for microstructure mechanical testing in static conditions, the knowledge of elastic moduli derived from those findings is not sufficient to explain the mechanical response of these structures in a dynamic regime. Our study established a method to investigate the viscoelastic material characteristics, which needs to be taken into account when designing nano- and micro-mechanical components used in dynamic stress conditions. Bending recovery measurements were carried out on photopolymer nano-wires submerged in liquid media. It was shown that the studied photopolymer materialsare well described by the mechanical model of standard linear solids. The direct comparison of the theoretical predictions and the experimental results allowed us to identify the effect of internal friction on the photopolymer mechanical properties. The internal damping originates partially from the uncured part of thephotoresinand partially from the solvent molecules penetrating into the polymer network.

The elastic and/or viscoelastic character of photopolymer materials can be utilized in many different applications, including passive and active micro-rheology, microfluidic actuators, light robotics for single-cell manipulations,etc. We give an overview of the previous work in this fieldand show the possible future development areas.

Acknowledgement
This work was supported by the Slovak Research and Development Agency (grants APVV-15-0665, APVV-18-0285) and by the Slovak Ministry of Education (grant KEGA No. 012 UVLF – 4/2018).

α- Lactalbumin amyloid fibrillization in acidic pH - dependence on Hofmeister cations

A. Antošová[1], M. Gančár[1], E. Bystrenová[2], Z. Lučkayová[3], M. Baťková[1], Z. Bednáriková[1], Z. Gažová[1]

[1]*Institute of Experimental Physics Slovak Academy of Sciences, Watsonova 47, 040 01 Kosice, Slovakia*
[2]*Consiglio Nazionale delle Ricerche - Istituto per lo Studio dei Materiali Nanostrutturati (CNR-ISMN) via P. Gobetti 101, 40129 Bologna, Italy*
[3]*Institute of Biology and Ecology, Faculty of Science, Pavol Jozef Šafárik University in Košice*
e-mail: antosova@saske.sk

Protein aggregation into amyloid fibrils is implicated in the pathogenesis of many amyloid-related diseases as well as the formation of smart bionanomaterials.Many data about the amyloid aggregation of non-disease associated proteins such as hen egg white lysozyme or insulin was published in the last decades[1]. On the other hand, a comprehensive study of amyloid fibril formation for a non-disease associated proteinlike α-lactalbumin (α-LA) is still missing. α-LA is a small (123 aa) acidic Ca^{2+}binding protein involved in the regulation of lactose biosynthesis as a component of lactose synthase. It has been found that Ca^{2+} depleted α-LA,in its molten globular state at low pH,forms amyloid fibrils *in vitro*[2].

Using a multi-technique approach, we have examined the effect of different cations from Hofmeister series (NH_4^+, Cs^+, K^+, Na^+, Cu^+,Mg^{2+}, Ca^{2+}) in the form of chloride saltson the amyloid formation of Ca^{2+}-depleted α-lactalbumin (α-LA). Thekinetics, the content of β-structure and amyloid fibril morphology have been studied using ThT fluorescence, infraredand CD spectroscopy, Congo red assay and AFM microscopy.The effect of cations on kinetic parameters of α-LA amyloid formation (length of lagphase and aggregation constant of growth phase)is strongly correlated totheirpositionin the Hofmeister series. The highest aggregation constants were observed for the outermost cations in the Hofmeister series, namely Mg^{2+} and NH_4^+. However, the formed fibrils prepared in $MgCl_2$have different secondary structure arrangement (Fig. 1B dashed line) and different morphology of fibrils (Fig. 1A) compared to fibrils prepared in presence of NH_4Cl in which the fibrils are longer and more twisted (Fig. 1C).

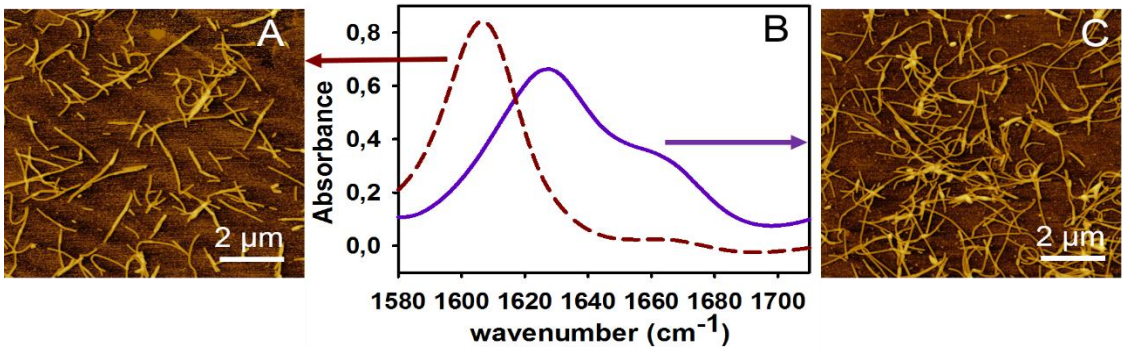

Fig. 1. AFMimages of α-LA fibrils prepared in the presence of $MgCl_2$ (A) and NH_4Cl (C).FTIR spectraof α-LA fibrils formed in presence of $MgCl_2$ (B-brown dash line) and NH_4Cl (B-solid violet line).

The obtained results might contribute to a better understanding of the processes of amyloid self-assembly of globular proteins.

Acknowledgment
This work was supported by the research grants VEGA 2/0145/17,APVV-18-0284, ITMS 313011T533 (DIAGNAD), and the MIUR grant (PRIN 20173L7W8K).

References

[1] F. Chiti, C. M. Dobson, Ann. Rev. Bioch. 75 (2006), 333-366.
[2] J. Goers, S. E. Permyakov, E. A. Permyakov, V. N. Uversky, A. L. Fink, Biochemistry 41 (2002), 12546-12551.

Spectrally- and time-resolved microscopy study of the interaction of microplastics with *Chlorella sp.* algae

A. Marček Chorvátová[1,2] and D. Chorvát[1]

[1] *Department of Biophotonics, International Laser Center, Ilkovičova 3, 814 04 Bratislava, Slovakia.*
[2] *Department of Biophysics, FNS, Univ. Ss Cyril and Methodius, J Herdu 1, 917 02 Trnava, Slovakia.*
e-mail: Alzbeta.Marcek.Chorvatova@ucm.sk

Microplastics represent a serious environmental pollution of the 21st century. Understanding their interactions with living organisms and finding ways of their removal is a prerequisite for keeping our environment healthy. Algae are aquatic organisms playing a key role in photosynthesis. Deep understanding of algal cell response is essential to predict how ecosystems may be affected by the environmental pollution and/or other human activities. The brightest endogenous fluorophores in plants are chlorophylls, the main electron donors and acceptors in photosynthesis. We have previously demonstrated application of fluorescence spectroscopy and microscopy tools to record endogenous fluorescence in *Chlorella* algae [1-2], as well as tested the effect of environmental stressors on these endogenous properties [2-3].

Our aim was to examine endogenous fluorescence of sweet water algae *Chlorella sp.* by spectroscopy and microscopy methods and to monitor cell behavioural changes under influence of latex beads (amine-modified or carboxylate-modified polystyrene of 1.0 or 0.03 µm mean particle size, labelled with yellow-orange fluorescence ex/em 470nm/505nm, Sigma-Aldrich). We tested the effect of fluorescently-labelled latex beads (Fig. 1) on spectrally- and time-resolved autofluorescence in *Chlorella* algae. Our first experiments demonstrate the feasibility to evaluate the responsiveness of these algae to microplastics. Performed research will lead to proposal of new biosensing tools for monitoring of the environmental pollution in water and finding approaches for its removal.

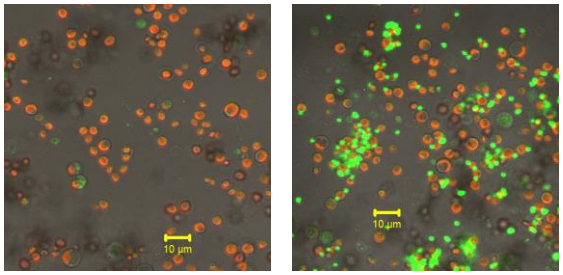

Fig. 1. Laser scanning confocal microscopy imaging of *Chlorella sp* algae, exc. 450nm, composite image of the green spectral region 480-520nm, red spectral region 620-680nm and transmission image in control conditions (left) and in the presence of fluorescent carboxylate-modified polystyrene beads of 0.03 µm (right), scale 10 µm.

Acknowledgement
This work is supported by VEGA No. 2/0123/18, as well as the Integrated Initiative of European Laser Infrastructures LASERLAB-EUROPE V (grant agreement no. 871124, European Union's Horizon 2020 research and innovation programme).

References

[1] T. Teplicky, M. Danisova, M. Valica, D. Chorvat, D. Jr., and A. Marcek Chorvatova A. A., AEEE Journal 15 (2017), 362-367, doi 10.15598/aeee.v15i2.2015.
[2] Marcek Chorvatova A., Uherek M., Mateasik A., Chorvat D. Jr.: Time-resolved endogenous chlorophyll fluorescence sensitivity to pH: study on *Chlorella sp.* algae. Methods and Applications in Fluorescence 8 (2020): 024007, doi 10.1088/2050-6120/ab77f4.
[3] Z. Pavlinska, D. Chorvat Jr., A. Mateasik, M. Jerigova., D. Velic, N. Ivosevic DeNardis, A. Marcek Chorvatova, 2020: Fluorescence responsiveness of unicellular marine algae *Dunaliella* to stressors under laboratory conditions. Journal of Biotechnology X 6 (2020), 1-10, doi 10.1016/j.btecx.2020.100018.

Sequential determination of 90Sr and 210Pb in bone samples using molecular recognition technology product AnaLig® Sr-01

S. Dulanská[1], I. Coha[2], M. Nodillo[2] and Ž. Grahek[2]

[1]Institute of Medical Physics, Biophysics, Informatics and Telemedicine, Faculty of Medicine, Comenius University, 813 72 Bratislava, Slovakia

[2] Division for Marine and Environmental Research, Ruđer Bošković Institute, Bijenička cesta 54, Zagreb, Croatia, 10000, Zagreb, Croatia

e-mail: dulanskas@gmail.com

Radioactive isotopes ^{210}Pb and ^{90}Sr, accumulate in bones and procedures for their determination usually include radiochemical methods prior their detection. This work describes a novel method for simultaneous determination of ^{210}Pb and ^{90}Sr in bone samples by using molecular recognition technology product AnaLig®Sr-01 gel, commercially available from IBC´s Technologies Inc. This material was initially used for strontium isolation.

Important drawback is that it also binds lead ions. This fact is used to develop a simple and rapid method for their simultaneous determination. Suitability and effectiveness of AnaLig®Sr-01 gel was validated by analysis of certified reference animal bone material, supplied by *International Atomic Energy Agency (*IAEA A-12) and ^{210}Pb reference sample. The developed single column method was used to determine the activity concentrations of ^{90}Sr and ^{210}Pb in bones of wild boars, deers and goats from different regions of Slovakia and Croatia (Fig.1). The proposed simple and effective method can be easily implemented in any radiochemical laboratory and the obtained results could be used for monitoring environmental areas of interest. The recoveries of both isotopes were high in all tested samples, 100 % for Pb and around 80 % for Sr. This is very important considering low activity concentration of radionuclides in environmental samples. The activity concentration of ^{210}Pb correlated well with age of the animal (R^2 = 0.94), whereas for ^{90}Sr no correlation was found (R^2 = 0.05).

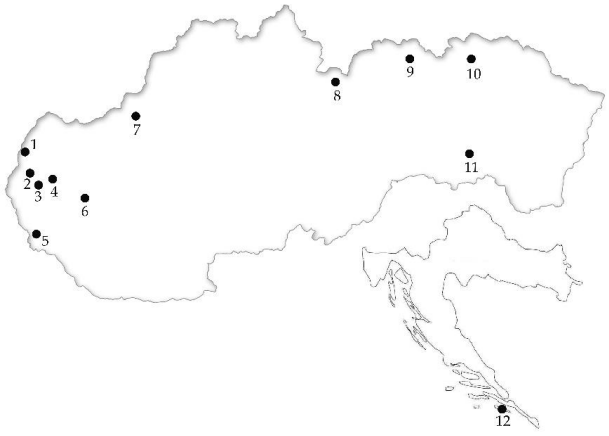

Fig. 1. Map of Slovakia and Croatia with locations of places where animals were hunted: 1 Sekule, 2 Závod, 3 Rohožník, 4 Plavecké Podhradie, 5 Bratislava, 6 Trnava, 7 Trenčín, 8 Tatry, 9 Stará Ľubovňa, 10 Bardejov, 11 Košice, 12 Mljet

Acknowledgement

This work was supported by the project of the Slovak Research and Development Agency under the contract No. APVV-17-0150.

Luminal Eu^{3+} interferes with luminal Ca^{2+} regulation of the cardiac ryanodine receptor

M. Gaburjáková[1], J. Gaburjáková[1] and J. Almassy[2]

[1] *Institute of Molecular Physiology and Genetics, Centre of Biosciences, Slovak Academy of Sciences, Dúbravská cesta 9, 840 05 Bratislava, Slovakia.*

[2] *Department of Physiology, Faculty of Medicine, University of Debrecen, Debrecen 4002, Hungary.*

e-mail: marta.gaburjakova@savba.sk

In cardiac muscle, the ryanodine receptor (RYR2) functions as a Ca^{2+} release channel in the sarcoplasmic reticulum and plays a pivotal role in Ca^{2+} cycling required for rhythmic muscle contraction. Dysregulation of the RYR2 channel by luminal Ca^{2+} has been implicated in a life-threatening, stress-induced arrhythmogenic disease [1]. The mechanism of this regulatory process is under debate, and it has been attributed to Ca^{2+} binding on the cytosolic face (the Ca^{2+} feedthrough mechanism: permeation of luminal Ca^{2+} via the RYR2 pore in the lumen-to-cytosol direction) and/or the luminal face of the RYR2 channel (the true luminal mechanism). The molecular nature and location of the luminal Ca^{2+} site is unclear.

Our aim was to provide further strong evidence in support of the luminal Ca^{2+} site on the RYR2 channel using a trivalent cation, Eu^{3+}. Because trivalent cations possess high binding affinities for Ca^{2+} sites and do not permeate Ca^{2+} channel pores [2], Eu^{3+} is an excellent experimental tool for directly manipulating only the luminal component of RYR2 regulation by luminal Ca^{2+}.

At the single-channel level, we found that luminal Eu^{3+} modified the caffeine-activated RYR2 channel when bathed with luminal Ca^{2+}. No appreciable effect was revealed for luminal Ba^{2+} (mimicking the absence of luminal Ca^{2+}). Importantly, distinct RYR2 gating modes acquired in the presence of luminal Ca^{2+} or Ba^{2+} were resistant to luminal Eu^{3+}. Under our experimental conditions, essential determinants of the Ca^{2+} feedthrough mechanism (such as the Ca^{2+} current and RYR2 sensitivity to cytosolic Ca^{2+}) were not affected. This implies that the RYR2 cytosolic face was not likely involved in the observed changes. Our results indicate that two spatially distinct Ca^{2+} sites, accessible from the RYR2 luminal side even when the channel is closed, likely mediate true luminal regulation by independently controlling RYR2 sensitivity to caffeine and gating behavior [3].

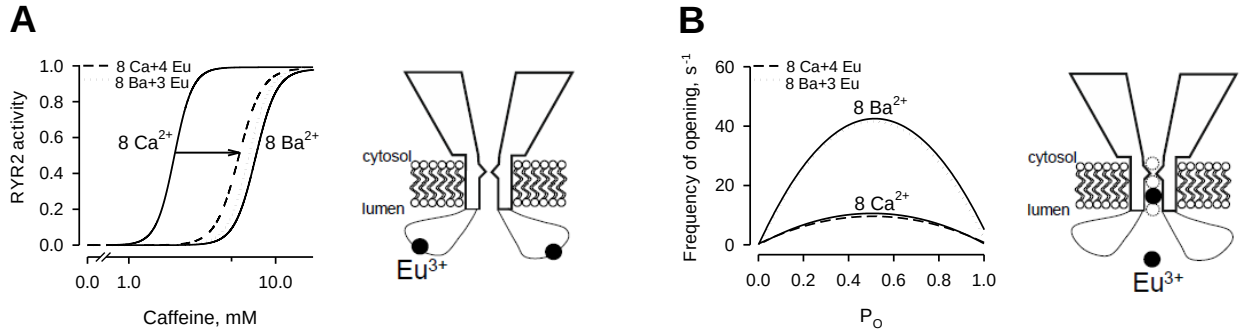

Fig. 1. (A) RYR2 responsiveness to caffeine (left) is likely controlled by a luminal-facing Ca^{2+} site (right). (B) RYR2 gating behavior (left) is presumably regulated inside the channel pore (right).

Acknowledgement

This work was supported by the Slovak Scientific Grant Agency (VEGA 2/0011/18 and VEGA 2/0008/20) and EU Structural Fund (ITMS 26230120009).

References

[1] W. Chen, R. Wang, B. Chen et al., Nat Med 20 (2014), 184-192.

[2] J.B. Lansman, J Gen Physiol 95 (1990), 679-696.

[3] J. Gaburjakova, J. Almassy, M. Gaburjakova, Bioelectrochemistry 132 (2020), 107449.

Regulation of the $Ca_V2.2$ channel by Grina/TMBIM3 protein resembles that by G-protein-coupled receptors

L. Lacinová[1,2], R.T. Mallmann[3], L. Moravčíková[1], B. Jurkovičová-Tarabová[1], N. Klugbauer[3]

[1] Center of Biosciences, Institute of Molecular Physiology and Genetics, Bratislava, Slovakia
[2]Faculty of Natural Sciences, University of Ss. Cyril and Methodius, Trnava, Slovakia
[3] Institut für Experimentelle und Klinische Pharmakologie und Toxikologie, Albert-Ludwigs-Universität, Freiburg, Germany
e-mail: lubica.lacinova@savba.sk

$Ca_V2.2$ channels are high-voltage activatedcalcium channels expressed exclusively in neurons. They are recognized for their unique role in nociception. Most investigated modulatory pathway regulating the $Ca_V2.2$ channels is G-protein-coupled receptor (GPRC) activated pathway leading to current inhibition by Gβγ subunit of G-protein.Pharmaceutical inhibition of $Ca_V2.2$ channels by an activation of GPRC e.g. by opioid drugsis a common strategy for treatment of chronic and/or neuropathic pain.

We have applied the yeast split-ubiquitin system with its specific advantages to search for interaction partners of the $Ca_V2.2$ channel and identified several proteins directly interacting with the channel [1, 2]. Some of them appeared to be able to inhibit the channel. Most interesting interaction partner was Grina/TMBIM3 protein, which inhibited the channel by a mechanism resembling that of GPRC [3].

When coexpressed with $Ca_V2.2$ channels,Grina/TMBIM3 protein significantly suppressed the current amplitude up to 50% and slowed the kinetics ofcurrent activation. This effect was accompanied by a significant shift of the voltage dependencies of activationtime constants towards more depolarized voltages. Application of a stimulus protocol including a strong depolarizingpulse relieved inhibition of current amplitude by Grina/TMBIM3. When Grina/TMBIM3 was present,inactivation by an action potential-like train of pulses was diminished. Both observations resemble mechanism ofhow the release of G-protein βγ subunits following activation of GPCR inhibits Ca_V2 channels. The impact of Grina/TMBIM3 and G-protein βγ subunits are rather comparable with respect to suppression of current amplitude andslowing of activation kinetics. Furthermore, both modulators had the same effect on current inactivation whenevoked by an action potential-like train of pulses. Kinetics of relief of current inhibition during strong depolarization and its restoration during prolonged repolarization was similar for both Grina/TMBIM3 and G-protein βγ subunits.

Acknowledgement
This work was supported by the VEGA grant No 2/0143/19and Slovak Research and Development Agency under the contract No. APVV-15-0388.

References

[1] R.Mallmann, T.Wilmes, L.Lichvárová, A.Bührer, B.Lohmüller, J.Castonguay, **L. Lacinova** and N.Klugbauer,Scientific Reports(2013),Article number: 1777
[2] R. Mallmann, K. Ondacova, L. Moravcikova, B. Jurkovicova-Tarabova, M.Pavlovicova, L. Lichvarova, V. Kominkova, N. Klugbauer, **Lacinova L.,**Pflugers Arch. 471, (2019), 861–874.
[3] R. Mallmann, L. Moravcikova, K. Ondacova, L. **Lacinova,**N. Klugbauer, Cell Calcium 80, (2019), 71–78.

Modelling calcium spark at different cardiac ryanodine receptor distributions

B. Iaparov[1,2], I. Zahradník[1], A. Zahradníková[1]

[1]*Department of Cellular Cardiology, Institute of Experimental Endocrinology, Biomedical Research Center, Slovak Academy of Sciences, Dúbravská cesta 9, 841 04, Bratislava, Slovakia*

[2]*Insitute of Experimental Physics, Slovak Academy of Sciences, Watsonova 47, 040 01, Košice, Slovakia*

e-mail: bogdan.iaparov@savba.sk

Calcium ions play a central role in excitation–contraction coupling (ECC) by being themessenger linking electrical activation to mechanical contraction of cardiac myocytes.The most of calcium ions incardiac myocytes pass through the ryanodine receptors (RyRs) that form the calcium release sites (CRSs) on the membrane of sarcoplasmic reticulum.Calcium release from individual CRSs can be observed using calcium sensitive fluorescent dyes as intracellular calcium sparks. Recent experimental data show heterogeneity of RyR distribution inside the CRS of cardiac myocytes [1-3]. It is not clearwhether RyR distribution in the CRS influences properties of calcium sparks (amplitude, spatial and temporal properties).

We developed a basic stochastic model of a CRS, which allows to manipulate RyR distributioninto arbitrary patterns. RyR activity was approximated by a two-state gating model conforming to published RyR properties such as sensitivity to allosteric activation by Ca^{2+} ions and sensitivity to competitive/non-competitive inhibition by Mg^{2+} ions. [4-5]. Calcium dynamics was treated using the linearized buffered diffusion approximation [6].

The results of the Monte-Carlo (MC) simulations and the mean-field (MF)simplification [7], which allows a huge decrease in computational demands, showed a significant influence of RyR distribution on calcium spark properties. However, MF simulations did not reproduce the results of MC simulations for RyR distributions observed experimentally.

MC simulations produced three types of calcium released events, namely quarks, blips and sparks, with characteristics responsive to the RyR distribution. We introduced ameasure of the RyR distribution calledvicinity$v$, defined as:

$$v = \frac{1}{\sqrt{N_{RyR}}(N_{RyR}-1)} \sum_i \sum_{j,j\neq i} \frac{1}{r_{ij}}$$

where N_{RyR} is the number of RyRs in the CRS and r_{ij} is the distance between the i^{th} and j^{th}RyR.The vicinity was foundto be a reasonable predictor of the calcium spark activity at different RyR distributions.While being simple, this model can befurther improved, and it makes this approach promisingfor studies on dynamics of calcium release.

Acknowledgement

The research was supported by Russian Foundation for Basic Research according to the research project no 18-31-00153, by grants from the Slovak Grant Agency (VEGA 2/0143/17), the Slovak Research and Development Agency (APVV-15-0302), by the Government of the Russian Federation, Program 02.A03.21.0006 and by the Ministry of Education and Science, projects 5719 and 2277. Our study was performed using the Uran supercomputer of the Krasovskii Institute of Mathematics and Mechanics.

References

[1] Asghari P et al. (2014). *Circ Res*, 115: 252-262.
[2] Jayasinghe I et al. (2018). *Cell Rep*, 22:557-567.
[3] Asghari Pet al. (2020). *eLife*, 9: e51602.
[4] Zahradníková Aet al. (2010). *J Gen Physiol*, 136, 101-116.
[5] Iaparov BI et al. (2019). *Eur. Biophys. J*, 48: 579-84.
[6] Naraghi M,Neher E. (1997). *J Neurosci*, 17: 6961-6973.
[7] Groff JR, Smith GD. (2008). *Biophys J*, 95: 135-154.

Our experience in risk assessment related to electromagnetic fields

J. Míšek[1], J. Jakuš[1], M. Veterník[1], I. Tonhajzerová[2], M. Kopáni[3], V. Jakušová[4], N. Višňovcová[1], K. Sládičeková[1], D. Parízek[1], L. Janoušek[5] and J. Vojtek[6]

[1]Dept. of Medical Biophysics, JFMED in Martin, Comenius University Bratislava, Mala Hora 4, 036 01 Martin, SR.
[2] Dept. of Physiology, JFMED in Martin, Comenius University Bratislava, Biomedical Center, Mala Hora 4, 036 01 Martin, SR.
[3]Institute of medical physics, biophysics, informatics and telemedicine, FMED in Bratislava, Comenius University Bratislava, Sasinkova 2, 813 72 Bratislava, SR.
[4]Dept. of Public Health, JFMED in Martin, Comenius University Bratislava, Mala Hora 4, 036 01 Martin, SR.
[5]Dept. of Electromagnetic and Biomedical Engineering, FEIT, University of Zilina in Zilina, Univerzitna 1, 010 26 Zilina, SR
[6]ELPRA-Technik, Kolonia Hviezda 104, 036 08 Martin, SR
e-mail: jakub.misek@uniba.sk

The lecture proposes the research experience at the Department of Medical Biophysics, JFMED in Martin, CU in Bratislava related to electromagnetic fields (EMF) and their effects on living organisms, which the beginnings date back to 2009.

Our experiments in humans focused on determining the responses of the Autonomic Nervous System (sympathetic, parasympathetic nerve activities) after exposure to a generated radiofrequency signal [1]. The aim of the study in humans (grammar school students: 25 exposed; 25 control) at exposure to EMF limit values was to analyze heart rate variability (HRV) as an indicator of autonomic nervous system (ANS) excitability and reactivity. The results showed no statistically significant changes in HRV of the control group and physiological parameters (body temperature and blood pressure) in both groups. However, the results revealed an increase in parasympathetic activity in the spectral as well as time domain parameters of HRV analysis in the supination position in the exposed group compared to the control group. The numeric simulation revealed increased absorption in some parts of the CNS. At the end of this study, we confirmed that short-term exposure to EMF limits can significantly modulate ANS activity, and that the ortho-clinostatic test is adequate to investigate the effects of EMF fields in humans.

The new exposure system using mobile communication frequency bands was developed at the department [2]. This selective system allows in vitro as well as in vivo experimental procedures to be performed on cells and other biological tissues, as well as on small laboratory animals. It uses a real telecommunication signal from base stations. The system was tested on group of the experimental animals (rabbits) which were exposed to occupation levels of EMF. The aim of this study [3] was to evaluate HRV in awake (Group 1) as well as anesthetized animals (Group 2) after exposure to above-limits EMFs. In both groups, we observed a slight increase in vagal tone. These results correspond to the results in humans. Temperature changes revealed an increase in central temperature with maximum in 60 min of the exposure in group 1. We attribute this to the direct effect of EMF on biological tissue. Group 2 was not characterized by a significantly elevated temperature, which is attributed to the attenuated function of the thermoregulatory system caused by the anesthetics. In conclusion, we can hypothesize the potential effect of EMF on some structures of the brain´s tissue with subsequent hyper or hypoactivity of the relevant segments either directly or through a compensatory mechanism. Further research, focusing mainly on the modulation of neurotransmitters and the overall activity of specific regions of the CNS, is necessary.

Our department has established close cooperation with the Institute of Medical Physics, Biophysics, Informatics and Telemedicine, FMED, CU in Bratislava. The research in a pilot study led to the demonstration of dystrophic changes in Purkinje cells as well as the formation of iron deposits in several areas of the brain [4] after exposure the rabbits by occupational EMF intensities.

In cooperation with the Department of Public Health JFMED in Martin, CU in Bratislava, our staff participates in epidemiological questionnaire studies, monitoring of EMF in the environment, especially adolescent students at high school and areas with increased movement of people (shopping centers, schools, etc.). These spaces are often "EMF shielded", increasing the radiation power from the cell phone [5]. Analysis of spaces in schools, shops and restaurants has shown an increase in EMF intensity in the case of data communication [6].

The research groups agree that the non-thermal effects of long-term EMF exposure play an important role in assessing the effects of these fields on human health. The currently valid limit values are obsolete for the needs of modern world. These standards are adapted from short-term exposures and thermal effects. However, they do not consider cumulative, long-term low-level EMF, which can also cause the so-called non - thermal bioelectromagnetic effects.

Acknowledgement
This work was supported by Slovak Research and Development Agency under the contract no. APVV-19-0214 and project VEGA 1/0173/20 and VEGA 1/0166/17.

References

[1] Misek J., Belyaev I., Jakusova V., Tonhajzerova I., Barabas J., Jakus J. 2018. Heart rate variability affected by radio frequency electromagnetic field in adolescent students. Bioelectromagnetics, 39(4):277-288.

[2] Misek J., Vojtek J., Veternik M., Kohan M., Jakusova V., Spanikova G., Belyaev I., Jakus J. 2018. New radiofrequency exposure system with real telecommunication signals. Advances in Electrical and Electronic Engineering, 16 (1): 101 – 107.

[3] Misek J., Veternik M., Tonhajzerova I., Jakusova V., Janousek L., Jakus J. 2020 Radiofrequency electromagnetic field affects heart rate variability in rabbits. Physiological Research. [Accepted; In Press].

[4] Kopani M., Filova B., Sevcik P., Kosnac D., Misek J., Polak S., Kohan M., Major J., Zdimalova M., Jakus J. 2017. Iron deposition in rabbit cerebellum after exposure to generated and mobile GSM electromagnetic fields. Bratisl Med J, 118 (10): 575 – 579.

[5] Míšek J., Jakušová V., Špigúthová D., Jakuš J. 2016. Meranie limitných hodnôt mobilného telefónu v priestoroch budov s nízkou intenzitou signálu. [In Slovak] Životné podmienky a zdravie, Nový smokovec, pp. 16-22.

[6] Kohan M., Spronglova M., Visnovcova N., Misek J., Jakusova V., Jakus J. 2020 Monitoring of data transmission and changes in values of electromagnetic field in living environment. Communications, 22(1):3-8.

Handbook of electromyographictechniques EMG atlas of conductivitystudies

Ondrej Boško, Michal Šimera, Ivan Poliaček

Department of medical biophysics, Jessenius Faculty of Medicine in Martin
Comenius University in Bratislava, Malá Hora 4, 03601 Martin
e-mail: bosko1@uniba.sk

Electromyography (EMG) is an important method of diagnosing neuromuscular diseases. There is a lack of practical literature for individual medical specializations, which deals with detailed clinical procedures in clinical diagnostics.

So far, the following has been published in the Slovak language: " Základná príručka elektromyografických techník – EMG atlas " [1]. Due to the technological possibilities of the time, the publication provides only a schematic representation of the location of EMG electrodes and not for all currently used montages. From this publication, doctors are learning the basic techniques of electromyographic diagnostics to this day. The current basic diagnostic procedures in EMG have changed and the instrumentation has undergone its natural technological development.

Due to the new and more modern EMG technology and wider possibilities of information distribution, we decided to develop a new manual of electromyographic techniques, which will contain all commonly used electromyographic montages for conductivity studies with detailed textual and pictorial (photographic) description.

To demonstrate the most commonly used diagnostic procedures, we used the Natus UltraPro S100 EMG instrument with Viking 22.1 software. When placing the electrodes, we used the methodological manual Cibulčik and Šóth (1998). Surface plate and ring electrodes (Nicolet) were used as recording electrodes, Ten20 conductive paste and NuPrep abrasive paste were used to reduce the transient resistance. We demonstrated the methodical procedures for the examination of the nerves of the upper and lower limbs. For the upper limb: n. medianus, n ulnaris, n. radialis. For the lower limb: n. tibialis, n.suralis, n. peroneus, n. peroneus superficialis. Characteristics of examinations of motor and sensitive functions of peripheral nerves were developed for all mentioned nerves (if they are comonly performed for a given nerve). The methodology of examination of the given nerve contains a list of recording electrodes with a description of their location on the limb, including a photograph, a description of the location of the grounding electrode and a description of stimulation sites. For each examination, reference values according to Liveson (1992) [2] and Cibulčik and Šóth (1998) [1] will be given.

We plan to publish this manual in electronic form in the form of a web page and later also in paper form.

Acknowledgment
This works was supported by VEGA 1/0092/20.

References

[1] Cibulčík, František, and Jozef Šóth. EMG atlas : základná príručkaelektromyografickýchtechník. Martin: Osveta, 1998. Print.

[2] Liveson, Jay A., and Dong M. Ma. Laboratory reference for clinical neurophysiology. New York: Oxford University Press, 1992. Print.

Analysis of iron in rabbit cerebellum after exposure to generated and mobile GSM electromagnetic fields

M. Kopani[1], J. Panik,[1] B. Filova[1], J. Misek[3], M. Kohan[3], J. Jakus[3], P. Povinec[2], Š. Polák[4]

[1]Institute of Medical Physics, Biophysics, Informatics and Telemedicine, Faculty of Medicine, Comenius University, Bratislava, Slovakia
[2]Centre for Nuclear and Accelerator Technologies (CENTA), Faculty of Mathematics, Physics and Informatics, Comenius University, Bratislava, Slovakia
[3]Department of Medical Biophysics, Jessenius Faculty of Medicine, Comenius University, Martin, Slovakia
[4]Institute of Histology and Embryology, Faculty of Medicine, Comenius University, Bratislava, Slovakia
e-mail: martin.kopani@fmed.uniba.sk

Electromagnetic radiation can impair structure and function of cells and tissues [1]. It can lead to accumulation of some chemical elements. The aim of this study was to examine iron accumulation in rabbit cerebellum after exposure to real telecommunication GSM signal characterized by frequency band 1805 – 1870 MHz and generated radio-frequency electromagnetic field (RF EMF) under carrier frequency 1788 MHz generated by functional generator Agilent N9310A. Histochemical analysis of iron distribution by light and electron microscopy with energy-dispersive microanalysis and particles induced X-ray emission (PIXE) analysis revealed dystrophic changes of Purkinje cells in irradiated groups and iron containing deposits located in various parts of *cerebellum*. Others elements detected in these deposits were C, O, Na, Mg, Al, Si, P, S, Cl, Ca. Focal concentration of iron in the sample after exposure to generator signal was found. Inductively coupled plasma mass spectrometry (ICP MS) showed differences of iron concentration among groups. We suggest that changes probably reflect thermal effects of RF EMF on cells and tissues. We found higher iron accumulation as a result of either higher blood brain barrier (BBB) permeability or actuation and redistribution of endogenous iron. Since ICP MS obtained results showed differences of iron concentration among groups it may indicate higher BBB permeation occurs. We suggest that iron accumulation may be result of impairment of BBB but actuation or aggregation of endogenous iron in extra- and intracellular space cannot be ruled out.

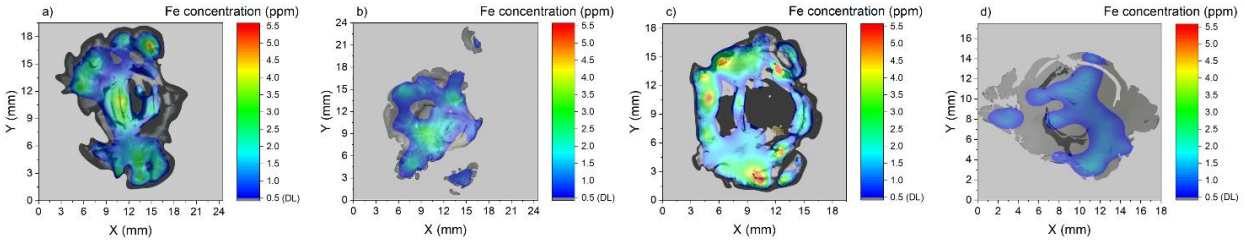

Fig. 1. Rabbit, cerebellum, PIXE. Iron concentration in rabbit cerebellum for four different groups: a) generator, b) GSM + generator, c) GSM, d) control.

Acknowledgement
This work was supported by the Slovak Research and Development Agency under the contract No. APVV-0189-11and APVV- 16-0039 and the Ministry of Education, Science, Research and Sport of the Slovak Republic No. VEGA 1/0173/20.

References

[1] WM Williams, ST Lu, M Del Cerro, W Hoss, and SM Michaelson, IEEE Trans Microw Theory 32 (1984), 808–818.

Simulations of unilateral vagal cooling effect on cough reflex

L. Martvoň[1], I. Poliaček[1]

[1] *Department of Medical Biophysics, Jessenius Faculty of Medicine in Martin, Comenius University in Bratislava, Malá hora 4, 03601 Martin, Slovakia.*
e-mail: martvon5@uniba.sk

Cough is a main respiratory defensive reflex. Cough can be elicited by both mechanical and chemical stimulation of the airway mucosa and is mediated by Aδ and C-fibers, respectively. These fibers project to the neurons of nucleus of the solitary tract (NTS). Excitatory afferent drive for the cough network is produced by activation of ionotropic glutamatergic receptors). Cough network generates cough motor pattern, which is transmitted by descending neural pathways to inspiratory and expiratory muscles.

We attempted to simulate effects on cough obtained from *in vivo* experiments [1], using neural simulator developed at University of South Florida, Tampa USA [2]. The study of Simera et. al [1] is dedicated to various modulations of afferent signal to the cough network and their effect on the output characteristics of cough (cough number, inspiratory and expiratory muscle activity intensities and time characteristics). Specifically, we focused on unilateral cooling of vagus nerve. We hypothesized that reducing afferent information to half would result in the same decrease of respiratory muscle activity as was seen *in vivo* experiments. We simulated this reduction by cutting various parameters of afferent neurons (number of fibers in population, number of terminals and synaptic strength) to half, which all resulted in mild decrease of output signal, contrary to *in vivo* experiments. Further decrease in number of fibers (1/10 of the original count) in afferent population resulted in satisfactory decrease in cough number, however the effect on respiratory muscle activities were uneven. We then embraced more complex changes in afferent neural population (simultaneous change in count of fibers, number of terminals, synaptic strength and extended delay time), with different effects on inspiratory and expiratory cells of the NTS, which resulted in desired outcome. Results of our simulations show that 1) processing of afferent signal at the level of NTS neurons is nonlinear and 2) processing of afferent information is different for inspiratory and expiratory components of cough.

In spite of a significant progress in our understanding of neural control of the cough reflex, our current level of knowledge is still not capable to achieve effective treatment of various pathologies of this defensive reflex. Still, animal models are providing us with invaluable knowledge of reflexes of the respiratory tract. However, there is a big potential in revisiting previously conducted experiments by the means of computational modeling. These simulations may provide insights that may lead us to better understand and/or improve present-day model of cough generation.

Acknowledgement
This work was supported by the Scientific Grant Agency (VEGA) under the contract No. 1/0166/17, 1/0092/20.

References

[1] M. Simera, I. Poliacek, M. Veternik, L. Babalova, Z. Kotmanova, J. Jakus. Changes in vagal afferent drive alter tracheobronchial coughing in anesthetized cats. Respir Physiol Neurobiol 230:36-43 2016.

[2] R. Shannon, D. M. Baekey, K. F. Morris, B. G. Lindsey. Ventrolateral medullary respiratory network and a model of cough motor pattern generation. J Appl Physiol 1998; 84: 2020±2035.

Modeling of calcium sparks in cardiac myocytes

I. Zahradník[1], B. Iaparov[1,2], A. Zahradníková[1]

[1] *Department of Cellular Cardiology, Institute of Experimental Endocrinology, Biomedical Research Center, Slovak Academy of Sciences, Dúbravská cesta 9, 841 04, Bratislava, Slovakia.*

[2] *Insitute of Experimental Physics, Slovak Academy of Sciences, Watsonova 47, 040 01, Košice, Slovakia.*

e-mail: ivan.zahradnik@savba.sk

Release of calcium ions in cardiac myocytes takes place at special structures known as dyads. The structure of cardiac dyads can be studied *in situ* in molecular detail [1-3]. However, the function at molecular level can be studied only *in vitro* [4], while *in situ* function can be studied only at cellular level [5]. Since the exact relationship between structure and function of dyads and their calcium release sites (CRS) is not accessible experimentally, we employed our recently developed modeling approach [6] to investigate how the structure of calcium release sites controls their function. Understanding of molecular factors is crucial for understanding mechanisms of excitation contraction coupling and their role in health and disease.

We defined the calcium release sites as components of the dyad, with accent on organization and function of ryanodine receptors. We simulated the calcium release function in a model that employed the latest data on spatial distribution and clustering of RyRs [1, 2], on calcium diffusion in a cytosolic buffer [7], and on RyR channel gating [6] adjusted to simulate the resting physiological state of myocytes. Simulated traces of group RyR behavior showed either no activation of calcium spark, or transient activation of a small group of RyRs in CRS, or stationary activation of a large group of RyRs during 200 ms following the first RyR opening. Simulated calcium sparks revealed that the arrangement of RyRs to checkerboard, side-by-side, or random form is much less important than the number and surface density of RyRs in the CRS. The kinetic parameters, probability of occurrence and amplitude of the simulated transient and stationary CRS events could be well described by a weighed function of the number of RyRs, inter-RyR distances, and RyR single-channel calcium current. The CRS model could predict a change in spark activity after rearrangement of RyRs in a CRS in response to changed intracellular conditions. Examination of the defined parametric space of CRSs illustrated the exploratory potential of correct *in silico* models to emulate difficult-to-perform experiments. These results explain the synergy between geometrical arrangement of cardiac dyads and calcium flux through RyRs based on the law of mass action.

Acknowledgement

The research was supported by SAV-TUBITAK JRP/2019/836/RyRinHeart, Russian Foundation for Basic Research (RFBR) project 18-31-00153, by grants from the Science Grant Agency (VEGA 2/0143/17), the Slovak Research and Development Agency (APVV-15-0302), by the Government of the Russian Federation, Program 02.A03.21.0006 and by the Ministry of Education and Science, projects 5719 and 2277, and by the Research & Development Operational Program funded by the ERDF (BIOMED, grant number ITMS: 26240220087). Our study was performed using the Uran supercomputer of the Krasovskii Institute of Mathematics and Mechanics.

References

[1] Asghari, P., Scriven, D. R., Sanatani, S., Gandhi, S. K., Campbell, A. I., & Moore, E. D. (2014). *Circ Res*, 115(2), 252-262.

[2] Jayasinghe, I., Clowsley, A. H., Lin, R., Lutz, T., Harrison, C., Green, E., ... & Soeller, C. (2018). *Cell Rep*, 22(2), 557-567.

[3] Asghari, P., Scriven, D. R., Ng, M., Panwar, P., Chou, K. C., van Petegem, F., & Moore, E. D. (2020). *eLife*, 9, e51602.

[4] Zahradníková A, Dura M, Györke I, Escobar AL, Zahradník I, Györke S. (2003) .*Am J Physiol Cell Physiol*. 285(5), C1059-1070.

[5] Janicek R., Zahradníková A. Jr, Poláková E., Pavelková J., Zahradník I., Zahradníková A. (2012). *J Physiol.* 590(20), 5091-5106.

[6] Iaparov, B. I., Moskvin, A. S., Zahradník, I., & Zahradníková, A. (2019). *Eur Biophys J*, 48(6), 579-584.

[7] Naraghi, M., & Neher, E. (1997). *J Neurosci*, 17(18), 6961-6973.

Enhancedsinglet oxygen production by photo-damaged AsLOV2 domain: experiments and modeling

Andrej Hovan[1], Martina Petrenčáková[1], Tibor Kožár[2], Daniel Jancura[1], Pavol Miškovský[2], Gregor Bánó[1]& Erik Sedlák[2]

[1]Department of Biophysics, Faculty of Science, P.J. Šafárik University, Jesenná 5, 041 54, Košice, Slovakia
[2]Center for Interdisciplinary Biosciences, Technology and Innovation Park, P. J. Šafárik University, Jesenná 5, 041 54, Košice, Slovakia
e-mail: andrej.hovan@student.upjs.sk

During the last decade, FMN (flavin mononucleotide) containing genetically-encoded singlet oxygen photosensitizing proteins have been developed for PDT (photodynamic therapy) applications. Such photosensitizers can be targeted by means of various tags. However, when FMN is encapsulated in protein environment, the quantum yield of $^1O_2$ production by FMN is significantly diminished due to its interactions with surrounding amino acid residues. Recently, an increase of $^1O_2$ production yield, was in such cases achieved by a decrease of quenching of the cofactor excited states by weakening of the protein-FMN interactions while still forming a complex.

An alternative approach, which we suggest here, relies on the blue light irradiation-induced dissociation of FMN to solvent. This dissociation prevents the protein-FMN interactions and thus increases the quantum yield of $^1O_2$ production. Our suggestion is based on the study of the irradiation effect on two variants of the LOV2 domain from *Avena sativa*; wild type, AsLOV2 wt, and the variant with a replaced cysteine residue, AsLOV2 C450A.We detected oxidation of several amino acids as well as irradiation-induced conformational changes in both AsLOV2 variants. A thorough analysis of these observations indicates that irradiation-induced increase in $^1O_2$ production is caused by a release of FMN from the protein. Moreover, an increased FMN dissociation from AsLOV2 wt in comparison with AsLOV2 C450A points to a role of C450 oxidation in repelling the cofactor from the protein.

Acknowledgement
This work was supported by the research grants provided by Slovak research and development agency (APVV-15- 0069 and APVV-15-0485) and by the research grant VEGA 1/0557/20.

References

[1] Baier, J. et al. Singlet oxygen generation by UVA light exposure of endogenous photosensitizers. Biophys. J. 91, 1452–1459, https:// doi.org/10.1529/biophysj.106.082388 (2006).
[2] Westberg, M., Bregnhoj, M., Etzerodt, M. &Ogilby, P. R. Temperature Sensitive Singlet Oxygen Photosensitization by LOV-Derived Fluorescent Flavoproteins. The journal of physical chemistry. B 121, 2561–2574, https://doi.org/10.1021/acs.jpcb.7b00561 (2017).
[3] Torra, J. et al. Tailing miniSOG: structural bases of the complex photophysics of a favin-binding singlet oxygen photosensitizing protein. Sci Rep 9, 2428, https://doi.org/10.1038/s41598-019-38955-3 (2019).
[4] Ruiz-Gonzalez, R. et al. Singlet oxygen generation by the genetically encoded tag miniSOG. J. Am. Chem. Soc. 135, 9564–9567, https://doi.org/10.1021/ja4020524 (2013).

Microinjection of neuroactive modulator into the ventral respiratory group – computer simulations

M. Veterník, L. Martvoň, J. Míšek, J. Jakuš, I. Poliaček

Department of Medical Biophysics, Jessenius Faculty of Medicine in Martin, Commenius University in Bratislava, Slovakia
e-mail: marcel.veternik@uniba.sk

The ventral respiratory column generates rhythmical respiration and is divided into four compartments: the Bötzinger complex (BOT), pre-Bötzinger complex (pre-BOT), rostral ventral respiratory group and caudal ventral respiratory group. BOT is a neuronal population containing expiratory augmenting neurons. The BOT region and surrounding reticular formation also contain a smaller number of expiratory units with decrementing discharge patterns, as well as other related respiratory neurons. The BOT area and the pre-BOT are important in generating respiratory rhythm and modulating respiratory motor activity. It is also known that the respiratory network in BOT / pre-BOT is a significant part of the neural network that generates a central pattern of cough reflex.

The impact of D, L – homocysteic acid microinjection (non-specific glutamate receptor agonist that causes excitation of neurons) into the BOT area was observed on computer model of quiet breathing and cough reflex. Integrated signals from neural populations innervating main respiratory motor neurons inspiratory phrenic and expiratory lumbar were obtained from simulations. We analysed durations and amplitudes of phrenic and lumbar activity during quiet breathing and cough reflex, number of coughs elicited by 10 s long stimulation. Fibre population providing virtual DLH related excitation signal to expiratory neural populations with augmenting discharge pattern was added after control simulations. The excitation had 2 levels, DLH1 represented excitation by higher number of fibres and terminals and by lower synaptic strength (simulated higher number of excitatory inputs), DLH2 represented excitation by lower number of terminals and by higher synaptic strength (simulated higher effect of excitatory inputs).

Our simulations have demonstrated a high level of analogy with the cough reflex and breathing changes observed in the experiments. Simulated excitations in the area of the BOT led to cough depression represented by the decrease in the number of coughs and the neuronal activity of the lumbar nerve neuronal population during cough. Despite the shortening of phrenic activity during cough (compared to quiet breathing), which was not observed in animal experiments, our simulations confirm the ability of the computer model to simulate functional processes in neural populations. Our results suggest that a suitable computer model of a functional neural network is capable to confirm and predict the results obtained on animals.

Acknowledgement
This work was supported by Slovak Research and Development Agency under the contract no. APVV-19-0214 and by projects VEGA 1/0166/17, VEGA 1/0092/20, and VEGA 1/0173/20.

Accuracy of open probability and open time estimation from single-channel records

A. Zahradníková[1], B. Iaparov[1,2], and I. Zahradník[1]

[1]*Department of Cellular Biophysics, Institute of Experimental Endocrinology, Biomedical Research Center, Slovak Academy of Sciences, Dúbravskácesta 9, 845 05 Bratislava, Slovakia.*
[2]*Institute of Experimental Physics, Slovak Academy of Sciences,Watsonova 47, 040 01 Košice*
e-mail: alexandra.zahradnikova@savba.sk

Transmembrane ion flux in living cells is mediated by ion channels and depends on their number, conductance, and open probability. Gating of channels is sensitive to experimental conditions and is characterized by open probability P_O and mean open time $t_O$that are determined in single-channel experiments. Datasets of individual experimental records of single-channel activity measurements represent compound random samples of stochastic gating continuous in time. The aim of this study was to understand the relationship between the accuracy (trueness and precision) of $P_O$and $t_O$determination and the method of single-channel activity data collection.

Two simple gating models with a single closed time and one of two open times were used of simulation of a long sequence of openings and closures comprising up to 50000 events. Simulated single-channel activity of sequential channel gating events was partitioned into records of different duration (5 - 30 s). Collections of 8 - 1024 records were combined into datasets. P_O and t_O estimates of individual datasets were statistically evaluated.We found that the trueness of P_O determination, defined as relative systematic errore_S – normalized absolute difference between the estimated and the true value, depends on the average number of channel openings per record(Fig. 1A). The level of precision of $P_O$and $t_O$determination was defined using the notion of precision level e_R^α. To reach a precision levelof e_R^α, therelative random error of estimate has to be less than e_R^αin α% of independent random datasets.In the tested models, the precision levelsof P_O and $t_O$depended on the number of channel openings in the whole dataset and on the coefficient of variation of mean open timeCV_{to} (Fig.1B,C).In the tested models, estimation of P_O required twice as many openings to reach the same precision level as t_O estimation.

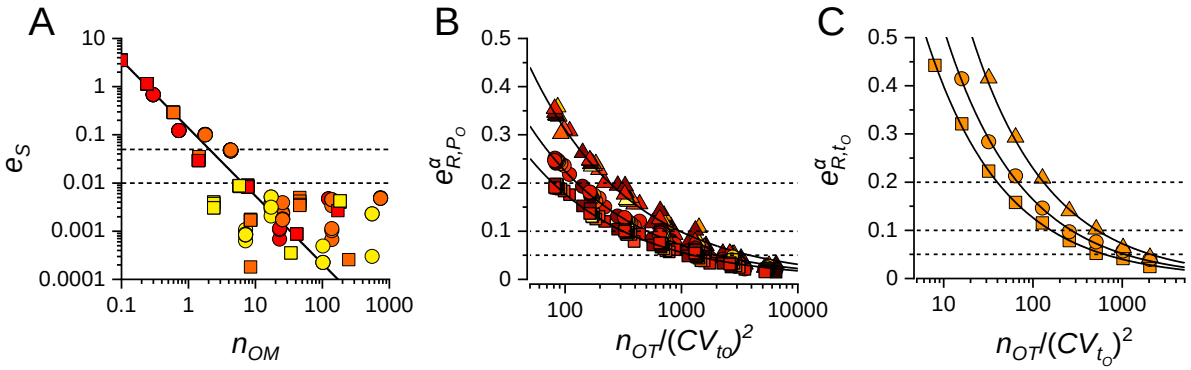

Fig. 1. Trueness and precision of P_O and t_O estimation.A –Relative systematic error e_S of P_O estimates depends on the mean number of openings per record n_{OM}.Dashed lines correspond to 1% and 5% levels of systematic srror. Solid line - the best fit of the data by the equation $e_S = A/(n_O)^B$ (A = 0.138 ± 0.003 and B = 1.41 ± 0.01). Colorsrepresentdifferent record durations; different symbols stand for different mean open time. B, C–Precision levels of open probability(B) and open time(C) as functions of normalized number of openings in the dataset$n_{OT}/(CV_{t_O})^2$. Squares, circles and triangles denote values of precision limitcorresponding to α of 80, 90 and 98%. In B, colors represent different open times and coefficients of their variation.Dashed lines markprecision levels of 0.05, 0.1, and 0.2.

Next we have derived general, model-independent relationships relating the coefficients of variation of $P_O$to coefficients of variation of t_O and t_C. We found that while the precision of t_O depends on the number of openings and on the coefficient of variation of open time, the precision of

P_O depends on the number of openings, level of open probability, and on the coefficients of variation of open as well as closed times.Precise estimation of P_O may require collecting up to 16×more openings that analogous estimation of t_O (Fig. 2). These findings allow planning of single-channel experiments for the required accuracy of P_O determination over a large span of open probabilities. According to the presented results, planning and evaluating single-channel experiments should include definition of the required precision level$e_R^\alpha$for P_O and $t_O$and determination of the number of openings necessary to achieve the required level of precision.

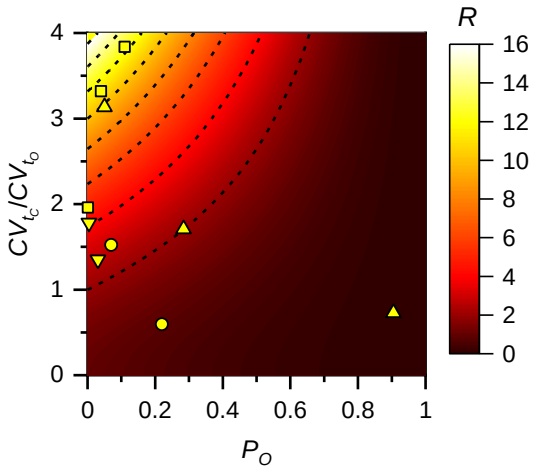

Fig. 2. The relationship between the ratio CV_{t_C}/CV_{t_O}, open probability P_O and the ratio R between the number of openings needed to obtain the same relative error of open probability estimation and that of open time estimation. Squares, circles, up triangles and down triangles represent the estimated values of P_O, CV_{t_E} andCV_{t_C}/CV_{t_O} for RyR2 channels activated by calcium [1], adenosine [2], ATP [3] and AMP [4], respectively.

Acknowledgement
This work was supported by the Slovak Research and Development Agency grant APVV-15-0302, by SAV-TUBITAK project JRP/2019/836/RyRinHeart, by the Science Grant Agency grant VEGA 2/0143/17 and by the Research & Development Operational Program funded by the ERDF (BIOMED, grant number ITMS: 26240220087).

References

[1] Zahradnikova, A., and I. Zahradnik. 1995. Description of modal gating of the cardiac calcium release channel in planar lipid membranes. *BiophysJ.* 69:1780-1788.
[2] Chan, W.M., W. Welch, and R. Sitsapesan. 2000. Structural factors that determine the ability of adenosine and related compounds to activate the cardiac ryanodine receptor. *Br J Pharmacol.* 130:1618-1626.
[3] Kermode, H., A.J. Williams, and R. Sitsapesan. 1998. The interactions of ATP, ADP, and inorganic phosphate with the sheep cardiac ryanodine receptor. *BiophysJ.* 74:1296-1304.
[4] Ching, L.L., A.J. Williams, and R. Sitsapesan. 1999. AMP is a partial agonist at the sheep cardiac ryanodine receptor. *Br J Pharmacol.* 127:161-171.

DNA aptamers in biosensors and in targeted drug delivery

T. Hianik

Department of Nuclear Physics and Biophysics, FMFI UK, Mlynska dolina F1, 842 48 Bratislava, Slovakia
e-mail: Tibor.Hianik@fmph.uniba.sk

Aptamers are single stranded DNA or RNA molecules that are selected by method of Systematic Evolution of Ligands by EXponencial enrichment (SELEX) toward various targets, such as proteins, drugs, biomarkers, viruses, bacteria or whole cells [1]. In a solution aptamers fold into 3D structure containing binding site for the target. The affinity of aptamers to their targets is in the micromolar to the subnanomolar range and can therefore be comparable and in certain cases even better than, those of antibodies for the same targets. In contrast with antibodies, aptamers are selected *in vitro*. In comparison with antibodies they are more stable and flexible. Already developed aptamer can be reproduced with high accuracy. In addition, aptamers can be chemically modified by various labels that allowing them to be immobilized at various surfaces at which can serve as receptors in biosensors [2]. The chemical modification also increases the aptamer stability. Electroactive, optical labels, quantum dots and nanoparticles can also be conjugated with aptamers, which allowing signals amplification using electrochemical, optical and piezoelectric methods. Aptamers can be connected to the AFM tips, which allowing measurement of the forces between aptamer and its target at the solid support or at the surface of the cell [3]. In addition aptamers can be used as a probe for imaging of the specific molecules at the surfaces and thus allowing analyzing their lateral distribution. Nanocarriers modified by aptamers are very effective for targeted drug delivery.

This contribution is focused on the introduction into the structure and physical properties of DNA aptamers and on demonstration of several applications of aptamers as a receptors in targeted drug delivery and in diagnosis of the cancer by means of detection of cancer markers at the surface of the cells using thickness shear mode acoustic method (TSM) and single molecule force spectroscopy (SMFS).

Acknowledgement
This work was supported by Agency for Promotion Research and Development (Projects No. APVV-14-0267 and by Science Grant Agency, grant No. VEGA 1/0419/20.

References

[1] C. Tuerk and L. Gold, Science 249 (1990) 505–510.
[2] T. Hianik and J. Wang, Electroanalysis 21 (2009) 1223–1235.
[3] A. Poturnayova, M. Burikova, J. Bizik and T. Hianik, ChemPhysChem 20 (2019) 545-554.

Ultrasound-propelled nanomotors modified with fluorescein-labeled aptamers and dendrimers as potential treatment for breast cancer

V. Subjakova[1,2], M. Beltrán-Gastélum[2] , B. Esteban-Fernández de Ávila[2], H. Gong[2], Z. Garaiova[1,2], M. Ionov[3], P. Lekshmy Venugopalan[2], T. Hianik[1] and J. Wang[2]

[1]Faculty of Mathematics, Physics and Informatics, Comenius University, Mlynska Dolina F1, 842 48 Bratislava, Slovakia
[2]Department of Nanoengineering, University of California San Diego, La Jolla, California, 92093, USA
[3]Department of General Biophysics,Faculty of Biology and Environmental Protection, University of Lodz, Lodz, Poland

Nano/micromotors are synthetic nano/microscale structures capable of converting chemical fuel or external energy into mechanical movement [1]. Various nanomotors are showing promising potential towards diverse biomedical application including diagnostics, targeted drug delivery and active delivery of therapeutics [2]. We have demonstrated ultrasound (US)-propelled graphene-oxide (GO) coated gold nanowires (AuNWs), functionalized with fluorescein-labeled DNA aptamers (FAM-AIB1-apt) as nanomotors for qualitative intracellular detection of overexpressed AIB1 oncoproteins in MCF-7 breast cancer cells. AIB1, also known as steroid receptor coactivator 3 (SRC-3), belongs to the p160 steroid receptor family and acts as a transcriptional coactivator. AIB1 plays important roles in regulation growth signaling pathways and is frequently overexpressed mostly in breast cancer.

The current sensing strategy is based on an attractive OFF-ON intracellular fluorescent switching. The fluorescence signal is quenched while FAM-AIB1-apt is adsorbed on GO/AuNWs (signal OFF) due to fluorescence resonance energy transfer. Then, in the presence of the specific target AIB1, the FAM-AIB1-apt is released from the GO/AuNWs surface leading to a fluorescence signal recovery. The fast movement of nanomotors under the US field facilitated accelerated intracellular uptake and resulted in a faster aptamer binding with the target protein and thus faster fluorescence recovery. The propulsion behavior of the aptamer functionalized nanomotors greatly enhanced the fluorescence intensity compared to static conditions. Negligible fluorescence intensity was observed in negative control HFF-1 cells as well as in positive control MCF-7 treated with nonspecific fluorescein-labeled aptamers. This new aptamer functionalized nanomotor-based strategy offers considerable potential for further development of sensing methodologies towards early diagnosis of breast cancer [3]. US-propelled nanomotors were also demonstrated for active delivery of dendrimers. The resulting complexes were tested as active intracellular transporters being propelled by US fields and using breast cancer cells as a model [4].

Acknowledgement
This work was supported by the European Commission within the project Innovative technology for the detection of enzyme activity in milk (Formilk) under grant agreement number 690898 /H2020-MSCA-RISE-2015 and by Agency for Promotion Research and Development under the contracts APVV-14-0267, SK-PL-18-0080, SK-BY-RD-19-0019 and by Polish Ministry of Science and Higher Education, Science Grant Agency, grant No. VEGA 1/0419/20.

References

[1] J. Wang, Nanomachines: Fundamentals and Applications, Wiley-VCH: Weinheim (2013).
[2] J. Wang, R. Dong, H. Wu, Y. Cai1, B. Ren, Nano-Micro Lett. 12 (2020), 11-20.
[3] M. Beltrán-Gastélum, B. Esteban-Fernández de Ávila, H. Gong, P. Lekshmy Venugopalan, T. Hianik, J. Wang, V. Subjakova, ChemPhysChem. 20 (2019) 3177-3180.
[4] Z. Garaiova, G. Bolat, B. Esteban-Fernández de Ávila, H. Gong, N. Sanz del Olmo, P. Ortega, F. Javier de la Mata, S. Michlewska, J. Wang, T. Hianik, Clinical Oncology and Research 2 (2019), 1-5.

Hypericin hydrophobic interactions with anti-apoptotic members of Bcl2 family

Katarina Stroffekova[1], Anastasia Doroshenko[1], Silvia Tomkova[1], and Tibor Kozar[2]

[1]Department of Biophysics, Faculty of Natural Sciences, PJ Safarik University, Jesenna 5, Kosice, Slovakia;
[2]Center of Interdisciplinary Biosciences, TIP-Safarik University, Jesenna 5, Kosice, Slovakia;
e-mail: katarina.stroffekova@upjs.sk

Upregulation of anti-apoptotic Bcl2 family members (Bcl2, Bcl_{XL}, Mcl1) is present in many types of cancer cells and underscores their resistance to apoptosis. To circumvent this, the inhibitors of anti-apoptotic Bcl2 members, termed BH3 mimetics, have been explored [1]. Recently, we have discovered that hypericin (Hyp), a naturally occurring photosensitive compound,had significant effects on ultrastructure, mitochondria function and metabolism, and Bcl2 proteins [2].We have hypothesized that Bcl2-Hyp interactions might be one possible mechanism underlying these effects.

Our aim was to test how Hyp interacts with anti-apoptotic members of the Bcl2 family (Bcl2 and Mcl1) and compare these interactions to known BH3 mimetics such as gossypol (Goss) and ABT263. We have shown that Hyp binds into the Bcl2 hydrophobic groove comprised of BH3 and BH1 domains [3]. In addition, the molecular docking revealed that Hyp may also interact with other anti-apoptotic members of the Bcl2 family, Bcl_{XL} and Mcl1 comparableto panBcl2 BH3 mimetics. We tested thesepredictions by immunocytochemistry, fluorescent spectroscopy and cell viability assay to investigate interactions between Hyp and anti-apoptotic Bcl2 members.

We have explored interactions of BH3 and BH1 domains and Hyp further. Our results show that Hyp interacts with BH3 and BH1 peptides in concentration dependent manner and shows the stronger interactions than Goss and ABT263. In addition, we have also studied interaction of three compounds, Hyp, Goss and ABT-263, with whole purified Bcl2 and Mcl1proteins by fluorescence spectroscopy. Our findings indicate that Hyp interacts stronger than Goss or ABT263 with the Bcl2 protein. The Goss is the strongest interactor with Mcl1 protein followed by Hyp and the ABT263. Our findings indicate that Hyp may function in cell signaling pathways as a novel BH3 mimetic molecule and has the potential to enhance other cancer treatments.

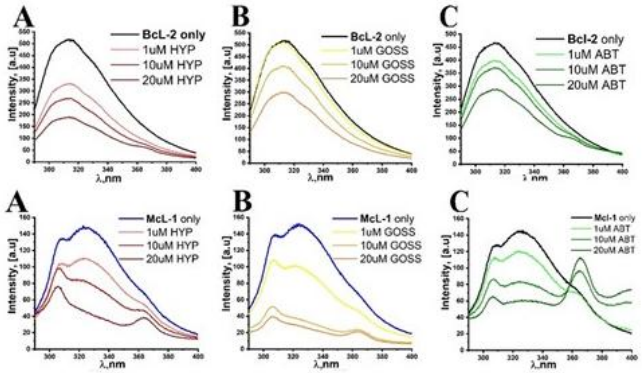

Fig. 1. The fluorescence quenching spectra of Bcl2 and Mcl1 protein (1μM) with different concentration of Hyp (A), Goss (B) and ABT-263 (C).

Acknowledgement
This work was supported by the Slovak Grant Agency (VEGA 1/0425/15 and 1-0421-18) and by the Slovak Research and Development Agency (APVV-15-0485 and APVV-16-0158).

References

[1] Delbridge, ARD &A StrasserThe BCL-2 proteinfamily, BH3-mimetics and cancertherapy.CellDeath and Differentiation (2015) 22, 1071–1080.
[2] Huntosovaet. al. Assessinglight-independenteffects of hypericin on cellviability, ultrastructure and metabolism in humanglioma and endothelialcellsToxicology in Vitro 40 (2017) 184–195.
[3] Stroffekova et al. Importance of Hypericin-Bcl2 interactionsforbiologicaleffects at subcellularlevels. Photodiagnosis and PhotodynamicTherapy 28 (2019) 38–52.

Education of Biophotonics in Slovakia: from past activities to future concepts

S. Hustava[1] and A. Marček Chorvátová[1,2]

[1] Department of Biophysics, FNS, Univ. Ss Cyril and Methodius, J Herdu 1, 917 02 Trnava, Slovakia.
[2] Department of Biophotonics, International Laser Center, Ilkovičova 3, 814 04 Bratislava, Slovakia.
e-mail: stefan.hustava@ucm.sk

Biophotonics is a modern science that aims to study the interaction of light with living cells, tissues or organisms, but also includes the development and validation of new optical and imaging diagnostic techniques. The Biophotonics industry is one of the fastest growing industries in need of an increasing number of specialized professionals. Biophotonics therefore presupposes interdisciplinary knowledge, e.g. knowledge at the interface of disciplines such as physics (optics, laser physics, biophysics), biomedical engineering, biology, chemistry, biotechnology, informatics as well as medicine and biomedicine [1]. The development of the field of Biophotonics is thus closely related to the increasing use of Biophotonics in cell and tissue diagnostics, the emergence of nanotechnology and their use in Biophotonics, as well as the development of new imaging systems. The concept of the design of an international project for teaching Biophotonics is thus highly desirable for Slovakia from the point of view of modern education [2].

Currently, in the field of Biophotonics, there are training activities at the level of M.Sc. and Ph.D that, together with development of novel Biophotonics tools for higher education [3], allowing at least basic preservation of the Biophotonic education. In the future, education in Biophotonics in Slovakia needs to be improved by more profound collaboration with large state-of-the-art laser, microscopy and biomedical imaging infrastructures, namely via new biomedical and biotechnology infrastructures in Europe, including Laserlab Europe [4] or EuroBioImaging [5]. To be part of these infrastructures is a fundamental condition for a successful international cooperation in Biophotonics education. Only in this way can students gain the latest knowledge at the interface of optics, photonics, biophysics, but also chemistry, molecular biology, physiology, biomedicine and nanobiophotonics.

Our aim in the future is to actively participate in educational activities with specialized workplaces at European universities cooperating within other EU projects (eg Laserlab Europe V, CARLA, COST projects, etc.). It is also highly desirable to improve existing schemes, such as the European Erasmus plus or Marie-Curie Fellowship programs and/or double diploma programs, including development of international teams within European Universities [6]. At the same time, the design of such a education must be preceded by the improvement of teaching and support of modern higher education in Slovakia.

Acknowledgement
This work is supported by KEGA 005UCM-4/2018 and NFP313010T458 z OPVaI-VA/DP/2018/1.1.3-10.

References

[1] Marcek Chorvatova A 2019: The concept of education of Biophotonics in Slovakia (in Slovak: Koncepcia výučby Biofotoniky na Slovensku. ***Fotonika 2019,*** Proceedings of the 14th annual scientific meeting of ILC: 18-21.
[2] Marcek Chorvatova A: Conception of an international project proposal for teaching of Biophotonics at the European level (in Slovak: Koncepcia návrhu medzinárodného projektu pre výučbu Biofotoniky na Európskej úrovni). ***Fotonika 2020,*** Proceedings of the 15th annual scientific meeting of ILC: *in press*.
[3] Hustava S., Marcek Chorvatova A 2019: Biophotonics tools for higher education: equivalent circuit model of the plasma membrane of excitable cells. ***Proceeding of ANS 2019:*** 6-11.
[4] https://www.laserlab-europe.eu/ or
[5] https://www.eurobioimaging.eu/
[6] https://ec.europa.eu/programmes/erasmus-plus/programme-guide/part-b/three-key-actions/key-action-2/european-universities_sk

Calcium signaling and contractility in cardiomyocyte of Wolframin invalidated rats

M. Cagalinec[1,2,3], A. Zahradníková Jr[1], J. Pavelková[1], S. Kureková[4], M. Hoťka[3] and A. Zahradníková[1]

[1] *Department of Cellular Cardiology, Institute of Experimental Endocrinology, Biomedical Research Center, Slovak Academy of Sciences, Dubravska cesta 9, 84505 Bratislava, Slovakia*

[2] *Centre of Excellence for advanced materials application, Slovak Academy of Sciences, Dubravska cesta 9, 84511 Bratislava, Slovakia*

[3] *Department of Neurophysiology and Neuropharmacology, Center for Physiology and Pharmacology, Medical University of Vienna, Schwarzspanierstraße 17A, 1090 Vienna, Austria*

[4] *Department of Biophysics and Electrophysiology, Institute of Molecular Physiology and Genetics, Centre of Biosciences, Slovak Academy of Sciences, Dubravska cesta 9, 84005 Bratislava, Slovakia*

e-mail: michal.cagalinec@savba.sk

Wolfram syndrome (WS) is a rare recessive disorder caused by mutations in the Wfs1 gene encoding the wolframin protein (Wfs1). Wfs1 is located in the membrane of endoplasmic reticulum (ER) and is involved in ER stress, mitochondrial function and calcium signalling. For the latter, in Wfs1 deficient neurons the cytosolic calcium response after stimulation has been significantly depressed [1] and it has been demonstrated that Wfs1 co-immunoprecipitates with SERCA [2]. Beyond brain and pancreas, Wfs1 is highly expressed in the heart [3]. Since calcium is the principal trigger of cardiomyocyte contraction and since Wfs1 is highly expressed in the cardiac tissue, we have evaluated calcium metabolism and contractility in the Wfs1 exon5-deleted ($Wfs1^{-e5/-e5}$) cardiac myocytes using confocal microscopy, patch-clamp and molecular biology.

In four months old male rats, invalidation of Wfs1 resulted in a significant increase of the amplitude of myocyte contraction as well as in prolongation of contraction in field-stimulated myocytes (Fig.1 left). Calcium transients of the Fluo-3/AM stained $Wfs1^{-e5/-e5}$ myocytes, recorded simultaneously with contractions, showed significantly prolonged calcium transient, but no significant change of the amplitude (Fig. 1 right). Moreover, sarcoplasmic reticulum calcium content was not changed in the absence of functional Wfs1, as revealed by caffeine application.

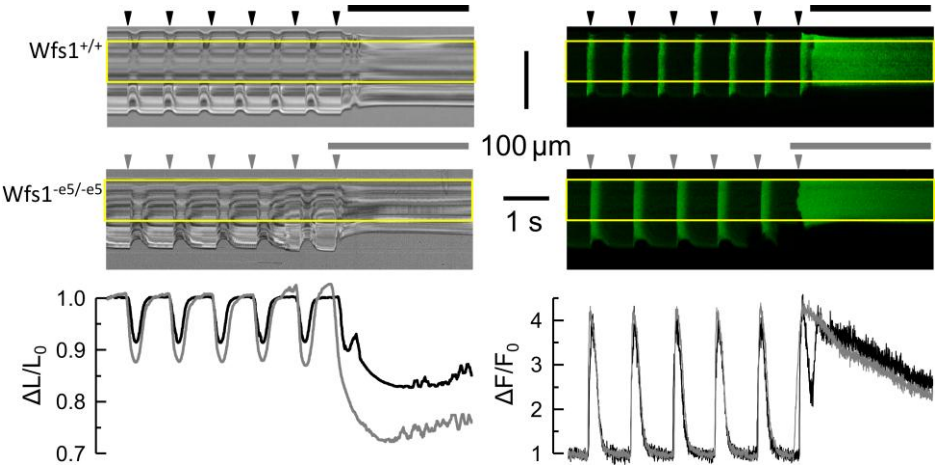

Fig. 1. Typical records of sarcomere length and cytosolic Ca^{2+} in response to field stimulation (arrowheads). *Left column* – transmitted light records of line-scans along the myocyte long axis. Deflections correspond to contractions of the myocyte. *Right column* – fluorescence records of calcium signal in confocal line-scans corresponding to the contraction records (left). The yellow rectangles denote the analyzed region. *Top row* – $Wfs1^{+/+}$ myocyte. *Middle row* – $Wfs1^{-e5/-e5}$ myocyte. Horizontal lines – applications of caffeine. *Bottom row* – the time course of changes in the relative sarcomere length (left) and cytosolic calcium signals (right) corresponding to the top and middle row records (black - $Wfs1^{+/+}$, grey - $Wfs1^{-e5/-e5}$).

The change in contractility could result from a change of the calcium current (the trigger for calcium release) and/or from a change of calcium release itself. Calcium currents showed no statistically significant differences between parameters of the current-voltage curves between the groups (Fig. 2A). The efficiency of calcium current to induce calcium release was estimated according to [4] from the extent of calcium release-dependent inactivation of calcium current. The voltage dependence of inactivation was not significantly different but the fraction F_{iV} of inactivated calcium current was significantly larger in $Wfs1^{-e5/-e5}$ than in $Wfs1^{+/+}$ myocytes (Fig. 2B). When calcium release was triggered by tail calcium currents evoked after +60 mV prepulses of variable duration, known to selectively induce only the calcium release-dependent component of inactivation [4], the dependence of inactivation on prepulse duration was not significantly different between the two myocyte groups but the fraction F_{it} of inactivated calcium current was again significantly elevated in $Wfs1^{-e5/-e5}$ myocytes (Fig. 2C).

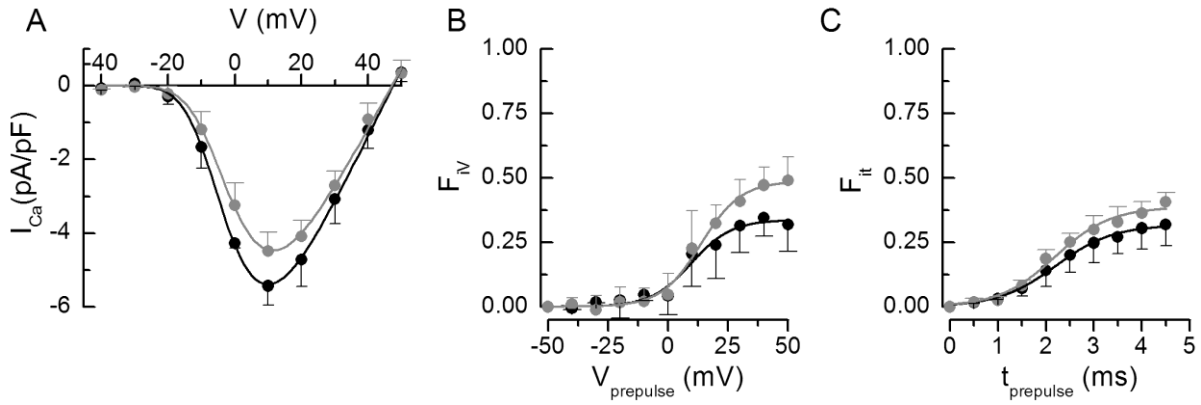

Fig. 2. Analysis of calcium currents. **A:** Voltage dependence of the peak calcium current amplitudes. The curves represent the respective fits by the equation $I_{Ca}(V) = g_{max} (V - V_r) / (1+\exp(-(V - V_{1/2}) / V_S))^4$. **B:** Fractional inactivation of the test pulse calcium current amplitude by variable prepulse voltages of 5-ms duration. The curves represent the respective fits by the Boltzmann equation. **C:** Fractional inactivation of the test pulse calcium current amplitude by prepulses to +60 mV of variable duration. The curves represent the respective fits by the Boltzmann equation. In all panels, black – $Wfs1^{+/+}$, grey – $Wfs1^{-e5/-e5}$. Data are given as mean ± S.E.M.

In addition, we have observed a decrease in expression of the plasma membrane sodium-calcium exchanger in $Wfs1^{-e5/-e5}$ myocytes both at the mRNA and at the protein level, whereas the expression levels of L-type calcium channel, ryanodine receptor type 2, SERCA2 and calsequestrin2 were not different.

The decrease of NCX expression might slow down extrusion of Ca^{2+} from the myocytes, leading to prolongation of calcium transient, and curtailing of calcium current due to increased calcium release-dependent inactivation of I_{Ca}. This would explain the unchanged SR calcium content.

Acknowledgement
This work was supported by SASPRO grant No. 0063/01/02, APVV-15-0302, VEGA 2/0169/16, VEGA 2/0143/17 and ITMS 26230120006.

References

[1] M. Cagalinec, M. Liiv, Z. Hodurova, M.A. Hickey, A. Vaarman, M. Mandel, A. Zeb, M. Kuum, D. Safiulina, V. Choubey, E. Vasar, V. Veksler and A. Kaasik, PLoS Biol (2016), 14(7), e1002511.
[2] M. Zatyka, G. Da Silva Xavier , E.A. Bellomo, W. Leadbeater, D. Astuti, J. Smith, F. Michelangeli, G.A. Rutter and T.G. Barrett. Hum Mol Genet (2015), 24 (3), 814-827.
[3] T. Yamada, H. Ishihara, A. Tamura, R. Takahashi, S. Yamaguchi, D. Takei, A. Tokita, C. Satake, F. Tashiro, H. Katagiri, H. Aburatani, J. Miyazaki and Y. Oka, Hum Mol Genet (2006), 15(10), 1600-1609.
[4] A. Zahradníková, Z. Kubalová, J. Pavelková, S. Györke and Ivan Zahradník, Am J Physiol Cell Physiol (2004), 286(2), C330-341.

2D spectral analysis of highly autofluorescent samples

A. Zahradníková jr.[1], M. Novotová, Jasna Marinovic[2], and I. Zahradník

[1] *Department of Cellullar Cardiology, Institute of Experimental Endocrinology, Biomedical Research Center, Slovak Academy of Sciences, Dúbravská cesta 9, 845 05 Bratislava, Slovakia*

[2] *Department of Physiology, University of Split School of Medicine, Croatia*

e-mail: ueensash@savba.sk

Autofluorescence of tissue samples is a serious obstacle in immunofluorescent imaging, as it interferes with fluorescence signal of labels. Especially problematic is the high background in glutaraldehyde-fixed samples, which is inevitable in biopsies primarily targeted for electron microscopy analysis.

Here we used 2D spectral analysis of biopsies from human hearts from elderly ischemic patients (men, 66 – 73 y) that were fixed in Karnovsky's Fixative (2% formaldehyde and 2.5% glutaraldehyde in 0.1 M sodium phosphate buffer) and embedded in paraffin. In addition to the increased background, high local autofluorescence was present in intracellular bodies, presumably ceroid/lipofuscin granules.

We have used Leica TCS SP8 X with white laser to create Λ-λ scans of 15 μm thick tissue slices. The samples were treated by xylene to remove paraffin, rehydrated, permeabilized in PBS containing 0.1% Triton X-100 and blocked in 1% BSA in PBS with 0.1% Tween-20. A subgroup of samples was quenched by 10 mM CuSO4 in 50 mM ammonium acetate buffer. The remaining samples were incubated in 10 μg/ml WGA-Texas Red conjugate in antibody solution buffer (1% BSA in PBS, pH 7,4) at 4°C overnight and after washing in PBS for 3x 15 min incubated at 4°C overnight with mouse anti-CytC antibody (ab13575, 1:200) and then for 2h at RT with goat anti-mouse-Star635P conjugate (Abberior 2-0002-007-5, 1:100) in the antibody solution buffer. All slides were mounted using ProLong Gold mounting buffer.

Images were obtained by sequential excitation by laser light in 10 nm increments between 470 and 670 nm. At each excitation wavelength, emission was recorded at 20-nm bandwidth in the 480 – 785 nm range in 15 nm increments. A 2D plot of fluorescent intensities from the whole images as well as from regions of interest showed high autofluorescence intensities at blue excitations (470 – 500 nm in quenched and up to 540 nm in unquenched samples) in the whole range of emission wavelengths, and high autofluorescence with a small Stokes shift at a majority of excitation wavelengths (Fig. 1).

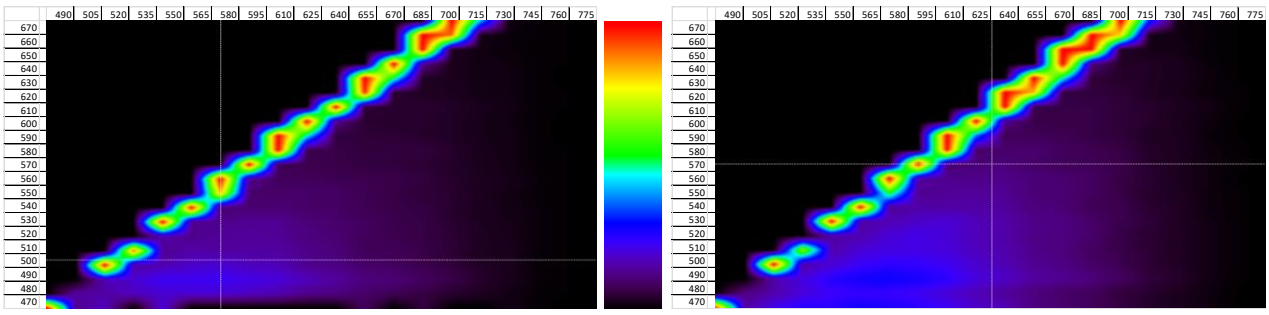

Fig. 1. Autofluorescence signal intensities from quenched (left).and unquenched (right) samples. Excitation wavelengths are on the vertical axis, while emission windows are on the horizontal axis. Relative intensity scale is in the center.

Nevertheless, comparison of fluorescence intensities of negative controls and fluorescently labeled samples revealed specific excitation/emission pairs that were not present in the unlabeled images and could therefore be attributed to specific labeling by WGA or anti-CytC antibody. The labeling-specific excitation/emission pairs correspond to excitation wavelength of 560 and emission band of 610-650 nm for WGA and two pairs – 590 and 640 nm excitation wavelengths and 660-710 and 715-760 nm emission windows for Star 635P-conjugated antibody (Fig. 2).

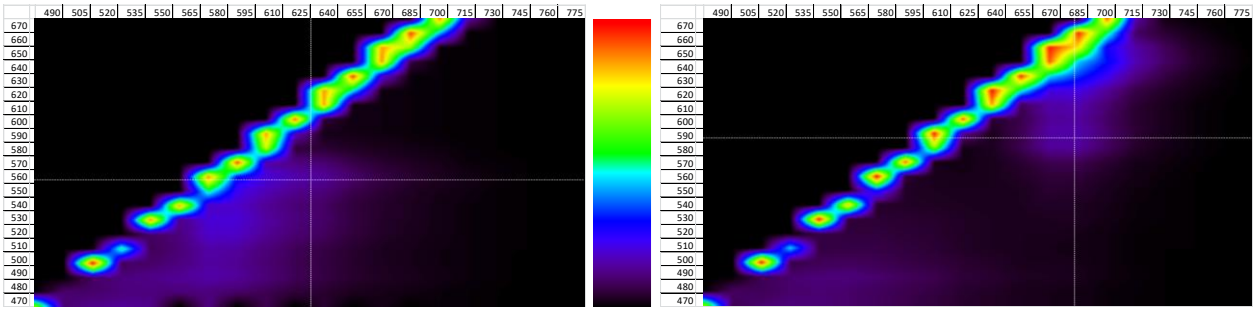

Fig. 2. Fluorescent signal intensities from Texas Red-conjugated WGA (left).and Star 635P-conjugated secondary antibody (right). Excitation wavelengths are on the vertical axis, while emission windows are on the horizontal axis. Relative intensity scale is in the center.

Overlay of images from the specific excitation-emission pairs enabled us to clearly distinguish the sarcolemma, CytC aggregates and autofluorescent granules (Fig. 3).

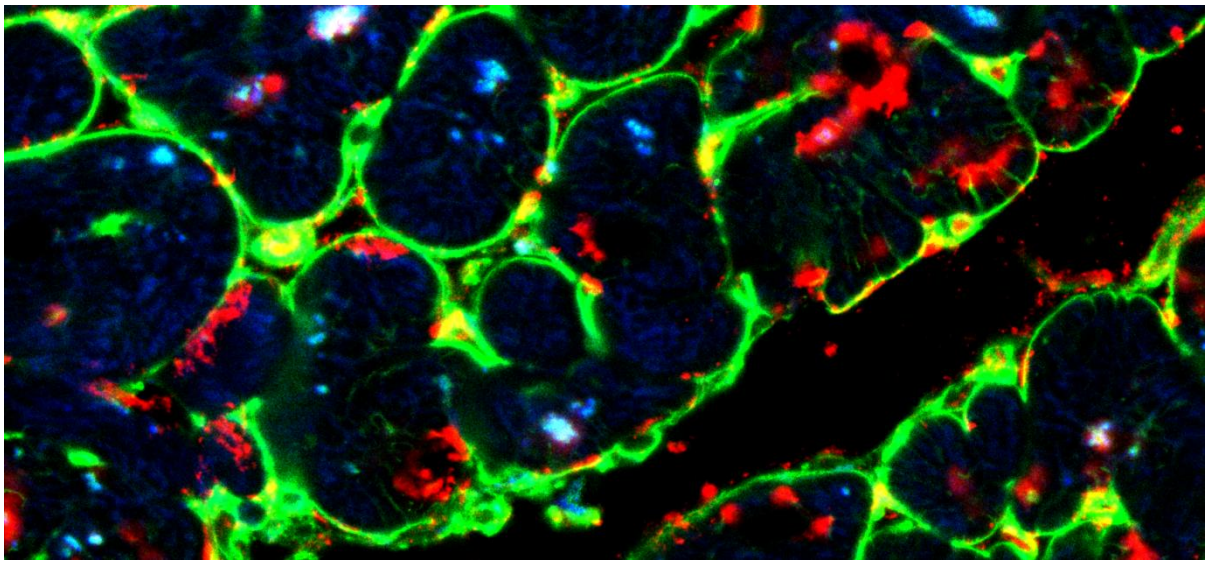

Fig. 3. Overlay of images acquired from the autofluorescence (blue), WGA-Texas Red (green) and Star-635P (red) fluorescence.

Acknowledgement
This work was supported by the Research & Development Operational Program funded by the ERDF (BIOMED, grant number ITMS: 26240220087)and by ERA-CVD_JTC2019-055.

Pseudo-peroxidase activity of cytochrome *c* and its structural consequences

N. Tomášková[1], G. Yassaghi[2], T. Kožár[3], R. Varhač[1], A. Musatov[4], P. Man[2], P. Novák[2], and E. Sedlák[1,3]

[1]*Department of Biochemistry, Faculty of Science UPJŠ, Moyzesova 11, Košice, Slovakia*
[2]*BioCeV - Institute of Microbiology, Průmyslová 595, Vestec, Czech Republic*
[3]*Center for Interdisciplinary Biosciences, Technology and Innovation Park UPJŠ, Jesenná 5, Košice, Slovakia*
[4]*Department of Biophysics, Institute of Experimental Physics SAS, Watsonova 47, Košice, Slovakia*
e-mail: erik.sedlak@upjs.sk

Cytochrome *c* (cyt *c*), in addition to its function as an electron shuttle in respiratory chain, is able to perform as a pseudo-peroxidase with a critical role during apoptosis.

We show that pseudo-peroxidase activity, measured by guaiacol oxidation and the ferrous oxidation in xylenol orange methods, correlates with the accessibility of the heme iron, which was assessed from the association rate constant of cyanide binding to cyt *c* [1].

Incubation of cyt *c* with an excess of hydrogen peroxide lead to a suicide inactivation of the protein, which is accompanied by heme destruction and covalent modification of numerous amino acid residues. Although steady-state reaction of cyt *c* with an excess of hydrogen peroxide represents non-physiological conditions, they might be used for analysis of the so-called first-hit amino acid modifications in *in vivo*. Oxidation of tyrosine residues 67 and 74, detected by mass spectrometry bottom-up approach, are the first amino acid residues modifications found upon incubation with hydrogen peroxide. The positions of the oxidized tyrosines suggest a possible migration pathway of hydrogen peroxide-induced radicals from the site of heme localization to the protein surface. Analysis of a size of folded fraction of cyt *c* upon limited incubation with hydrogen peroxide indicates that the early oxidation of amino acids triggers an accelerated destruction of cyt *c*. Position of tunnels from molecular dynamics simulation structures of cyt *c* points to a location of amino acid residues exposed to a higher concentration of reactive oxidants that are thus likely more prone to covalent modification [2].

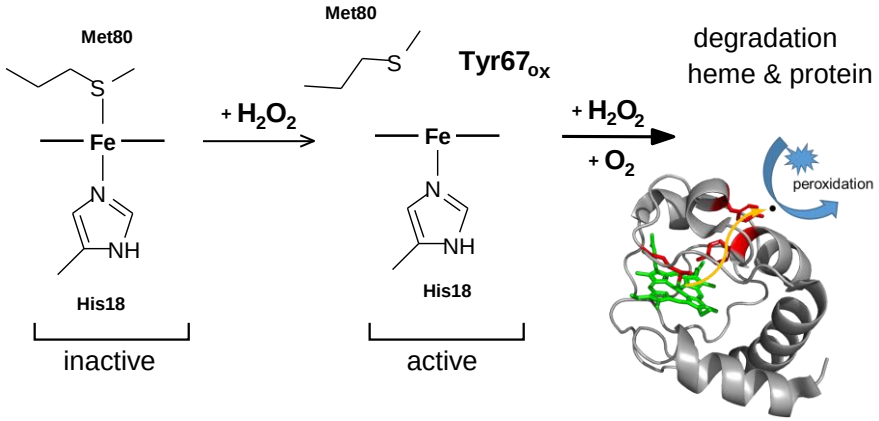

Fig. 1. Schematic representation of the heme region of cyt *c* in the inactive and active conformation upon interaction with hydrogen peroxide.

Acknowledgement
This work was supported by Slovak Research and Development Agency under the contract No. APVV-15-0069 and by grant VEGA 2/0009/17 from Ministry of education, research, and sport.

References

[1] N. Tomášková, R. Varhač, V. Lysáková, A. Musatov, and E. Sedlák, Biochim. Biophys. Acta - Proteins Proteom. 1866 (2018), 1073-1083.
[2] N. Tomášková, G. Yassaghi, T. Kožár, M. Petrenčáková, D. Jancura, P. Man, P. Novák, and E. Sedlák E (submitted)

Observing Hsp70 mechanics during the hydrolysis of a single ATP molecule

Anubhuti Singh[1], Matthias Rief[1], Gabriel Žoldák[2]

[1] Physics Department E22, Technical University of Munich, Garching 85748, Germany,
[2] Center for Interdisciplinary Biosciences, Technology and Innovation Park, P. J. Šafárik University, Jesenna 5, 041 54 Košice, Slovakia
e-mail: gabriel.zoldak@upjs.sk

DnaK is an ATP-regulated Hsp70 chaperone, which is a central molecular chaperone of the protein quality control network in the cell [1]. Once ATP is bound to the nucleotide-binding domain (NBD) of DnaK, the closed substrate-binding domain (SBD) opens its binding cleft and, at the same time, the SBD α-subdomain engages the N-terminal lobe of the NBD. Overall, the SBD undergoes a dramatic ~10 Å displacement of its lid subdomain to allow the exchange of substrates [2]. Here, we can show that a significant conformational change of the SBD can be observed in single-molecule mechanical experiments during a single ATP hydrolysis event.

Recently, single-molecule force experiments have focused on nanomechanics of the individual domains of Hsp70 [3, 4] while mechanical investigations of the two-domain protein that consists of NBD and SBD domains in various ATP/ADP and peptide bound states were missing. In this study, we designed the full-length DnaK construct for optical trapping experiments, which includes the introduction of N and C terminal cysteines, their modification by DNA-maleimide conjugates and hybridize the protein-cysteine-maleimide-DNA construct with a single-stranded overhang of longer DNA handles attached to functionalized beads (see [3, 4] and references therein). Force-extension curves of the apoform of Hsp70 revealed contour-length increases and rupture forces, which are in excellent agreement with the reported fingerprints of the NBD and SBD domains. The NBD fingerprint consists of a single unfolding event at 30 pN with the contour length of ca. 134 nm. The SBD fingerprint consists of two unfolding events at 15 and 20 pN with 22 nm and 39 nm contour-length increase. To study slow conformational exchanges between various Hsp70 states, we applied a pulling speed of 20 nm/s.

Interestingly, in our first set of experiments at a slow pulling speed of the Hsp70 chaperone, we observed that the first peak of the SBD unfolding event display downward overshoot-like behavior , which was consistently seen for the isolated SBD domain as well. We interpreted this unusual behavior as the binding of the part of the unfolded helical lid of the Hsp70 by the still-folded beta subdomain of the SBD. Such auto-inhibited conformation of Hsp70 was observed earlier under conditions that destabilize SBD, and it is attributed to the presence of Hsp70 recognizable sequence motif HLLH as a part of the own sequence. If true, such overshoot kinetics can be suppressed in the presence of a peptide substrate. Indeed, the auto-inhibition behavior of the Hsp70 chaperone disappeared when the peptide substrate was added to the solution. To by-pass such autoinhibitory behavior, we decided to switch to the so-called DnaK*ye variant of the Hsp70 chaperone, which does not show such auto-inhibitory conformation [5].

To observe ATP/ADP cycling of the Hsp70 protein DnaK*ye, the protein was incubated in the presence of large excess of MgATP in the presence of the 50 μM σ^{32} peptide substrate [6]. Under given conditions, the ATP cycle depends on the situation whether DnaK*ye has bound peptide substrate or not (Fig. 1A, rates at zero load). To confirm the identity of a single DnaK*ye molecule, the caught protein was first pulled to 40-50 pN, and unfolding of both domains was monitored. Based on the worm-like-chain (WLC) fit, the refolding of both domains can be observed. Hence, verification of the correct pulling geometry and folding status enables us in later cycles to watch the mechanical properties of SBD*ye in a two-domain DnaK*ye (Fig1B). During a

series of force-extension traces, the cycling of SBD*ye between various states can be observed (Fig1B). We showed that SBD*ye in the ATP-only state is in a weak mechanical state, which can unfold at low forces (Fig.1B red) while in the ADP state, SBD*ye is in a mechanical highly stable state which unfolds at 40-50 pN (not shown). Hence, by monitoring SBD*ye mechanical stability, we can assign an ATP/ADP state of DnaK*ye. Because of a slow ADP exchange, even under highly supersaturating ATP conditions, ADP states exist transiently (red-to-blue transitions, Fig.1C). After dissociation, an ATP molecule binds quickly and SBD*ye transform into mechanically weak state. Hence, we were able to monitor the hydrolysis of a single ATP molecule during the Hsp70 cycle.

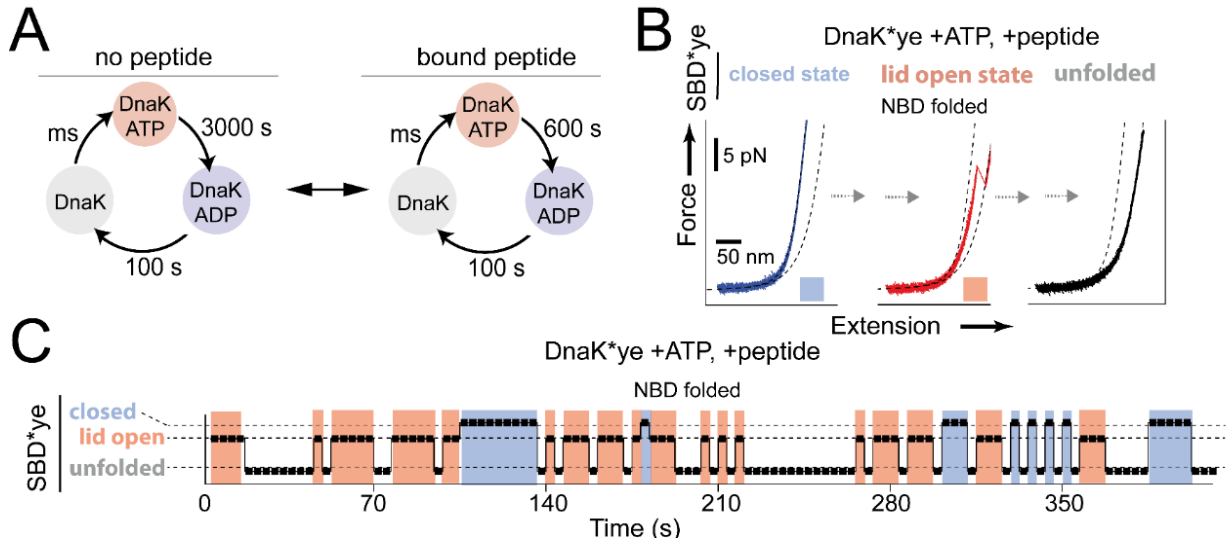

Fig. 1. (A) ATP cycle of Hsp70 in the absence or presence of bound NR peptide. (B) Force-extension curves of DnaK*ye in the presence of Mg2+ATP and peptide. The protein was pulled to 20 pN; only ATP-form can unfold at these forces. Three different force-extension patterns are possible: SBD*ye is folded and does not unfold during the cycle (ADP form), is folded and does unfold (ATP-form), or it SBD*ye is initially unfolded (no information about the state). (C) Cycling between ATP (red)/ADP (blue) form or unfolded SBD*ye (no color). A transition from red to blue indicates the hydrolysis of a single ATP molecule.

Acknowledgement
This work was supported by Slovak Grant Agency VEGA No 1/0175/19 and by the Slovak Research and Development Agency under Contract No. APVV-18-0285.

References

[1] M.P. Mayer, Trends Biochem Sci. 38 (2013), 507-514
[2] R. Rosenzweig, N.B. Nillegoda, M.P. Mayer, and B. Bukau, Nat. Rev. Mol. Cell. Biol. 20 (2019), 665-680.
[3] S.S. Mandal, D.R. Merz, M. Buchsteiner, R.I. Dima, M. Rief, and G. Žoldák, Proc. Natl. Acad. Sci. USA. 114 (2017), 6040-6045.
[4] D. Bauer, D.R. Merz, B. Pelz, K.E. Theisen, G. Yacyshyn, D. Mokranjac, R.I. Dima, M. Rief, and G. Žoldák, Proc. Natl. Acad. Sci. USA. 112 (2015), 10389-10394.
[5] J.F. Swain, E.G. Schulz, and L.M. Gierasch, J. Biol. Chem. 281(2006), 1605-1611.
[6] J.S. McCarty, S. Rüdiger, H.J. Schönfeld, J. Schneider-Mergener, K. Nakahigashi, T. Yura, and B. Bukau, J. Mol. Biol. 256 (1996), 829-837.

A guide on calcium signalling in cardiac myocytes

I. Baglaeva[1,2], I. Zahradník[1], B. Iaparov[1,2] and A. Zahradníková[1]

[1] Department of CellularCardiology, Institute of ExperimentalEndocrinology, Biomedical Research Center, Slovak Academy of Sciences, Dúbravská cesta 9, 841 04, Bratislava, Slovakia.

[2]Institute of ExperimentalPhysics, Slovak Academy of Sciences, Watsonova 47, 040 01, Košice, Slovakia.

e-mail: iuliia.baglaeva@savba.sk

This presentation aims to serve as an introductory guide into the molecular processes behind heart contraction and into the experimental procedures for observation of cardiac myocytes.

The heart is a vital organ that beats and pumps the blood to all parts of the body. Thus, the heart does mechanical work. The signal for performing work is provided by the conduction system of the heart that sends electrical signal from pacemaker cells to the myocardium for contraction [1]. The electrical signal and the mechanical response are coupled by a subcellular mechanism called cardiac excitation-contraction coupling (ECC). Calcium ions play a key role in ECC both as signalling elements and as regulators of the molecular contractile machinery [2,3].

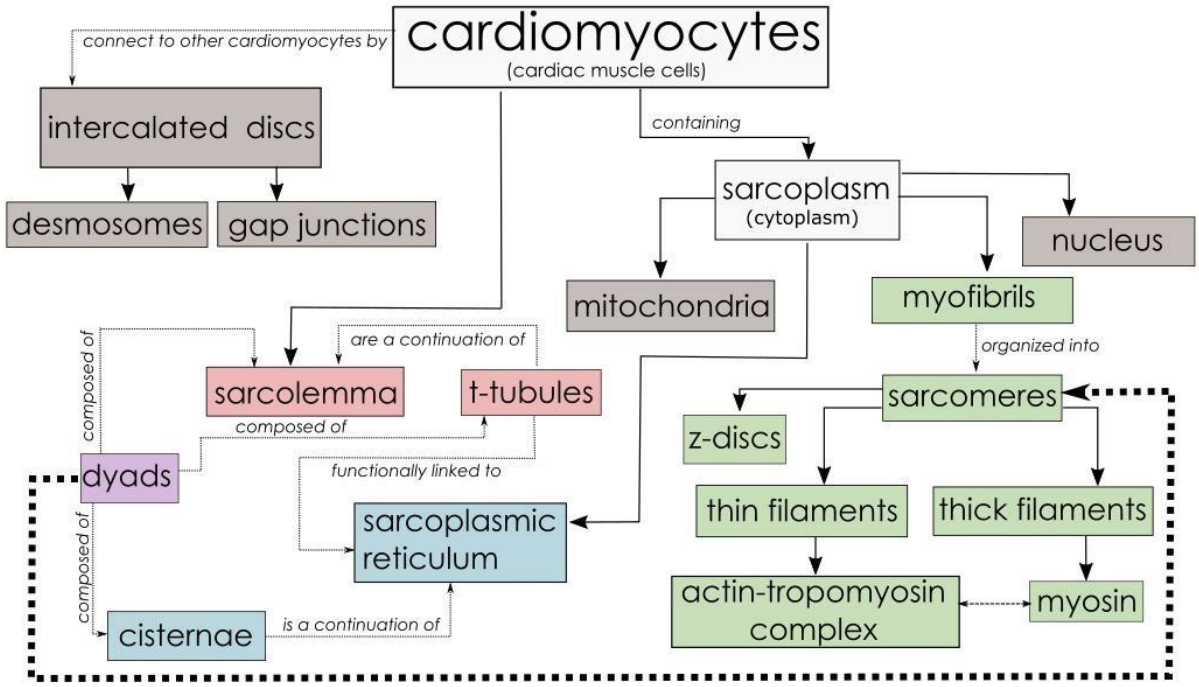

Fig. 1. Schematic description of a cardiomyocyte. The systems responsible for different functions are color-coded as follows: electrical excitation - red; calcium release - blue; excitation-contraction coupling - purple; mechanical work - green; other functions - grey.

Cardiomyocytes join end-to-end through intercalated discs and are composed of sarcolemmaandsarcoplasm, which contains nucleus, myofibrils and mitochondria. The structure of cardiomyocytes and the functional relationship between activation and contraction are shown in Fig. 1.

An electrical signal comes from the conduction system of the heart, moves across the sarcolemma into the t-tubules, and induces opening of voltage-gated calcium L-type-channels in the cell membrane. Then Ca^{2+} from the extracellular space flows into the dyadic space between the tubule and the sarcoplasmic reticulum cisterna. This process activates ryanodine receptors (RyRs), which release Ca^{2+} from the sarcoplasmic reticulum (SR) into the cytosol, creating a local calcium release. Multiple releases from different dyads sum to create the cytosolic calcium transient [3]. The

elevated cytosolic calcium binds to troponin C in the myofilaments, which enables interaction between actin and myosin [1].After contraction Ca^{2+} unbinds from troponin C and is removed from the cytosol. Most of Ca^{2+} is transported back into the SR with the help of the sarco/endoplasmic reticulum Ca^{2+}-ATPase,SERCA. A smaller part of Ca^{2+} is removed from the cell in exchange for $Na^{+}$by the Na^{+}- Ca^{2+} exchanger (NCX) and pumped out by the plasma membrane Ca^{2+}-ATPase (PMCA).

In each cardiac cycle, the amount of calcium influx from the extracellular space must be equal to calcium efflux back to the extracellular space, and the amount of calcium released from the SR must equal the amount of calcium uptake back to the SR - otherwise the cell would either gain or lose Ca^{2+}. Imbalances between Ca^{2+} entry and exit can only occur transiently and then they result in changes of the amplitude of the Ca^{2+} transient and thence contractility [3].

Acknowledgement
This work was supported by the Research & Development Operational Program funded by the ERDF (BIOMED, grant number ITMS: 26240220087).

References

[1] Arnold M. Katz, Physiology of the Heart 4-ed. - Philadelphia: Lippincott Williams & Wilkins, (2006), 644p.
[2] Donald M. Bers, (2002). Cardiac excitation–contraction coupling, *Nature* 415(6868), 198-205.
[3] Eisner, D. A., Caldwell, J. L., Kistamás, K., & Trafford, A. W. (2017). Calcium and excitation-contraction coupling in the heart.*Circ Res*, 121(2), 181-195.

The role of salt-bridge stability in the initial steps of insulin fibrillation

Z. Bednarikova[1]*, B. N. Ratha[2]*, R. K. Kar[2], S. A. Kotler[3], S. Raha[4], S. De[5], N. C. Maiti[6], A. Bhunia[2], Z. Gazova[1]

[1] Department of Biophysics, Institute of Experimental Physics SAS, Watsonova 47, 040 01 Košice, Slovakia.
[2]Department of Biophysics, Bose Institute, P-1/12 CIT Scheme VII (M), Kolkata 700054, India
[3]National Center for Advancing Translational Sciences, National Institutes of Health, Rockville, Maryland 20850, USA
[4]Department of Physics, Bose Institute, 93/1 APC Road, Kolkata 700009, India
[5]School of Bioscience, IIT Kharagpur, Kharagpur 721302, India
[6]Division Structural Biology and Bioinformatics, CSIR-Indian Institute of Chemical Biology, Kolkata 700032, India
**Authors contributed equally*
e-mail: bednarikova@saske.sk

Insulin is an excellent amyloid model protein for understanding amyloidogenesis, and its fibrils formation and structural characterization are well reported. However, the knowledge of early events during insulin fibrillation is still obscure [1].

Therefore, we have studied how structural and sequence similarity of insulin variants from human (HI), bovine (BI), and the modified glargine (GI) influence their thermal stability and aggregation propensity. We investigated the structural features and kinetics of fibrils formation using thioflavin T assay, atomic force microscopy (AFM) and NMR to shed a light on the role of B-chain C-terminal dynamics and salt-bridge stability in the initial steps of insulin fibrillation. Kinetic analysis of insulins fibrillization showed that fibrils formation of GI is slower than BI and HI. The longer lag phase of GI fibrillization was confirmed also by AFM imaging. After 42 h, BI and HI formed protofibrillar and fibrillar species; but, only globular oligomers of GI were observed. These data point to higher stability of GI due to two additional Arginine residues, Arg31B and Arg32B. NMR experiment showed atomic contacts and residue specific interactions, particularly the salt-bridge and H-bond formed among C-terminal residues Arg31B, Lys29B and Glu4 in GI. We propose that enhanced the stability of native GI by strengthening salt bridge can retard tertiary collapse, a crucial biochemical event for oligomerization and subsequent fibril formation.

Our data indicate that fluctuation of the C-terminal residues of the insulin B-chain play a key role in the growth phase of insulin aggregation.

Acknowledgement
This work was supported by projects from Slovak Research and Development Agency APVV-18-0284, VEGA 0145/17, and ITMS 313011T533 (DIAGNAD).

References
[1] Ratha et al. J. Phys. Chem. B 2020, 124 (7), 1125-1136

Glyphosate SERS detection: looking for the detection limits

F. Belén Fuenzalida[1], D. Jancura[1], S. Sanchez-Cortes[2], P. Miškovský[3,4], Z. Jurašeková[1]

[1] *Department of Biophysics, Faculty of Science, P. J. Šafárik University, Jesenná 5, 040 01 Košice, Slovakia.*
[2] *Institute of the Structure of Matter, IEM-CSIC, Serrano 121, 28006 Madrid, Spain*
[3] *Technology and Innovation Park, P. J. Šafárik University, Šrobárová 2, 041 80 Košice, Slovakia*
[4] *SAFTRA photonics, s.r.o., Moldavská cesta 51, 040 11 Košice, Slovakia*
e-mail: zuzana.jurasekova@upjs.sk

Glyphosate ((N-phosphonomethyl)glycine, Figure 1) is one of the world's most popular, non-selective and broad-spectrum herbicide which directly pollutes the environment and contaminated foods [1, 2]. It is an active ingredient of the commercial *Roundup* (known and used also in the Slovak Republic) which is very often and commonly applied against weeds. The Glyphosate's use is not banned currently, however, its safety for human health is a subject of wide debate. Glyphosate is considered toxicologically harmful and presents potential association with human carcinogenesis and other chronic diseases, including mental and reproductive behaviors which is associated mainly with its accumulation in the water at the environments [1, 3]. Moreover, current European legislation allows Glyphosate's use until December 2022 [4]. In general, detection of pesticides residues is an essential step in regulating and monitoring the levels of pesticides. Thus, the issue of the Glyphosate monitoring is becoming increasingly important.

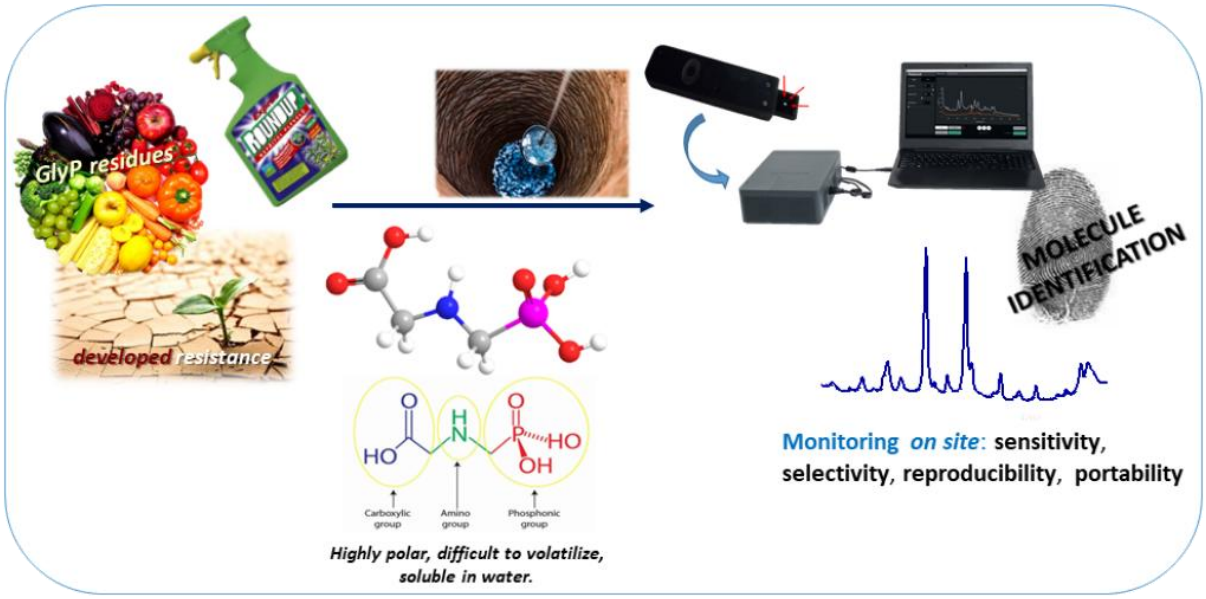

Fig. 1. Glyphosate is one of the most commonly-used and non-selective herbicides in agriculture, which may directly pollute the environment and threaten human health. It works by blocking an enzyme essential for plant growth. In the recent years, certified laboratories developed selective residue method for testing of glyphosate residues in water samples. However, the main drawback of this method is too high polarity of glyphosate. Raman spectroscopy technique is suitable for pesticide detection in aqueous solution. In addition, increased Raman signal acquired by employment of appropriate SERS substrates transforms Raman spectroscopy from a structural analytical method into a structurally sensitive nano-probe able to detect very low concentration of molecules down to the single-molecule level.

Since the 1980s, glyphosate residue determination has been and is still conducted by chromatographic methods combined with mass spectroscopy. However, these techniques are suffering from complex cleanup process and multiple derivative operation steps what results in an expensive and slow detection and quantification of glyphosate. In addition, glyphosate has no fluorescence group that can be detected by fluorescence detector. [1, 2] Raman spectroscopy as a technique of the *fingerprint* provides specific structural information at the level of molecules. On

the other hand, surface-enhanced Raman spectroscopy (SERS) can magnify molecular vibrations in a system and allows to detect even a single molecule. SERS technique consists of the Raman signal of a molecule in the proximity of a nanostructured noble metal surface that is enhanced by the enormous electromagnetic field concentrated in the interphase. This effect is related to localized plasmon resonances of the metal [5]. Therefore, definition of conditions and the development of technology for sensitive and selective SERS glyphosate detection, that would not be time-consuming and materially demanding and would be also feasible *on site*, represents a hot topic research project. Our aim is to develop methodology based on SERS technique for the sensitive and selective detection of glyphosate and to determine its detection limits.

Acknowledgement
This work is supported by the Scientific Grant Agencies of the Ministry of the Education of Slovak Republic (APVV-19-0580 and VEGA 1/0557/20). This work has also been financially supported by MINECO (Project FIS2017-84318-R).

References

[1] A. L. Valle, F. C. C. Mello, R. P. Alves-Balvedi, L.P. Rodrigues, L.R. Goulart, *Environ. Chem. Lett.* 17 (**2019**) 291-317.
[2] M. Xu, Y. Gao, Y. Li, X. Li, H. Zhang, X. X. Han, B. Zhao, L. Su. *Spectroschim. Acta A* 197 (**2018**) 78-82.
[3] K. Z. Guyton, D. Loomis, Y. Grosse et al. *Lancet. Oncol.* 16 (**2015**) 490-491.
[4] https://ec.europa.eu/food/plant/pesticides/glyphosate_en
[5] M. Moskovits, D. P. DiLellla, K. J. Maunard. *Langmuir* 4 (**1998**) 67-76.

The reactivity of the C-terminal anti-tau antibody shows differences possibly due to the changes in the global folds of tau isoforms

O. Cehlár[1,2], L. Horňáková[1,3], J. Šinský[1], J. Hanes[1,2] and R. Škrabana[1,2]

[1] *Institute of Neuroimmunology of Slovak Academy of Sciences, Dubravska cesta 9, 84510 Bratislava, Slovakia*
[2] *Axon Neuroscience R&D Services SE, Dvorakovo Nabrezie 10, 81102 Bratislava, Slovakia*
[3] *Department of Biochemistry, Faculty of Natural Sciences, Comenius University, Ilkovicova 6, 84215 Bratislava, Slovakia*
e-mail: ondrej.cehlar@savba.sk

Alzheimer's disease (AD) is the most common cause of dementia and thus a disease that radically reduces the quality of life not only for patient but also for the patient's family. An important role in the development and progression of this disease is played by the accumulation of two proteins, namely the tau protein and β-amyloid, caused by changes in their structures.

The structural insights into the pathological and physiological tau protein conformations may help to answer the key questions of the pathogenesis of AD and other tauopathies. All isoforms of tau protein consist of four main domains and differ according to number of N-terminal inserts (0N, 1N, 2N) and repetitive domains (3R, 4R). An important regulatory role is played by C-terminal domain which is believed to be responsible for inhibition of tau protein aggregation [1].

We have been studying the kinetics of the interaction of an antibody DC39C, which epitope lies inside the last 12 C-terminal amino acids of tau, with various tau proteins by surface plasmon resonance. According to recent insights in the structure of tau protein obtained by cross-linking guided discrete molecular dynamics, where tau molecule was modelled as a rather globular and compact [2], epitope for DC39C antibody should be hidden in between the beta strand of first N-terminal insert and N-terminus of tau protein (Fig. 1). Global conformation that was observed by FRET method supports that C-terminal domain is hidden between MTBR and N-terminal domain [3]. Our results had shown that isoforms without N-terminal inserts bind to DC39C antibody better than isoforms containing them; same results were obtained when truncated tau from N-terminal domain was used. To support our kinetic data and their link to the tau global folds, we have performed chemical crosslinking with mass spectrometry analysis.

Subsequently, we measured the kinetics of filament formation by fluorescence with ThT via heparin-induced aggregation to observe the effect of C-terminal domain removal on aggregation compared to the full length and truncated tau (151-391/ 3R) which causes Alzheimer´s like pathology in the rat model [4]. The shortest construct of tau protein (1-391/3R) indicated very rapid filament formation; slightly slower filament formation was observed when tau protein without C-terminal domain was used, and the slowest filament formation when isoform tau 39 (2N3R) was used. These findings also support the hypothesis of C-terminal domain inhibition of tau aggregation.

Fig. 1. Model of tau40 molecule (longest tau human CNS isoform-2N4R) obtained using short distance cross-linking guided discrete molecular dynamics simulations [2].

Acknowledgement
This work was supported by the Scientific Grant Agency of the Ministry of Education of the Slovak Republic (Grant No. 2/0145/19) and by the Slovak Research and Development Agency (Grant No. APVV-19-0531).

References

[1] Abraha, A., Ghoshal, N., Gamblin, T. C., Cryns, V., Berry, R. W., Kuret, J. & Binder, L. I., J Cell Sci 113, (2000), 3737-3745.
[2] Popov, K. I., Makepeace, K. A. T., Petrotchenko, E. V., Dokholyan, N. V. & Borchers, C. H., Structure 27, (2019), 1710-1715 e1714.
[3] Jeganathan, S., von Bergen, M., Brutlach, H., Steinhoff, H. J. & Mandelkow, E., Biochemistry-Us 45, (2006), 2283-2293.
[4] Filipcik, P., Zilka, N., Bugos, O., Kucerak, J., Koson, P., Novak, P. & Novak, M., Neurobiol Aging 33, (2012) 1448-1456.

Ultrafiltration and size-exclusion chromatography for the isolation of exosomes

D. Džubinská[1], M. Zvarík[1], Z. Garaiová[1], L. Šikurová[1], I. Waczulíková[1]

[1] *Department of Nuclear Physics and Biophysics, Faculty of Mathematics, Physics and Informatics of the Comenius University, Mlynská dolina F1, 842 48 Bratislava, Slovakia*
e-mail: dzubinska2@uniba.sk

Exosomes belong to the group of extracellular vesicles (EVs). These spherical membrane structures with a diameter of 30 - 150 nm are involved in many biological processes, predominantly in the intercellular communication. EVs encapsulate proteins, RNA, lipids and metabolites whose changes reflect the biological state of the body. They occur in blood, lymph fluid, urine, as well as malignant ascites [1]. Exosomes have been reported as being secreted by a wide range of cells, but cancer cells secrete at greater rates and amounts. Especially in the condition of bladder cancer, where cancer cells are in direct contact with urine, EVs released into the urine could be a specific source of biomarkers [2]. Likewise, EVs circulating in the blood come from various tissues and their isolation can provide information about the pathological process [3]. Thus, there is an immense potential for the use of EVs for biomarker detection in clinical settings [1]. Additionally, by removing the internal components of the isolated exosomes and following uptake of the dendrimer nanoparticles into exosomes to provide the hybrid nanoparticles, which can be used as vectors in therapy [6]. Interestingly, an appealing feature of EV-based biomarker analysis is the significant reduction in the sample complexity compared to whole body fluids [1]. Currently, several techniques based on physicochemical and biochemical properties of exosomes are used to aid isolation of exosomes. The currently ongoing experiments are focused on the technique of isolation of exosomes from urine and blood of patients with bladder cancer using ultrafiltration and size exclusion chromatography (SEC) [4,5]. The efficiency and quality of exosome isolation has been monitored by estimating the size and concentration of isolated exosomes. In order to detect biomarkers of bladder cancer, we have also focused on the metabolites encapsulated into the exosomal membrane and their subsequent HPLC analysis.

Acknowledgement
This work was supported by projects UK/256/2020, VEGA 01/0136/18 and NAWA EUROPARTNER PPI/APM/2018/1/00007/U/001.

References

[1] Boukouris, Mathivanan, Proteomics Clin Appl. 9(3-4). (2015) 358–367pp.
[2] Murakami et al., Oncotarget, (2018) 9, 32810–32821pp.
[3] Properzi F, Logozzi M, Fais S., Biomark Med.7 (2013) 769–778.
[4] Gheinani et al., Sci Rep; 8 (2018) 3945
[5] Theodoraki et al., Clin Exp Immunol.194, (2018) 67-78.
[6] Hong et al., United States Wisconsin Alumni Research Foundation (Madison, Wi, Us) Pub. No:20180369410 (2018)

Recombinant expression, purification and biophysical characterization of the λ-type IgG light chain

V. Džupponová[1], G. Žoldák[2]

[1] *Department of Biophysics, Faculty of Science, PavolJozefŠafárik University, Jesenná 5, 040 01 Košice, Slovakia*

[2]*Center for Interdisciplinary Biosciences, Technology and Innovation Park, Pavol Jozef Šafárik University, Jesenná 5, 041 54 Košice, Slovakia*

e-mail: veronika.dzupponova@student.upjs.sk

Light chain is part of IgG which consists of variable (V-domain) and constant domain (C-domain). The structure of both domains is composed of ca. 9 β – strands, which are assembled into compact typical immunoglobulin fold structure and covalently linked by a disulphide bond [1]. While sequence of C-domains is highly conserved, V-domains contain at certain positions hypervariable sequences, so-called CDRs (acronym of Complementarity Determining Regions). Because of their large sequence variability in CDRs, V- domains can have an increased tendency to form amyloid fibrils and aggregates. If light chain expression is dysregulated, high aggregation propensity of V-domainscan lead to severe pathologies such as amyloidosis and multiple myeloma [2].

Multiple myeloma (MM) is the second most common haematological malignancy, manifested by uncontrolled proliferation and accumulation of damaged plasma cells in the bone marrow. As a result of genetic dysregulation of heavy chain of immunoglobulin G (IgG) production, myelomatic plasma cells produce in very high concentration of light chain of IgG (LC) which is subsequently secreted into the bloodstream. From the blood circulation, LC is gradually captured in organs important for life, such as heart, kidney and liver, where due to the low colloidal stability of the LC it forms aggregates and at the final stage it forms the microscopic fibrils or amyloid deposits (for amyloidosis) [2, 3].

Understanding the molecular nature of protein aggregation and the effect of the physicochemical environment that accelerates the conversion of functional forms of proteins into pathogenic aggregates is a key to discovering the reasons for the high morbidity of these leukemic diseases and consequently the rational development of drugs that inhibit the formation of toxic aggregates [4].

For a first time in our laboratory, we have obtained highly pure recombinant human λ-type light chain. After controlled cytoplasmic expression of the protein in *E.coli*, we found that recombinant light chain protein accumulates exclusively in inclusion bodies. Following several purification steps, including oxidative refolding in the presence of GSH/GSSG shuffle, Q-sepharoseanion exchange chromatography, size-exclusion gel chromatography, the protein shows a single band on SDS/PAGE gel under reducing conditions. Circular dichroism in far UV region and differential scanning calorimetry have confirmed that the protein is correctly folded. The yield is 7.5 mg of the light chain protein per 1 L of bacterial culture.

Having a pure protein in our hands, we have now started excessive biophysical characterization Specifically, our goal is to understand mechanistic questions of the relation between conformational and colloidal stability.

Firstly, the colloidal stability of proteins is connected with solubility of proteins in native, partially unfolded or unfolded state. Molecular mechanism of colloidal stability involves two seemingly unrelated factors – the strength of the protein-protein interaction as well as the contribution of conformational stability that controls the integrity of the native protein. Low conformational stability can lead to partial unfolding that exposes portions of the protein with a tendency to aggregation [5]. Secondly, the conformational stability of proteins involves both – equilibrium and non-equilibrium folding/unfolding steps. In the case of multi-domain proteins, the unfolding mechanism can be more complex and hence *ad hoc*models have to be developed [6].

Acknowledgement
This work was supported by the research grants from the Slovak Grant Agency VEGA No 1/0175/19 and by the Slovak Research and Development Agency under the Contract no. APVV-18-0285.

References

[1] Branden C. and Tooze J. (1999) Introduction to protein structure, *Garland Publishing*, Inc., New York, 2nd ed.
[2] Blancas-Mejia L. M., Misra P., Dick C. J., Cooper S. A., Redhage K. R., Bergman M. R., Jordan T. L., Maar K., Ramirez-Alvarado M. (2018). Immunoglobulin light chain amyloid aggregation. *Chemical Communications.* 54, 10664-10674.
[3] Andrich K., Hegenbart U., Kimmich C., Kedia N., Bergen H. R., Schönland S., Wanker E., Bieschke J. (2016). Aggregation of Full-length Immunoglobulin Light Chains from Systemic Light Chain Amyloidosis (AL) Patients Is Remodeled by Epigallocatechin-3-gallate. *Journal of Biological Chemistry.* 292(6), 2328–2344.
[4] Xue W.-F., Homans S. W., Radford S. E. (2008). Systematic analysis of nucleation-dependent polymerization reveals new insights into the mechanism of amyloid self-assembly. *Proceedings of the National Academy of Sciences.* 105(26), 8926–8931.
[5] Ratanji K.D., Derrick J.P., Dearman R.J., Kimber I. (2014) Immunogenicity of therapeutic proteins: influence of aggregation. *J Immunotoxicol.* 11(2), 99-109.
[6] Nemergut M., Žoldák G., Schaefer J.V., Kast F., Miškovský P., Sedlák E. (2017) Analysis of IgG kinetic stability by differential scanning calorimetry, probe fluorescence and light scattering. *Protein Science.* 26(11), 2229-2239.

Ribosome display as a tool for directed evolution of haloalkane dehalogenases

V. Dzurillová[1], E. Sedlák[2]

[1]*Department of Biophysics, Faculty of Science, P.J. Šafárik University, Jesenná 5, 041 54 Košice, Slovakia*
[2]*Center for Interdisciplinary Biosciences, Technology and Innovation Park, P.J. Šafárik University, Jesenná 5, 041 54 Košice, Slovakia*
e-mail: veronika.dzurillova@student.upjs.sk

Haloalkane dehalogenases are microbial enzymes able to cleave carbon-halogen bonds in halogenated compounds yielding primary alcohol, halide ion and a proton. In addition, they act on prominent environmental pollutants in the process of dehalogenation, which has also a great value for biotechnology [1]. Nevertheless, further extension of these enzymes into practical applications is accompanied by obstacles such as low catalytic activity, stability, as well as product inhibition and insufficient enzyme selectivity. To overcome these limitations, protein engineering through directed evolution represents promising strategy.

Our study aims to investigate utilization of ribosome display in development of haloalkane dehalogenases for industrial applications. Ribosome display is powerful *in vitro* evolution technique used to select proteins from large libraries in order to improve desire protein property, such as affinity, stability or specificity. The main advantage of this method is its unique robustness. In fact, in one selection round we are able to screen for enriched mutants within sequence space up to 10^{12} variants. Selection criterion is usually binding against immobilized ligand [2].

Experimental set up for utilization of ribosome display, directed evolution approach in general, to engineer haloalkane dehalogenases with improved properties, consists of three basic steps: (i) creation of the library, (ii) selection step and (iii) characterization of the selected variants. There are several available strategies to generate directed evolution libraries ranging from point mutagenesis through gene recombination or shuffling, to different computational tools dedicated to designing DNA/protein libraries [3]. We chose the PCR-based method using mutagenic nucleotide analogs 8-oxo-GTP and dPTP and created initial library of DhaA variant H272F with mutational frequency 5 mutations per gene on average. This library was subsequently adopted to consecutive rounds of ribosome display during which mutant enzymes were selected against immobilized biotinylated chloroalkane. Capturing of the enzymes in selection step was mediated through formation of covalent bond between displayed enzyme and immobilized ligand[Fig.1] when in case of H272F only first part of the reaction takes place and proteins stayed captured [4]. As we were able to see positively evolving trend towards improved binders, this approach suggests the feasibility using ribosome display in evolution-directed engineering of haloalkane dehalogenases.

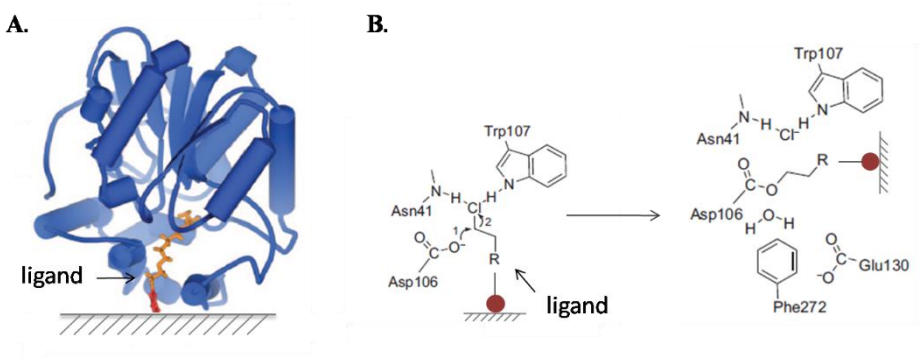

Fig. 1. A. Immobilization of mutant enzyme DhaA through biotinylated chloroalkane. B. Formation of covalent bond between chloroalkaneand Asp106 inside the catalytic site of DhaA H272F. Taken from Los, G.V. *et al.* [4].

Acknowledgement
We would like to express our thanks to prof. JiříDamborský for providing us plasmids carrying haloalkane dehalogenase genes. This work was supported by research grant provided by Slovak Research and Development Agency under the contract No. APVV-15-0069.

References

[1] Koudelakova, T., *et al*. Haloalkane dehalogenases: biotechnological applications. *Biotechnology Journal*, 2013, 8.1: 32-45.

[2] Plückthun, A. Ribosome display: a perspective. In: *Ribosome display and related technologies*. Springer, New York, NY, 2012. p. 3-28.

[3] Gillam, E. MJ; Copp, J. N.; Ackerley, D. F. Directed evolution library creation. *Methods in Molecular Biology* (*Totowa, USA: Humana Press*), 2014.

[4] Los, G.V., *et al*. HaloTag: a novel protein labeling technology for cell imaging and protein analysis. *ACS chemical biology*, 2008, 3.6: 373-382.

Polyphenols and metal (iron, copper) ion complexation characterized by optical (UV-Vis and Raman) spectroscopy

A. Espina[1], S. Sanchez-Cortes[2], Z. Jurašeková[1]

[1] *Department of Biophysics, Faculty of Science, P. J. Šafárik University, Jesenná 5, 040 01 Košice, Slovakia*
[2] *Institute of the Structure of Matter,IEM-CSIC, Serrano 121, 280 06 Madrid, Spain*
e-mail: zuzana.jurasekova@upjs.sk

Iron gall inks (IGIs) were probably the most important writing and drawing materials used from the Antiquity as well in the Middle Ages and even until to the modern times [1]. The frequent use of this type of ink is due to its simple preparation, good quality of the written records, their indelibility as well as no-clogging of writing pens and brushes [2]. Nevertheless, during the 20th century, they were progressively replaced by modern writing media based on synthetic dyes and colorants which do not show corrosive properties [3, 4]. In any case, a significant part of the human historical and cultural heritage found, exhibited and stored in libraries, archives, museums, galleries, *etc.* all over the world were recorded/made with the IGIs [4, 5]. Despite their historical importance and a huge number of studies dedicated to IGIs, there is only a little consensus on the chemical structure or composition of these complex compounds.

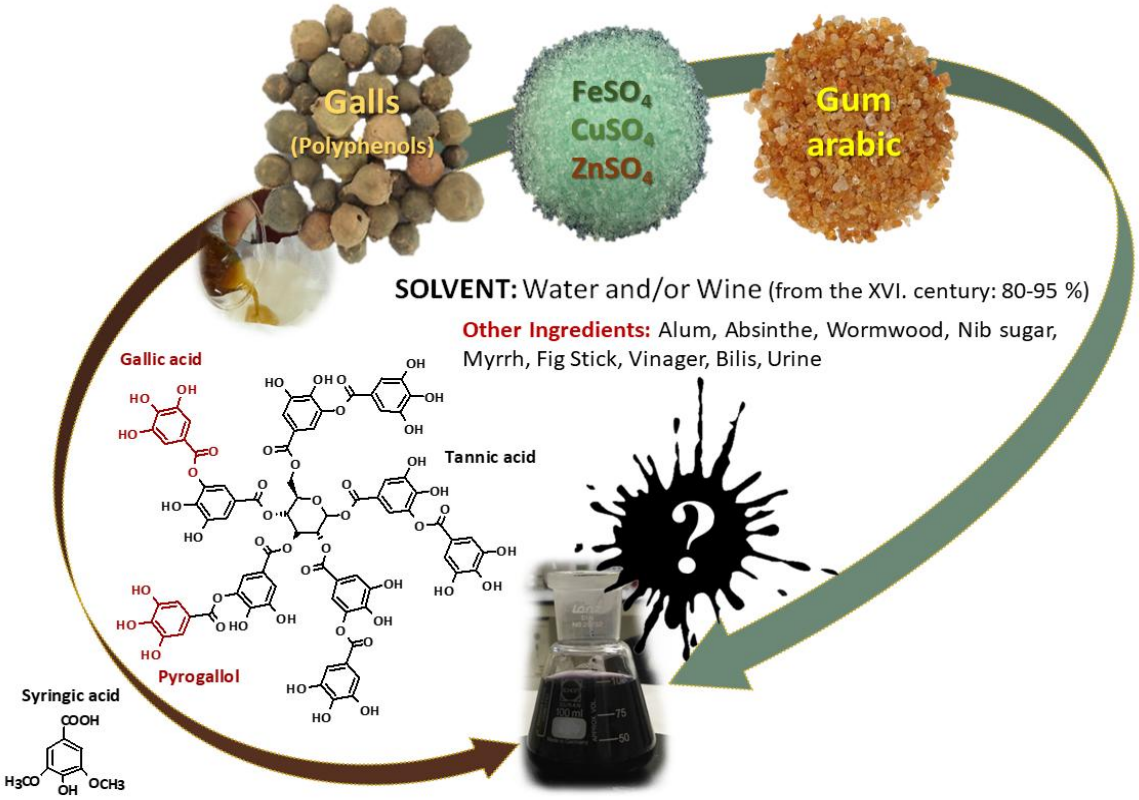

Figure 1. Main ingredients in the production of iron-gall ink. Formula structures of the studied (poly)phenol compounds.

Historical IGIs recipes typically consist of three or four basic ingredients: tannins, ferrous sulfates, Arabic gum and liquid medium [6, 7]. Hydrolyzable tannins are derivatives of the gallic acid and their function in the IGIs depends on their chelation properties to bind metal ions, especially iron ions. To analyze such complex systems, it is important to do an identification and characterization of their individual components. In addition, development of an appropriate analytical method is also an important task. That is why we focused during our research project on

studying complex formation of gallic acid and other structurally related (poly)phenolic – model – compounds (Pyrogallol, Syringic acid, Tannic acid) with iron and copper ions by means of optical spectroscopy, mainly by Raman and SERS techniques. Spectroscopy results confirmed the known fact that tannins possessing catechol or pyrogallol residues are excellent chelators of various metal ions. Besides, the effect of pH seems to be a crucial parameter in the preparation, use and degradation of IGIs deposited on different paper-based supports. In particular, the degree of polymerization processes and formation of new species followed by the interaction of phenolic compounds with metal ions are closely related with the pH variations. Therefore, this basic research is important not only to understand reaction mechanisms and kinetics of such complexes, but also to investigate IGIs present in *mock-up* samples and to detect them in different artifacts. Last but not least, to study tannins interaction with metal ions is also important regarding their antioxidant properties and corresponding biological consequences.

Acknowledgement
This work is supported by the Scientific Grant Agency of the Ministry of the Education of Slovak Republic (APVV-19-0580) and by the grant of Faculty of Science, P. J. Šafárik University in Košice (VVGS-PF-2020-1432). This work has also been financially supported by MINECO (Project FIS2017-84318-R).

References

[1] A. S. Lee et al. *Vib. Spectrosc.* 41 (**2006**) 170–175.
[2] E. Mert. A comparative study on chemical characterization of different ink ingredients used in ancient ornamented manuscripts, *Thesis*, Middle East Technical University, **2008**.
[3] M. Ďurovič a kol. Restaurování a konzervování archiválií a kníh, Paseka, Praha; Litomyšl (**2002**).
[4] L. Gál a kol. *Chem. List.* 108 (**2014**) 191-197.
[5] J. Kolar et al. *Anal. Chim. Acta* 555(**2006**) 167–174.
[6] J. Kolar, M. Strlic, M. *Iron Gall Inks: On Manufacture, Characterisation, Degradation and Stabilisation.* National and University Library, ISBN: 9789616551199, pgs. 253 (**2006**).
[7] B. Kanngießer et al. *Spectrochim. Acta Part B* 59 (**2004**) 1511–1516.
[8] M. Karamać. *Int. J. Mol. Sci.* 10 (**2009**) 5485-5497.

The cardiac ryanodine receptor provides an effective pathway for Zn^{2+} transport in cardiomyocytes

J. Gaburjakova[1] and M. Gaburjakova[1]

[1] *Institute of Molecular Physiology and Genetics, Centre of Biosciences, Slovak Academy of Sciences, Dubravska cesta 9, 840 05 Bratislava, Slovakia*
e-mail: jana.gaburjakova@savba.sk

Activation of a contractile apparatus essential for cardiomyocyte contraction requires Ca^{2+} release from the sarcoplasmic reticulum (SR) into the cytoplasm. Ca^{2+} ions are released through the cardiac ryanodine receptor (RYR2) that functions as a Ca^{2+} channel embedded in the SR membrane. Using a synchrotron X-ray induced fluorescence technique, it has been proposed that in cardiomyocyte additional physiological relevant divalent, Zn^{2+}, is buffered in intracellular structures highly consistent with the SR [1]. Zn^{2+} is essential for many cellular functions having a catalytic, structural or signaling function. Two families of Zn^{2+} transporters have been identified in membrane of the SR, namely ZIP and ZnT. Since the RYR2 channel is able to conduct in addition to Ca^{2+} also other divalents such as Ba^{2+}, Sr^{2+} or Mg^{2+}, we were interested whether the RYR2 channel with conductive pathway appropriately accommodated for various divalents could also function as an effective pathway for Zn^{2+} transport in cardiomyocytes.

Our aim was to investigate whether Zn^{2+} could permeate through the conductive pore of the RYR2 channel employing electrophysiological methods. RYR2 enriched microsomes were isolated from adult rat hearts by differential centrifugation and subsequently incorporated into the BLM, which mimics the native membrane environment by appropriate lipid composition. As a source of Zn^{2+} ions, we used $ZnCl_2$ with acceptable solubility at physiological pH of 7.35. Since we have not succeeded to record any activity of the RYR2 channel in the BLM using solely Zn^{2+} gradient as a driving force, we had to search for an alternative experimental approach. We considered detection of changes in reversal membrane potential U_m when manipulating concentration ratio of Ca^{2+} and Zn^{2+} on the luminal face of the RYR2 channel as a promising way. The permeability coefficient for Zn^{2+} was estimated by the theoretical equation of the total ionic current considering only positive ionic species (Ca^{2+}, Zn^{2+}, K^+, and $Tris^+$) present in experimental solutions.

From our experimental results, we could conclude that Zn^{2+} indeed permeates through the RYR2 channel and its permeability coefficient is three times lower than for Ca^{2+}. Because the RYR2 channel exhibits almost identical permeation characteristics for Mg^{2+} and Ca^{2+}, it is obvious that Zn^{2+} is less permeable through the RYR2 channel also in comparison to Mg^{2+}. This is interesting because Mg^{2+} and Zn^{2+} possess comparable charge density and similar ionic radius. The physiological relevance of our finding might be related to the presence of a specific protein structural motif - zinc finger- within the RYR2 channel. Recently identified zinc finger (type Cys_2His_2) is localized in the connection between the prolonged S6 transmembrane segment and the C-terminal domain. This connection is rigidified by Zn^{2+} coordinated by residues Cys-4874, Cys-4877, His-4894 and His-4899 (rat RYR2 numbering) [2] and it seems that mentioned rigidity is critical for RYR2 gating [3]. We assume that even small Zn^{2+} release from the SR, driven by a Zn^{2+} gradient, during each opening of the RYR2 channel might positively contribute to a stable Zn^{2+}environment around the zinc finger motif, and thus ensuring appropriate RYR2 gating.

Acknowledgement
This work was supported by the Slovak Scientific Grant Agency (VEGA 2/0011/18 and VEGA 2/0008/20) and EU Structural Fund (ITMS 26230120009).

References

[1] B. M. Palmer, S.Vogt, Z. Chen, R. R. Lachapelle, and M. M. LeWinter, J. Struct. Biol. 155 (2006), 12-21.
[2] K. Willegems, and R. Efremov, Adv. Exp. Med. Biol. 981 (2017), 179-204.
[3] W. Peng, H. Shen, J. Wu, W. Guo, X. Pan, R. Wang, S. R. Wayne Chen, and N. Yan, Science 354 (2016), aah5324-1-10.

Sequence-structure analysis of bacterial heat shock proteins 70

M. Gala[1], P. Pristáš[1] and G. Žoldák[2]

[1]*Institute of Biology and Ecology, Faculty of Science, P. J. Šafárik University, Košice, Slovakia*
[2]*Center for Interdisciplinary Biosciences, Technology and Innovation Park P. J. Šafárik University, Košice, Slovakia*
e-mail: Michal.Gala@student.upjs

Heat shock proteins 70 (Hsp70) are ubiquitous ATP-dependent chaperones (folding helpers) existing in all kingdoms of life. Structurally, canonical Hsp70 consists of two folded domains and C-terminal intrinsically disordered part. A nucleotide binding domain (NBD) binds ATP. A substrate binding domain (SBD) binds protein clients, and the binding affinity depends on ATP/ADP status of the NBD. The function of the C-terminal disordered part is less understood.

In the ATP-bound state, the SBD undergoes a conformational change which leads to the opening of the binding cleft and subsequently to the decrease in the binding affinity for a client. During the functional cycle of this chaperone, the ATP is hydrolyzed, which is used to drive conformational changes. After the ATP hydrolysis, structural rearrangements in the NBD domain trigger the closure of the SBD's binding pocket. The closure of the binding pocket leads to the capture of a client protein. In the SBD closed state, the client dissociates very slowly, and hence, the SBD closed state has a higher affinity to the client protein. Under *in vivo* conditions, ATP/ADP is controlled by the ATP levels and by the action of nucleotide-exchange factors (GrpE in *E. coli*) and other cochaperones (DnaJ). Co-chaperones regulate the ATP-ADP cycle of Hsp70 at different checkpoints.

The Hsp70 chaperone system from *E.coli* called DnaK have been identified as the first Hsp70 chaperone and it has been studied intensively. In addition, DnaK 3D structure has been solved using hybrid approach combining NMR spectroscopy and crystal structure determination. While the 3D structure offers valuable insights into a spatial localization of individual amino acids, the question how this complex nanomachine works have remained elusive. Recently, single-molecule force spectroscopy Hsp70 provided information on the mechanics of the domains [1-3] . These studies pointed out a strong interplay between mechanical vulnerable/stable regions in Hsp70 domains. Here we asked how such mechanical constraints are affected during the evolution of Hsp70. In particular, insertions/deletions can be highly disrupted for the mechanical interplay since such changes introduce a large shift in the register of the interactions.

To analyze the evolution of Hsp70s, we collected 244 sequences of Hsp70 from 12 bacterial phyla. In our collection, we included Hsp70 from recently sequenced extremophiles as well as clinically important bacterial species, and we performed multiple sequence alignment using MUSCLE algorithm [4] as implemented in MEGA-X [5]. In the collection of our sequences, the pairwise sequence identity is distributed around the median of ca. 56% with a standard deviation of ± 10%. Multiple sequence alignment was further processed and analyzed with the focus on: conserved residues/motifs, sequence variability, insertion/deletion (indel) occurrence and differences in selected attributes (e.g. amino acid composition or number of indels) between sequences of extremophilic and non-extremophilic bacteria. We found 109 conserved residues (>99.2% conserved). The NBD has 21.1 % conserved positions while the SBD has 12.4 % and, as expected, the C-terminus does not have any conserved position. Remarkable, two relatively long contiguous conserved sequence motifs located at the N-terminus (6-14, DnaK *E.coli* numbering) and at the NBD lobe-lobe interface (194-201, DnaK *E.coli* numbering). Interestingly, the bilobal NBD structure is a result of a gene duplication event and conserved stretches are located at N-

terminal part of both lobes [6]. Consistently, Wu-Kabat variability analysis showed that SBD and the C-terminal part are significantly more variable as compared to the NBD. The analysis of the indel incidents in Hsp70 shows that the large part of the SBD structure (431-595 residues) does not contain any indels. Given the gap positional frequency (ca. 30%) in the Hsp70 alignment, such indel-free region is highly unusual (of order 10^{-26}). We speculate that the absence of the indels in this region is the consequence of requirements for precise structural/geometrical mechanics of domains during Hsp70 allostery and hence insertion/deletion in the SBD domain can cause loss-of-function of such precisely balanced molecular machine.

Acknowledgement
This work was supported by the research grants from the Slovak Grant Agency VEGA No 1/0175/19 and by the Slovak Research and Development Agency under the Contract no. APVV-18-0285.

References

[1] S. S. Mandal, D. R. Merz, M. Buchsteiner, R. I. Dima, M. Rief and G. Žoldák, PNAS 114 (2017), 6040-6045.
[2] D. Bauer, D. R. Merz, B. Pelz, K. E. Theisen, G. Yacyshyn, D. Mokranjac, R. I. Dima, M. Rief, and G. Žoldák, PNAS 112 (2015), 10389-10394.
[3] S. Meinhold, D. Bauer, J. Huber, U. Merkel, A. Weißl, G. Žoldák and M. Rief, Biochemistry 58 (2019), 4744-4750.
[4] R.C. Edgar, Nucleic Acids Res. 32 (2004), 1792-1797.
[5] S. Kumar, G. Stecher, M. Li, C. Knyaz and K. Tamura, Mol. Biol. Evol. 35 (2018), 1547-1549.
[6] P. Bork, Ch. Sander and A. Valencia, PNAS 89 (1992), 7290-7294.

Amyloid aggregation of insulin: An interaction study of selected green tea constituents

Miroslav Gancar[1], Elena Kurin[2,*], Zuzana Bednarikova[1], Jozef Marek[1], Pavel Mucaji[2], Milan Nagy[2], Zuzana Gazova[1,*]

[1]Department of Biophysics, Institute of Experimental Physics Slovak Academy of Sciences, Watsonova 47, 040 01, Kosice, Slovakia
[2]Department of Pharmacognosy and Botany, Faculty of Pharmacy, Comenius University in Bratislava, Odbojarov 10, 832 32, Bratislava, Slovakia
e-mail: gazova@saske.sk

Exogenous insulin, used as a therapeutic agent for diabetes, forms insoluble deposits containing amyloid fibrillar structures in proximity of the administration site. We analysed the *in vitro* anti-amyloid activity of four green tea constituents: (-)-epigallocatechin gallate (EGCG), (-)-epicatechin (EC), gallic acid (GA) and caffeine (CF), and their equimolar mixtures. Regarding individually tested compounds, only EGCG inhibited the amyloid fibrillization of insulin. Molecular docking revealed that EGCG interacts with an essential amyloidogenic region of insulin chain B (Fig. 1). The individual EC, GA and CF molecules were ineffective. The presence of EGCG in equimolar binary – quaternary mixtures in combination with GA, EC, and/or CF was required for the inhibitory activity of most mixtures. Interestingly, individually inactive GA had a potentiating effect on the activity of EGCG in mixtures while EC and CF had a negative effect. We observed different amount of insulin amyloid aggregates the formed in the presence of studied green tea constituents and their mixtures. Moreover, the diverse morphology of aggregates indicates distinct types of aggregates. Results indicate that the biological activity of individual molecules is not directly applicable to the pooled samples effects prediction.

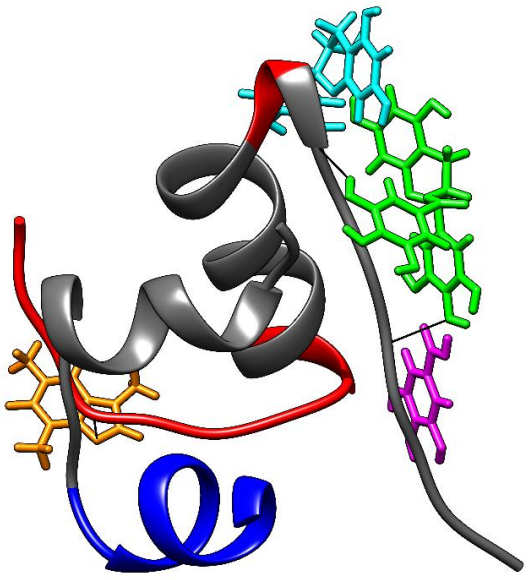

Fig. 1. Structure of human insulin at pH 1.9 (PDB ID: 2MVC) and best docking poses for studied compounds (GA - magenta; EGCG - green; EC - turquoise; CF - ochre) Calculated amyloidogenic regions are colored in grey.

Acknowledgement
This work was supported by VEGA grants 1/0359/18, 1/0290/16, 2/0145/17, APVV-18-0284 and ITMS 26210120012.

Liposomal locked-in dendrimers for development of cytostatic drugs

Z. Garaiová[1] , V. Šubjaková[1], J. Magiera[2], M. Holota[2], Š. Šutý[1], M. Ionov[2], S. Michlewska[2], I. Waczulikova[1], N. Sanz-del Olmo[3], F. Javier de la Mata[3], M. Bryszewska[2], T. Hianik[1]

[1]Faculty of Mathematics, Physics and Informatics, Comenius University, Bratislava, Slovakia
[2]Department of General Biophysics,Faculty of Biology and Environmental Protection, University of Lodz, Lodz, Poland
[3]Department of Organic and Inorganic Chemistry, and Research Institute in Chemistry "Andrés M. Del Río" (IQAR), University of Alcalá, Madrid,Spain. Networking Research Centre on Bioengineering, Biomaterials and Nanomedicine (CIBER-BBN), Spain. Instituto de Investigación Sanitaria Ramóny Cajal, IRYCIS
e-mail: garaiova.zuzana7@gmail.com

Hyperbranched dendritic polymers and liposomes have been intensively studied individually with promising results towards their potential use as drug carriers. This work focuses on the combination of liposomal and dendrimer technology for the development of a binary system, suitable for delivery of cytostatic drugs, which could potentially overcome deficiencies present in each individual group; thus, enable more efficient and safer chemotherapy.

We used fluorescently labeled carbosilane dendrimers FITC-CRD_{13} based on ruthenium that possess several unique anticancer properties [1]. Liposomes were prepared by hydration method using zwitterionic 1,2-dimyristoyl-sn-glycero-3-phosphocholine (DMPC). Locking dendrimers into the DMPC liposomes was performed by introducing FITC-CRD_{13} into the step of 1) dissolving lipids in organic solvent; 2) lipid film hydration. The samples were analyzed by transmission electron microscopy and fluorescent confocal microscopy. The microscopic images indicated the presence of dendrimers in the multilamellar liposomal structures forming vesicles of several micrometers. Size reduction of liposomes and their purification from unlocked dendrimers was performed by extrusion through 400nm polycarbonate membranes followed by several centrifugation steps. Preliminary results from the hemotoxicity assay show the concentration dependent hemolytic activity of dendrimers in concentration range of 0.5 μM – 5 μM, which seems to be reduced while being locked in liposomes.

Acknowledgement
This work was supported by the Slovak Research and Development Agency, APVV (Projects No. SK-PL-18-0080 and APVV-14-0267, SK-BY-RD-19-0019), VEGA 1/0756/20, COST CA17140 and Polish National Agency for Academic Exchange, NAWA (Pl-SK 2019–2020, Project No. PPN/BIL/2018/1/00150), by Polish Ministry of Science and Higher Education together with joint project EUROPARTNER: Strengthening and spreading international partnership activities of the Faculty of Biology and Environmental Protection for interdisciplinary research and innovation of the University of Lodz, which is financed by NAWA International Academic Partnership Programme. Authors also thanks funding by grants from CTQ2017-86224-P (MINECO), and SBPLY/17/180501/000358 Junta de Comunidades de Castilla-la Mancha (JCCM). CIBER-BBN is an initiative funded by the VI National R&D&i Plan 2008-2011, Iniciativa Ingenio 2010, the Consolider Program, and CIBER Actions and financed by the Instituto de Salud Carlos III with assistance from the European Regional Development Fund.

References

[1] S. Michlewska, M. Kubczak, M. Maroto-Díaz, N. Sanz del Olmo, P. Ortega, D. Shcharbin, R. Gomez Ramirez, F. Javier de la Mata, M. Ionov, M. Bryszewska, Biomolecules 2019, 9,411; doi:10.3390/biom9090411.

The polyphenol rottlerin: assessment of disassembly activity of protein aggregates and cytotoxicity

[A]I. Garcarova, [A] K. Siposova, [B] V. Huntosova, [A] A. Musatov

[a]Department of Biophysics, Institute of Experimental Physics, Slovak Academy of Sciences, Kosice, Slovakia
[a]Center for Interdisciplinary Biosciences, Technology and Innovation Park, P.J. Safarik University in Kosice, Kosice, Slovakia

Amyloid fibrils formed by normally soluble proteins, that assemble to form insoluble fibers, resistant to degradation are characteristic feature of many neurodegenerative and non-neuropathic amyloid-related diseases [1]. Over the last decades, there has been increased interest in the investigation of therapeutic potential of naturally occurring compounds, such as polyphenols. However, polyphenols are very abundant in nature and extremely diverse. Given their great heterogeneity, it is difficultto predicta structure-activity relationship, and a more appropriate approach is to combine a theoretical and experimental analysisto reveal their biological effects and the associated signal-transduction pathways [2].

In the present work, the anti-amyloid potential of polyphenolrottlerin was assessed on different proteins prone to aggregation, namely insulin, lysozyme, α-lactalbumin and β-lactoglobulin. Two different experimental approaches have been applied. First, the disassemblycapability of rottlerin was evaluated by addition of rottlerin to already pre-formed fibrils. Second, confocal fluorescence microscopy and cell viability assay were performed in order to assess the cytotoxicity of rottlerin. The efficiency of rottlerinto disassemble of pre-formed fibrils was found to be a time- and dose-dependent. The apparent DC_{50} values in the range from ~15 μM to ~30 μM suggest significant effectof rottlerin on the disaggregationprocess. In addition to ThT fluorescence assay kinetic studies the efficiency of rottlerin was confirmed by visualization of fibrils by atomic force microscopy. Especially significant was the finding that rottlerin possesses very strong and rapid ability to disassemble pre-formed fibrils. The disassembling effect of rottlerin was achieved during the first 5 min of incubation of rottlerin with pre-formed fibrils.

Cell viability was measured by MTT assay, performed on glioblastoma astrocytoma cells (U87MG) exposed to: i) intact amyloid fibrils (10 μM), ii) fibrils (10 μM) in the presence of rottlerin at molar ratios 1:1 and 1:0.5(fibrils to rottlerin)without previous incubation,and iii) mixture of fibrils (10 μM) pre-incubated with rottlerin for 24 hours at molar ratios 1:1 and 1:0.5(fibrils to rottlerin). While rottlerin did not induce significant changes detected by absorption as compared to control, cells treated with 10 μM amyloid fibril showed significantly reduced formazan production. However, viability of cells incubated in the presence of amyloid fibrils was improved after adding of rottlerin. Moreover, better cells survival was observed when treated with mixture of fibrils pre-incubated with rottlerin.Our *in vitro* studies indicate that the polyphenolrottlerin can be used for the rational design of potential therapeutics for amyloidogenesis and chemical modifications on rottlerin could be tested in the future as a promising strategy for the modulation of amyloidogenic proteins aggregation.

Acknowledgement
This work was supported by grants: VEGA No. 2/0009/17, 1/0156/18 andAPVV-15-453.

References:
[1] Stefani J., Dobson, C.M. (2003) *J. Mol. Med. (Berl.)*, **81:** 678-99
[2] Maioli E.*et al.* (2012) *Ann. N. Y. Acad. Sci.***1259**: 65-76

^{19}F labelling of 14-3-3ζ recombinant protein for ^{19}F NMR spectroscopy

Norbert Gašparik*, Aneta Kozeleková, Petr Louša, Jozef Hritz*

Central European Institute of Technology, Masaryk University, Kamenice 5, 625 00 Brno, Czech Republic
e-mail: norbert.gasparik@ceitec.muni.cz, jozef.hritz@ceitec.muni.cz

^{19}F NMR has been a very useful complementary approach to traditional NMR techniques - double labelling by ^{13}C and ^{15}N, especially due to the excellent magnetic properties of the ^{19}F isotope. 1) It has a spin ½ and strong dipolar coupling (useful in NOESY), 2) High sensitivity (83% relative to ^{1}H) and broad chemical shift range (up to 400 ppm), 3) ^{19}F is 100% abundant in nature and virtually non-present in biologically relevant samples [1-3]. Selective ^{19}F isotopic labelling is therefore an outstanding technique for monitoring region-specific changes in protein structure thanks to minimal background signal [4,5].

Here, we present our progress in the preparation of protein samples for ^{19}F NMR measurements, labelled with ^{19}F modified aromatic amino acids (AAs): 5-^{19}F-Trp, 4-^{19}F-Phe, and 3-^{19}F-Tyr. Distinct AAs had different incorporation efficiency rates, even though we used identical protocols. ^{19}F tryptophan was readily incorporated with 100% efficiency. However, the extent of ^{19}F phenylalanine and ^{19}F tyrosine incorporation ranged between 50-90%, presumably due to the similar biosynthetic pathways or non-optimal culture conditions. On the other hand, the amount and purity of samples was sufficient for pilot experiments, as demonstrated by well-resolved 1D ^{19}F NMR spectra.

Acknowledgement
This work was supported by the Ministry of Education, Youth and Sports of the Czech Republic within programme INTER-ACTION (project no. LTAUSA18168). This work has received funding from Czech Science Foundation, project no. 20-05789L. This research has been financially supported by the Grant Agency of Masaryk University, project MUNI/C/1562/2019. CIISB research infrastructure project LM2018127 funded by MEYS CR is gratefully acknowledged for the financial support of the measurements at the Josef Dadok National NMR Centre, Biomolecular interactions and crystallization and Proteomics Core Facilities.

References

[1] C. Frieden, S. D. Hoeltzli, J. G. Bann. *Methods Enzymol*. **380**, 2004, pp. 400-415.
[2] J. C. Jackson, J. T. Hammill, R. A. Mehl, *J. Am. Chem. Soc.* **129,** 2007, pp. 1160-1166.
[3] E. N. G. Marsh, Y. Suzuki, *ACS Chem. Biol*. **9**, 2014, pp. 1242-1250.
[4] J. G. Bann, J. Pinkner, S. J. Hultgren, C. Frieden. *PNAS* **99(2)**, 2002, pp. 709-714.
[5] C. Li, E. A. Lutz, K. M. Slade, R. A. S. Ruf, G-F. Wang, G. J. Pielak. *Biochemistry* **48**, 2009, pp. 8578-8584.

Time-resolved measurements of oxygenation and oxidative stress level in cancer spheroids

V. Huntošová[1], R. Seliga[1] and D. Horváth[1]

[1] *Center for Interdisciplinary Biosciences, Technology and innovation park, P. J. Safarik University in Kosice*
Jesenna 5, 041 54 Kosice, Slovakia
e-mail: veronika.huntosova@upjs.sk

Irregularities in oxygen supply and oxygenation of the tissue often reflect the injury and malformations of the tissue [1]. Low oxygenated tissues are often found in cancer. The efficacy of anticancer treatment depends on the level of cancer tissue oxygenation. Fluorescence microscopy represents the imaging method by which the molecular probes sensitive to oxygenation and oxidative stress can be identified within the living cells. However, fluorescence intensity-based techniques have limitations when detecting the molecular probes at low concentrations and in the presence of their quenchers (molecular oxygen and reactive oxygen species - ROS). For this reason, we have applied fluorescence and phosphorescence lifetime imaging of selected probes (curcumin, MitorTracker Orange CMTM/Ros (MTO), and $[Ru(Phen)_3]^{2+}$) localized in extracellular and intracellular space of cancer cells. The basal level of oxidative stress maintained in cells can be increased or decreased by external or internal stimuli. Curcumin represents the molecule that can decrease the ROS in the dark and induce oxidative stress after its irradiation. In this work, we have shown that MitorTracker Orange CMTM/Ros (MTO) dramatically varies its fluorescence lifetime in the presence of ROS along with the relocalization into the nucleus [2]. Finally, we focused on developing a time-resolved luminescence detection approach (Fig.1) to demonstrate both oxygen accumulation and oxidative stress levels in cancer spheroids in the presence of curcumin.

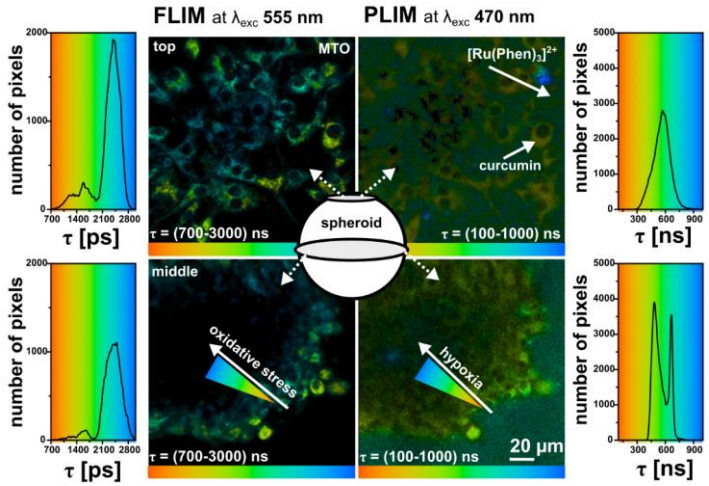

Fig. 1. Representative FLIM images of MTO and PLIM images of curcumin/$[Ru(Phen)_3]^{2+}$ applied in the U87 MG human glioma cells. FLIM and PLIM luminescence lifetime distribution histograms are plotted for each condition. The luminescence lifetimes are color-coded (minima- red, maxima - blue). The hypothesis of oxidative stress and hypoxia evolution in the spheroid is proposed by the white arrows.

Acknowledgement
This research was funded by the Ministry of education, science, research and sport of the Slovak Republic, grant numbers VEGA 1/0156/18 and VEGA 1/0421/18, and by Slovak Research and development agency, grant number APVV-15-0485.

References

[1] Huntosova, V., Wagnieres, G., 2018. CHAPTER 15 in Quenched-phosphorescence Detection of Molecular Oxygen: Applications in Life Sciences. The Royal Society of Chemistry, pp. 298-318.
[2] Tomkova, S.; Misuth, M.; Lenkavska, L.; Miskovsky, P.; Huntosova, V., 2018. Biochimica Et Biophysica Acta-Molecular Cell Research 1865 (4), 616-628

Estimation of activation energy of nonradiative processes in nicotinamide adenine dinucleotide *in vitro*

D. Chorvát[1] , A. Biathova[1,2] and A. Marček Chorvátová[1,2]

[1] *Department of Biophotonics, International Laser Center, Ilkovičova 3, 814 04 Bratislava, Slovakia.*
[2] *Department of Biophysics, FNS, Univ. Ss Cyril and Methodius, J Herdu 1, 917 02 Trnava, Slovakia.*
e-mail: dusan.chorvat@ilc.sk

Nicotinamide adenine dinucleotide (phosphate), NAD(P)H, is one of the main sources of endogenous fluorescence in living cells [1], including bacteria E-coli that are well known for their glycolytic metabolism, allowing to monitor non-invasively changes in metabolic oxidative state directly in these cells during biotechnological processes. Our aim was to examine time-resolved NADH fluorescence characteristics in various solvents to estimate the activation energy E_a for nonradiative processes of NADH molecule. In order to determine E_a, we used values of the fluorescence lifetime τ_1 recorded by time-resolved spectroscopy (BDL-473nm excitation laser, LP500 nm filter, HPM 100-40 photomultiplier array, SPC-830 TCSPC board; all Becker&Hickl, Germany) in different solvents, in dependence on the temperature T (in Kelvin), taking into consideration equation for non radiative rate constant k_{nr}: $k_{nr} = A.e^{(-Ea/RT)}$, $k_{nr} = 1/\tau - 1/\tau_r$

Where τ_r is radiative lifetime and R is universal gas constant. The value of E_a was thus estimated based on equation:

$$E_a = ln(1/\tau_1 - 1/\tau_r)/RT$$

Gathered results in different solvents (Fig. 1, red) were compared to a model (Fig. 1, green), where E_a was fitted using following relationship:

$$k_{nr} = A_0 . \eta^{\alpha'} . exp\,(-[E_0 + E_1 . \pi^* + E_2 . \beta + E_3 . \alpha] / RT)$$

where η is viscosity, E_x activation energy of processes, expressed as a function of solvatochromic parameters π^*, β and α. The use of a model of multiparametric activation energy and its dependence on the physicochemical parameters of the environment of the NADH molecule allowed us to observe that most pronounced effect is related to polarisability (π^*), then basicity (β) or acidity (α), and viscosity η as the least characteristics that affects observable fluorescence lifetime. Gathered results are a prerequisite for understanding of the influence of environmental changes on NAD(P)H autofluorescence in living cells.

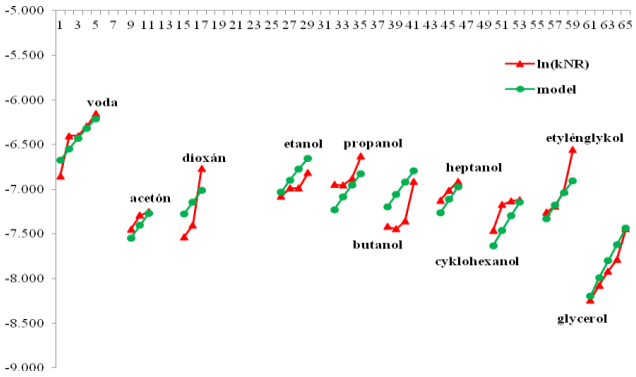

Fig. 1. Activation energy (y axes), calculated (green) and estimated experimentally (red) for different solvents.

Acknowledgement
We acknowledge support by APVV-15-0227, VEGA No. 2/0123/18, LASERLAB-EUROPE V (grant agreement no. 871124, European Union's Horizon 2020 research and innovation programme).

References

[1] Fluorescence Lifetime Spectroscopy and Imaging for Tissue Biomedical Diagnostics, Marcu L, French PMW, Elson DS V (Eds), CRC Press Publ (2014).

Determination of metabolites in urine of youths with depression

L. Ilavská[1], M. Morvová Jr.[1], J. Trebatická[3], Z. Ďuračková[2] and L. Šikurová[1]

[1] Department of Nuclear Physics and Biophysics, Faculty of Mathematics, Physics and Informatics of the Comenius University, Mlynská Dolina F1, 84248 Bratislava, Slovakia.
[2] Institute of Medical Chemistry, Biochemistry and Clinical Biochemistry, Faculty of Medicine of the Comenius University, Sasinkova 2, 81372 Bratislava, Slovakia.
[3] Department of Child Psychiatry, Faculty of Medicine of the Comenius University and National Institute of Child Diseases, Limbova 1, 83340 Bratislava, Slovakia..
e-mail: lucia.ilavska@fmph.uniba.sk

Depression is one of the neuropsychiatric disorders that is a serious global problem and is increasingly diagnosed in children and adolescents [1]. The disease is multifactorial and is affected by genetic, environmental, psychological, biological and biochemical factors, but its molecular basis in children and adolescents is not yet known. It has been hypothesized that disturbance of neurotransmitter metabolism (mainly serotonin) is responsible for the etiopathogenesis of depression [2]. The only known serotonin precursor is tryptophan. It is thought that increased tryptophan metabolism via the kynurenine pathway may be involved in the development of depression, which leads to decrease level of tryptophan for serotonin synthesis. Activation of the immune system also plays a key role, where neopterin in body fluids serves as a marker of cellular immune system activation [3]. In the study, we analyzed selected metabolites (tryptophan, kynurenine, neopterin) in urine by high performance liquid chromatography (HPLC) with absorption and fluorescence detection.

Acknowledgement
This work was supported by APVV–15–0063, UK/229/2020, KEGA 041UK-4/2020.

References

[1] TREBATICKÁ, J. et al. Súčasný pohľad na depresiu v detstve a adolescencii. In PSYCHIATRIA PRE PRAX. 2017. Vol. 18, no. 3, s. 95–99.
[2] MAES, M. et al. The new “5-HT” hypothesis of depression: cell-mediated immune activation induces indoleamine 2,3-dioxygenase, which leads to lower plasma tryptophan and an increased synthesis of detrimental tryptophan catabolites (TRYCATs), both of which contribute to th. In Progress in neuro-psychopharmacology & biological psychiatry. 2011. Vol. 35, no. 3, s. 702–21.
[3] A. TIEMEIER, H. et al. Plasma pterins and folate in late life depression: The Rotterdam Study. In Psychiatry Research . 2006. Vol. 145, no. 2–3, s. 199–206.

The effect of *PDR16* gene deletion on membrane potential in *Candida albicans*

J. Jacko[1], M. Morvová Jr.[1], A. Benčová[2], L. Šikurová[1], Y. Gbelská[2]

[1] *Faculty of Mathematics, Physics and Informatics, Comenius University, Mlynská dolina F1, 842 48 Bratislava, Slovakia*

[2] *Faculty of Natural sciences, Comenius University, Ilkovičova 6, 842 48 Bratislava, Slovakia*

email: jacko11@uniba.sk

Yeast has an irreplaceable place in science and industry. Especially in the food industry to produce baked goods, alcoholic beverages and dairy products. In science, and pharmaceutical industry they are widely used as a model organism. On another hand, certain yeast strains can act as primary or opportunistic pathogens. All yeasts diseases are treated with antifungal drugs. The most widespread and effective class of antifungal agents are azole drugs. At present, however, their increasing rate of azole antifungals resistance presents complications in the treatment of yeast infections. This is particularly important in *Candida*, especially *Candida albicans*. *Candida* are the most common cause of human opportunistic yeast infections worldwide, accounting up to 96% of yeast infections, where 50% of all cases are caused by *Candida albicans* [2].

The plasma membrane is the most important cell membrane and it plays a key role in drug resistance mechanisms. Its properties depend on the lipid and protein composition. One of the most abundant lipids in cell membranes is phosphatidylinositol (PITP). The *PDR16* gene encodes the major phosphatidylinositol transfer protein and is implicated in drug sensitivity. Deletion of the *PDR16* gene leads to increased susceptibility to azole antifungals, affects the phospholipid and sterol composition of the plasma membrane, and alters the total lipid composition in yeast membranes [3]. It has been shown that altered plasma membrane phospholipid and sterol composition can change membrane barrier function [4]. The membrane serves as a diffusion barrier to the movement of ions, especially to ions which are involved in membrane potential generation. The aim of this work is to study the effect of the *PDR16* gene deletion on the biophysical properties of *Candida albicans* membrane, namely the membrane potential as this attribute is notable in membrane barrier function.

The effect of the *PRD16* gene deletion on yeast transmembrane potential values was studied by shift in the emission maximum position ($\Delta\lambda_{max}$) in the fluorescence spectrum of the DiS-C_3(3) probe, after its incorporation into the sample. In our experiments, deletion of the *PDR16* gene did not have a significant effect on the $\Delta\lambda_{max}$ value of the deleted mutants, although the plasma membrane of the mutants was slightly hyperpolarized compared to the wild-type strain. This change is most likely due to a change in the lipid and/or sterol composition of the mutant membrane, which may lead to increased susceptibility to azole antimycotics.

Acknowledgement

This work was supported by Slovak Research and Development Agency under the contract No. VEGA 01/0697/18.

References

[1] BROWN, Sam P., Daniel M. CORNFORTH a Nicole MIDEO, 2012. Trends in Microbiology 20(7), 336–342.

[2] RAHENDRA, Prasad, 2017. *Candida albicans: Cellular and molecular biology*. 10.1007/978-3-319-50409-4.

[3] VAN DEN HAZEL, H. et al, 1999. J. of Biological Chemistry. 274(4), 1934–1941.

[4] LOFFLER, Jurgen, Hermann EINSELE, Holger HEBART, Ulrike SCHUMACHER, Claudia HRASTNIK a Gunther DAUM, 2000. FEMS Microbiology Letters 185(1), 59–63.

Polymeric micelles and endogenous lipoprotein nanoparticles as delivery systems of anticancer drug curcumin and photosensitizer hypericin

A. Jutková[1,2], S. Datta[3], D. Chorvát[4], P. Miškovský[5], D. Jancura[2,3] and J. Kronek[6]

[1] *Department of Biology and Genetics, University of Veterinary Medicine and Pharmacy in Košice, Komenského 73, 041 81 Košice, Slovakia*

[2] *Department of Biophysics, Faculty of Science, P. J. Šafárik University in Košice, Jesenná 5,041 54 Košice, Slovakia*

[3] *Center for Interdisciplinary Biosciences, Technology and Innovation Park, P. J. Šafárik University in Košice, Jesenná 5, 041 54 Košice, Slovakia*

[4] *Department of Biophotonics, International Laser Centre, Ilkovičova 3, 841 04 Bratislava, Slovakia*

[5] *Technology and Innovation Park, P. J. Šafárik University in Košice, Trieda SNP 1, 040 11 Košice, Slovakia*

[6] *Polymer Institute, Slovak Academy of Sciences, Dúbravská cesta 9, 845 41 Bratislava, Slovakia*

e-mail: annamaria.jutkova@uvlf.sk

Cancer is the second leading cause of the death in the world. Therefore, it is very important and crucial to develop an effective transport system of anticancer drugs for targeted distribution to the tumor cells in order to overcome undesirable side effects of conventional chemotherapy. Our aim was to construct polyoxazoline polymeric micelles, their physico-chemical characterization, and testing of these drug delivery systems as effective carriers of hydrophobic anticancer drug curcumin (CUR) and natural potent photosensitizer hypericin (HYP). The aim of this study was also to find the possibility of co-loading of CUR and HYP into the lipoprotein molecules - low density lipoproteins (LDL) and high density lipoproteins (HDL). The results of this work show that the size of all synthesised polyoxazoline polymeric micelles incorporated with CUR or HYP was less than 100 nm and therefore these micelles are suitable candidates for passive targeting of cancer tissues. CUR-loaded and HYP-loaded polyoxazoline polymeric micelles are highly stable for long-term storage and have high drug loading capacity. CUR inside polyoxazoline polymeric micelles is highly protected from the degradation and therefore this copolymer can be considered as an excellent stabilizer of CUR in aqueous solution. It has been also shown that CUR molecules can be successfully incorporated into lipoproteins, and LDL particles have a much higher loading capacity for CUR than HDL particles. We have found that CUR and HYP can be simultaneously incorporated into LDL with high level of efficiency without affecting each other.

Acknowledgement

The authors are thankful to the Slovak Grant Agency VEGA for the financial support in the project No.2/0124/18 and the Slovak Research and Development Agency for financial support in the project No. APVV-15-0485.

Effect of dimethyl sulfoxide on phase behaviour of liposomes as a model for cryopreservation of biological cells studied by calorimetry, positron annihilation and molecular dynamics simulations

I. Klbik[1,2], I. Maťko[1], O. Šauša[1], K. Čechová[1,2] and M. Melicherčík[2]

[1] *Institute of Physics, Slovak Academy of Sciences, Dúbravská cesta 9, 845 11 Bratislava, Slovakia.*
[2] *Department of Nuclear physics and Biophysics, Faculty of Mathematics, Physics and Informatics, Comenius University in Bratislava, Mlynská dolina, 842 48 Bratislava, Slovakia.*
e-mail: klbik3@uniba.sk

Liposomes are spherical supramolecular aggregates of lipid molecules. Lipids make up lipid bilayer which separates intraliposomal space from outside. Liposomes are used as model of biological cells as their membranes are build up by lipids. We use liposomes to model physicochemical events during cryopreservation of biological cells. Cryopreservation is a process where biological material susceptible to damage by unregulated chemical kinetics is preserved by cooling and storing at low subzero temperatures [1]. However, there is risk that comes with reaching low temperatures – formation of ice crystals as water is present in biological cells. Formation of intracellular ice is almost always lethal for the cells. It has been found that addition of some foreign substances into the cells medium, e.g. dimethyl sulfoxide or glycerol, can have cryoprotective effect and therefore substantially increase cell viability after thawing [2]. It is crucial to minimize toxic effect of these cryoprotective substances using low concentrated suspensions but high enough to secure cryoprotection [3]. There are some hypotheses concerning cryoprotective effects of dimethyl sulfoxide, but complete understanding is still lacking [3].

Our aim was to examine phase behavior of liposomal dispersions with dimethyl sulfoxide as cryoprotectant in concentration range of 0 – 10 vol. % with respect to water. Liposomes consisted of dimyristoylphosphatidylcholine. Emphasis was put on how dimethyl sulfoxide affects freezing of medium inside as well as outside of liposomes. Main method used was differential scanning calorimetry which allows for heat capacity scans in wide range of relevant temperatures for cryopreservation. Phase transitions are accompanied by change in heat capacity. As supporting methods we used: positron annihilation lifetime spectroscopy that can detect temperature induced changes in free volume characteristics with relevant information about phase behavior and also we used molecular dynamics simulations as a tool for tracking interaction between dimethyl sulfoxide and lipid bilayer during cooling and heating of the system as well for examination of phase behavior of water-dimethyl sulfoxide mixtures.

Our results indicate that dimethyl sulfoxide has major effect on phase behavior of liposomal dispersions, mainly: reducing the temperature at which intraliposomal medium freezes; raising the main phase transition temperature of lipid and enhancing structural integrity of freeze-thawed liposomes with increasing concentration of dimethyl sulfoxide in dispersions.

Acknowledgement
This work has been supported by grant APVV-16-0600 and VEGA 2/0157/17 project.

References
[1] D.E. Pegg, Meth. Mol. Biol. 368 (2007), 39-57.
[2] P. Mazur, Am. J. Physiol. 247 (1984), 125-142.
[3] T. Jang, et al. Integr. Med. Res. 6(1) (2017), 12-18.

Viscosity measurements using elastic polymer micro-cantilevers

J. Kubacková[1], G. T. Iványi[2], V. Kažiková[1], A. Strejčková[3], A. Hovan[4], G. Žoldák[5], G. Vizsnyiczai[2], L. Kelemen[2], G. Bánó[4] and Z. Tomori[1]

[1]Department of Biophysics,Institute of Experimental Physics,Slovak Academy of Sciences, Watsonova 47, 040 01 Kosice, Slovakia.
[2]Institute of Biophysics, Biological Research Centre, Temesvárikrt. 62, Szeged, Hungary.
[3]Department of Chemistry, Biochemistry and Biophysics, Institute of Biophysics, University of Veterinary Medicine and Pharmacy, Komenského 73, 04181 Košice, Slovak Republic.
[4]Department of Biophysics, Faculty of Science, P.J.Šafárik University, Jesenná 5, 041 54 Kosice, Slovakia.
[5]Center for Interdisciplinary Biosciences, Technology and Innovation Park, P.J. Šafárik University, Jesenná 5, 041 54 Kosice, Slovakia
e-mail: kubackova.jana@gmail.com

In this work we report on the fabrication of elastic microstructures and their use for viscosity measurement. Elastic 20 μm long head-and-neck-like micro-sized cantilevers with a thickness of approx. 0.3 μmare prepared by two-photon polymerization of trimethylolpropanetriacrylate, thebiocompatible photoresist calledOrmoComp®.The fabricated microstructures are equipped witha spherical head, which can be trapped by focused laser beams. A holographic optical tweezerssetup is used to manipulate the head of the cantilever and to bend it actively from the equilibrium position. After the release, the overdamped oscillations are recorded by video-tracking and are subjected to image analysis.The time dependence of the head position contains the information about the properties of both: the surrounding environment and the cantilever material.

The effect of solvent viscosity on the cantilever recovery motion is studied in details. Our results indicate that the elastic microstructures can be utilized for viscosity measurements in a straightforward way. Linear dependence is found between the recovery time of the overdamped cantilever oscillations and the viscosity of surrounding solution. The microstructures were tested by measuring the viscosity of aqueous glucose solutions and water-glycerol mixtures.

The small dimension of the structures opens the way for viscosity measurements in sub-microliter volumes, which may be of high interest in manyapplications. For example, injectable drug formulations in pharmacology can be mentioned, where the smallmeasured volume reduces the experimental demands on expensive samples.

Acknowledgement
This work was supported by the research grants from the Slovak Grant Agency Vega No. 2/0139/19 and APVV 15-0665.

Decomposition of AFM topographic surfaces: Modelling of growth curves

J. Marek , Z. Gazova

Department of Biophysics, Institute of Experimental Physics, Slovak Academy of Sciences, Watsonova 47, 04001 Kosice, Slovakia.
e-mail: marek@saske.sk

Nano-technologies are becoming synonymous with the present times. One of the requirements for their effective development is the need to characterize the properties of the investigated nano-objects. There are many experimental and theoretical approaches [1]. 3D imaging of the topographic surface using an atomic force microscope (AFM) allows you to get an idea about how objects look like at nanoscale. The autocorrelation function (ACF) method provides a fast and elegant estimate of the nanoparticle distribution parameters, but it has one significant drawback. Its cross-correlation component causes a large increase in error or it makes analysis impossible in the case of dense distributions [2].

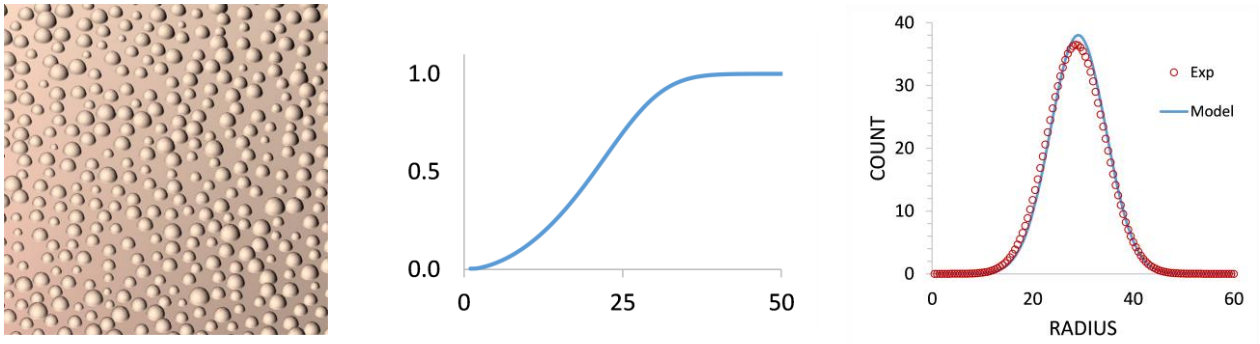

Fig. 1. Decomposition of half-sphere surfaces distribution. Simulated AFM topography (left), model growth curve (mid) and corresponding extracted size distribution (right). 3D view was made using Gwyddion software [3].

One possible solution to this problem is to use an image histogram of the distribution. By incorporating a statistical distribution function of the sizes of the given objects into a model of a topographic surface (e.g. from an AFM microscope, represented by a set of brightness values of individual pixels), its decomposition and acquisition of appropriate parameters of distribution functions is possible. Since the image histogram of such a surface is an invariant with respect to the relative position of the objects that make up the surface, the problem of cross-correlation of neighbouring objects will be solved. In this way, a method of analysis can be created for a quick and simple estimation of the distribution function of objects in an image. A by-product of this analysis is a possibility to model the curves of different growth processes through the cumulative function of object distribution (Fig.1).

Acknowledgement
This work was supported by VEGA grants No 02-0083-19 and No 02-0145-17.

References

[1] M. Hassellöv, J. W. Readman, J. F. Ranville and K. Tiede, Ecotoxicology 17 (2008), 344–361.
[2] J. Marek and E. Demjen, Journal of Nanoparticles Research 19 (2017), 208.
[3] D. Nečas and P. Klapetek, Central European Journal of Physics (Open Physics) 10 (2012), 181-188.

Human skin autofluorescence in health and eczema

M. Morvová Jr.[1], L. Šikurová[1]

[1] *Department of Nuclear Physics and Biophysics, Faculty of mathematics, physics and informatics Comenius University in Bratislava, Mlynská dolina F1, 842 48 Bratislava, Slovakia.*
e-mail: Marcela.Morvova2@fmph.uniba.sk

Human skin admittedly contains endogenous fluorophores distributed in various concentration in different skin layers [1]. The skin endogenous fluorophores include tyrosine, tryptophan, collagen, keratin, nicotinamide adenine dinucleotide, elastin and others [2]. All these fluorescent compounds exhibit changes in fluorescence characteristics related to modifications of skin functionality.

Our aim was to examine endogenous skin fluorescence (autofluorescence) by fluorescence spectroscopy method. We compare skin on fifth finger – *digitus minimus* of atopic dermatitis (eczema) and healthy skin (Fig. 1). The Luminescence Spectrometer LS 55 (PerkinElmer, Beaconsfield, UK) with Remote Fiber Optic Accessory (PerkinElmer) and BS Studio Software was used, as described previously [3]. The Excitation-Emission Matrix (EEM) was collected with excitation wavelength from 260 nm to 450 nm in 10 nm steps and emission wavelength from 280 nm to 650 nm with step 0.5 nm. The EEM represent the relation between the fluorescence intensity and excitation and emission wavelength.

Our preliminary experiments with complex fluorescence monitoring of eczema skin show differences in some regions of EEM in eczema skin and healthy skin. This emphasize the utilization of modern fluorescence techniques as prospective candidates for fast, safe, highly sensitive, and non-invasive monitoring of the human skin condition even in *in vivo* mode and its potential usage in dermatology.

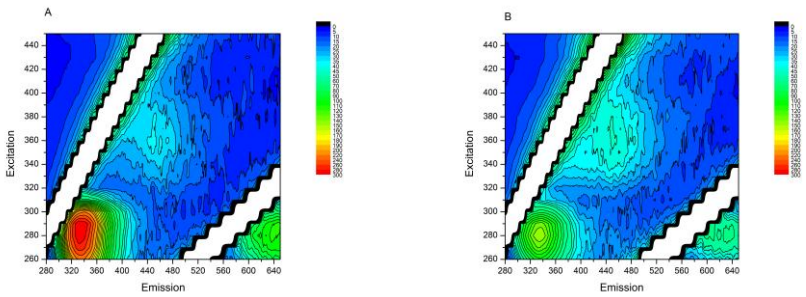

Fig. 1. The Excitation-Emission Matrix of skin autofluorescence on fifth finger – digitus minimus of (A) atopic dermatitis (eczema) and (B) healthy skin.

Acknowledgement
This work was supported by the NAWA EUROPARTNER PPI/APM/2018/1/00007/U/001, APVV_SK-BY-RD-19-0019 and KEGA 041UK-4/2020.

References

[1] W. Franco, E. Gutierrez-Herrera, N. Kollias and A. Doukas, British Journal of Dermatology. 174 (2016), 499-504
[2] N. Kollias, G. Zonios and G. N. Stamatas, Vibrational Spectroscopy. 28 (2002), 17-23.
[3] M. Morvová Jr., P. Jeczko and L. Šikurová, Skin Res Technol. 24 (2018), 599-605.

Effects of bis-coumarin homodimers on preformed amyloid fibrils of globular and intrinsically disordered proteins

B. Spodniaková[1], Z. Bednáriková[1], M. Gančár[1], A. Antošová[1], S. Hamuľáková[2], Z. Gažová[1]

[1]*Department of Biophysics, Institute of Experimental Physics SAS, Košice, Slovakia*
[2]*Department of Organic Chemistry, Institute of Chemistry, Faculty of Science, P. J. Šafárik University, Košice, Slovakia*

Presence of protein amyloid deposits is associated with pathologies of many amyloid-related disorders, including Alzheimer´s disease, Parkinson´s disease, diabetes mellitus, non-neuropathic lysozyme systemic amyloidosis, and others. We have studied effect of 4 compounds based on bis-coumarin homodimers connected via linker with increasing length (3-7 carbons)(Fig. 1) on amyloid fibrils of globular proteins (human insulin and hen egg white lysozyme) and intrinsically disordered protein ($A\beta_{40}$ peptide).

The ability of bis-coumarin homodimers to destroy amyloid fibrils was studied by means of ThT fluorescence assay, FTIR spectroscopy, and atomic force microscopy. We have found that the homodimers destroy protein amyloid fibrils differently. In the case of fibrils made of globular proteins, the destroying efficiency is weak for homodimers with short linker (3 and 4 carbons) but is significantly increased with linker length (Fig. 2). On the other hand, the studied compounds showed significantly higher efficiency to destroy fibrils of $A\beta_{40}$ peptide, but independent on the length of the linker.

The present work is a step towards understanding the relationship between the structure and anti-amyloid properties of compounds as an inevitable condition for design of potential treatment of amyloidosis.

MH3

MH4

MH

MH7

Fig. 1. Structure of studied bis-coumarinederivates.

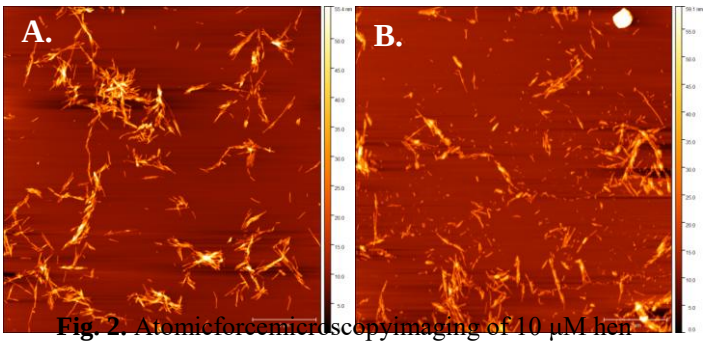

Fig. 2. Atomicforcemicroscopyimaging of 10 μM hen eggwhitelysozymefibrilsbefore(A) and after(B) incubationwithwith100 μM bis-coumarinhomodimere MH7. Lysozymefibrilswereprepared in glycine/NaCl buffer at low pH after 2h incubation at 65°C and 1200 rpm. The bar is 2 μm.

Acknowledgement
This work was supported by grants VEGA 2/0145/17, APVV 18-0284, and ITMS project 313011T553 (DIAGNAD).

Passive rheology using elastic micro-structures

A. Strejčková[1], J. Kubacková[2], A. Hovan[3], Z. Tomori[2] and G. Bánó[3]

[1]Department of Chemistry, Biochemistry and Biophysics, Institute of Biophysics, The University of Veterinary Medicine and Pharmacy in Košice, Komenského 73, 041 81 Košice, Slovakia
[2]Slovak Academy of Sciences, Institute of Experimental Physics, Department of Biophysics, Watsonova 47,040 01 Košice, Slovakia
[3]Department of Biophysics, Faculty of Science, P.J.Šafarik University, Jesenná 5, 041 54 Košice, Slovakia
e-mail: alena.strejckova@uvlf.sk

The theory of Brownian fluctuations of spherical particles in harmonic potentials was elaborated in connection with optically trapped beads in the past. This theory can be directly applied to the microscopic cantilever systems equipped with spherical particles at their end.In this case the harmonic potential is created by the cantilever itself (without optical trapping). It can be shown, that the power spectral density of such oscillations is given by a Lorentzian curve: $P(f) \sim 1/(f^2+f_c^2)$, where the corner frequency f_c is inversely proportional to the viscous damping of the system. It follows, that the viscosity of the surrounding medium can be evaluated from the power spectrum of the Brownian oscillations. Practically, it means that the end-bead oscillations are to be recorded during a certain period, so that the power spectrum can be calculated and fitted with a Lorentzian curve, using conventional mathematical methods. Our preliminary tests have confirmed the Lorentzian frequency dependence of the end-bead oscillations' power spectral density. The bead position was detected in back-scattered arrangement, using a few tens of micro-Watts 532 nm laser for illumination. The intensity of the back-reflected light was found to have a linear dependence on the bead position, when illuminating the microstructure edges. The power spectral density was analyzed to gain information on the surrounding medium viscosity.

Acknowledgement
This work was supported by the Slovak Research and Development Agency (grants APVV-15-0665, APVV-18-0285) and the Slovak Ministry of Education (grant KEGA No. 012 UVLF – 4/2018).

Fabrication and examination of magnetic zeolite nano/micro-particles for controlled drug release and modulation of amyloidogenesis

K. Šipošová[1], V. Hovhannisyan[2], D. Sedláková[1], A. Musatov[1], Sh.-J. Chen[2]

[1] Department of Biophysics, Institute of Experimental Physics SAS, Watsonova 47, 04001 Kosice, Slovakia.
[2] College of Photonics, National Chiao Tung University, No. 301, Gaofa 3rd Rd, Tainan 711, Taiwan.
e-mail: siposova@saske.sk

Both natural and synthetic nanoparticles have practical applications in a variety of areas, ranging from environmental remediation to an emerging multidisciplinary field that combines chemistry, engineering, physics, biology, and medicine. Additionally, over the last decades, there has been increased interest in the studies of *in vitro* and *in vivo* applications of NPs in radiation, photodynamic and thermal therapies. Proteins are important biological macromolecules that are fundamental to the proper functioning of cells and organisms; therefore, the impact of nanoparticles in living organisms at the protein level is a critical issue that is attracting increasing attention from researchers. In turn, natural zeolite nanoparticles, especially clinoptilolite zeolite (CZ) is a promising material for biomedicine and pharmaceutics due to its non-toxicity, thermal stability, expanded surface area, and exceptional ability to adsorb various atoms, organic molecules, photodynamic agents, and nanoparticles into micro- and mesopores.

Our aims were: i) to prepare magnetic nano/micro-particles of clinoptilolite type of natural zeolite as promising carriers for controlled drug delivery/release; and ii) to probe CZ particles as anti-amyloidogenic agents.

Adsorption of photodynamic active dyes and their release from CZ in the presence of biomolecules were quantitatively investigated by absorption and fluorescence spectrometry. Using multiphoton microscopy, we demonstrated that effective inducing of two-photon excited luminescence and second harmonic generation signals in nano/micro-particles of CZ by femtosecond near-infrared laser excitation can be successfully utilized in multiphoton imaging of CZ particles and the dye adsorption processes.

The amyloid aggregation process involves the association of peptides into supramolecular complexes, fibrils. Accumulation of formed fibrils are characteristic features for a range of, if not all, neurodegenerative disorders such as Alzheimer's, Huntington's, Parkinson's, as well as non-neuropathic amyloidosis. We have found that CZ particles affect amyloid aggregation of proteins, namely insulin and lysozyme in dose-dependent manner. Determined half-maximal inhibiting (IC_{50}) and half-maximal disassembly (DC_{50}) values of CZ particles were found to be in sub-miligram/mL concentrations range. Intriguingly, IC_{50} and DC_{50} values for insulin were one-half lower in comparison to those determined for lysozyme. In addition, anti-amyloid activity of CZ was enhanced after incorporation of magnetic (Fe_3O_4-based) nanoparticles into pores of CZ particles. This anti-amyloidogenic activity could be enhanced by co-application of external magnetic field and induction of hyperthermia or co-application of radiation. It is important to be noted that a synthetic zeolite (Zeolite Y) did not affect amyloid aggregation.

We could conclude, that CZ magnetic nano/micro-particles can be considered as safe and effective multimodal probes for MRI and optical imaging, thermo- and phototherapy as well as effective containers for controlled drug delivery not only for amyloid-related diseases.

Acknowledgement
This work was supported by grants: MVTS Amazon, SAS-MOST JRP 2017/6, VEGA No. 2/0009/17, APVV-15-453, EuroNanoMed Magbbris. The authors thank Zuzana Mitroova (Institute of Experimental Physics, SAS, Kosice, Slovakia) for the technical assistance.

Modeling of the effect of amphiphilic phosphorus dendrons on erythrocyte membrane fluidity measured in terms of fluorescence anisotropy

Šutý Š.[1], Garaiová Z.[1], Magiera J.[2], Ionov M.[2], Bryszewska M.[2], Shcharbin D.[3], Majoral J. P.[4], Hianik T.[1], Waczulíková I.[1]

[1] *Faculty of Mathematics, Physics and Informatics, Comenius University, Bratislava, Slovakia*
[2] *Faculty of Biology and Environmental protection, Department of General Biophysics, University of Lodz, Poland*
[3] *The State Scientific Institution "Institute of Biophysics and Cell Engineering of the NASB, Minsk, Belarus*
[4]*The Laboratoire de Chimie de Coordination Université de Toulouse, France*
e-mail: suty5@uniba.sk

Dendrons are artificially synthetized molecules representing a group of nanosized dendritic structures (dendrimer sections) which gain an interest for their possible therapeutic and anticancer properties[1]. Based on the compounds used for the synthesis avarious type of dendrons with tailored physicochemical properties can be prepared. We have studiedthree amphiphilic phosphorus dendrons (APDs) of the first and second generation: jq108 ($C_{124}H_{198}Cl_{10}N_{34}O_8P_8S_5$), jq170 ($C_{134}H_{218}Cl_{10}N_{34}O_8P_8S_5$) and jq111($C_{264}H_{418}Cl_{20}N_{74}O_{18}P_{18}S_{15}$), respectively.

Fluorescence anisotropy – inversely related to membrane fluidity – was calculated according to equation:$r = (I_{VV}-GI_{VH})/(I_{VV}+GI_{VH})$, where I_{VV} and I_{VH} = the vertical and horizontal intensities with respect to the vertical polarization of the excitation light, $G = I_{VH}/I_{VV}$ was grating correction factor. The relative change of fluorescence anisotropywas expressed as (r/r_0), where r and $r_0$were the observed and background anisotropiesof a probe DPH (1,6-diphenyl-1,3,5-hexatriene) or TMA-DPH (1-[4-(trimethyl-ammonium) phenyl]-6-phenyl-1,3,5-hexatriene) being intercalated in isolated erythrocyte membranes.Effect of ADPs on the anisotropy was measured in the range of1 μM - 110 μM.Since effects of ratios are multiplicative rather than additive, the logarithms of the (r/r_0) were analysed.

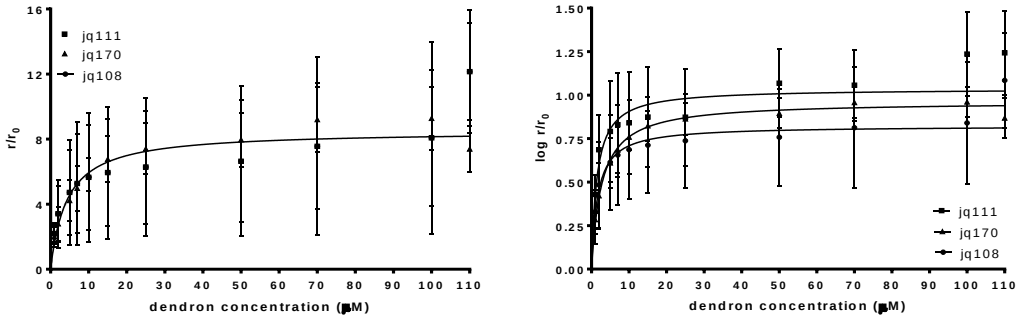

Fig. 1 Fluorescence anisotropy of DPH upon increasing concentrations of dendrons. Analysis with the original data on the ratio scale (Fig. 1 left). Analysis after logarithmic transformation (Fig. 1 right).

Using a nonlinear regression, we were able to prove significant differences in the effect of dendrons on the fluidity (P = 0.005, different curve for each data set; Fig. 1 right). The goodness-of-fit was quantified by coefficient of determination R^2, and the differences between the curves were tested using an extra-sum-of-squares F test. Analysis with the original data on the ratio scale failed to prove differences (P = 0.880, one curve for all data sets).Similar behaviour, but with higher steady-state anisotropy values was observed for TMA-DPH.

Acknowledgement
Supported by: the APVV (SK-PL-18-0080, APVV-14-0267, SK-BY-RD-19-0019), VEGA 1/0756/20, KEGA 041UK-4/2020 and by PL-SK 2019–2020 bilateral project of NAWA PPN/BIL/2018/1/00150; NAWA, PPI/APM/2018/1/00007/U/001.

References:

[1] C. E. Gutierrez-Ulloa, M. Yu. Buyanova, E.K. Apartsin, A.G. Venyaminova, F. Javier de la Mata, M. Valiente, R. Gómez,Org. Biomol. Chem. 15(2017), 7352 – 7364.

The fibril formation study of recombinant spider silk protein eADF4(C16) in different pH environments

Veronika Talafová[1], Martin Humenik[2], Gabriel Žoldák[3], Thomas Scheibel[2], and Erik Sedlák[3]

[1] Department of Biophysics, Faculty of Science, P. J. Šafárik University, Jesenná 5, 041 54 Košice, Slovakia
[2] Department of Biomaterials, Faculty of Engineering Science, University of Bayreuth Universitätsstraße 30, 95440 Bayreuth, Germany
[3]Center for Interdisciplinary Biosciences, P. J. Šafárik University, Jesenná 5, 041 54 Košice, Slovakia

Email: veronika.talafova@student.upjs.sk

Thanks to the remarkable combination of mechanical strength and elasticity as well as biocompatibility, the spider silk is an interesting subject of study in applied research [1-3].The spider silk formation in nature is a complex process including changes in pH, salt concentration and sheer forces which trigger transformation of highly concentrated protein solution into insoluble fibre [4].

This work focuses on a detailed analysis of fibril formation from the recombinant spider silk protein eADF4(C16) using spectroscopy methods (turbidity measurements, ThT and ANS fluorescence). Special focus is devoted to determination of a kinetic model of the self-assembly as well as an impact of chaotropic and kosmotropic ions on fibril morphology.We also studyinfluence of different pH environments onthe protein solubility.

Overall, we conclude thatthe model of secondary nucleation describes the self-assembly of recombinant spider silk protein eADF4(C16). Our results show divergent influences of ionic environments on the fibril formation.In this process, chaotropic ions act as inhibitorsand kosmotropic phosphate ions seem to be the most efficient. The results also illustrate that different pH environments, without the ion addition, significantly affect the transformation of recombinant spider silk protein intoaggregation structures.Low pH values (pH = 3,4,5) lead to the formation of fibrils. In environments with a pH higher than 5, the protein remains unfolded.

Acknowledgement
This work was supported by Slovak Research and Development Agency under the contract No. APVV-15-0069 and by grant VEGA 1/0175/19 from Ministry of education, research, and sport.

References:

[1] Schacht K, Scheibel T. Processing of recombinant spider silk proteins into tailor-made materials for biomaterials applications. CurrOpinBiotechnol. 2014;29:62-9.
[2] Aigner TB, DeSimone E, Scheibel T. Biomedical Applications of Recombinant Silk-Based Materials. Adv Mater. 2018;30:1704636.
[3] Humenik M, Lang G, Scheibel T. Silk nanofibril self-assembly versus electrospinning. Wiley Interdisciplinary Reviews: Nanomedicine and Nanobiotechnology. 2018:e1509.
[4] Humenik M, Scheibel T, Smith A. Spider Silk: Understanding the Structure–Function Relationship of a Natural Fiber. In: Howorka S, editor. ProgMolBiolTranslSci: Academic Press; 2011. p. 131-85.

Dynamics of heme region is main effector of cytochrome *c* peroxidase-like activity

N. Tomášková[1], R. Varhač[1], E. Sedlák[1,2]

[1]Department of Biochemistry, Faculty of Science, P.J. Šafárik University, Moyzesova 11, 041 54 Košice, Slovakia
[2]Center for Interdisciplinary Biosciences, Technology and Innovation Park, P.J. Šafárik University, Jesenná 5, 041 54 Košice, Slovakia
e-mail: natasa.tomaskova@upjs.sk

Cytochrome *c* (cyt *c*) is a well-known heme protein located on the external side of the inner mitochondrial membrane. The main function of cyt *c* is to shuttle electrons in mitochondrial respiratory chain between Complex III and Complex IV. Recently, it has been found out that cyt *c* plays important role in the activation of a programmed cell death cascade, can function as a cardiolipin-specific oxygenase that chemically oxidizes cardiolipin, and is an active player in regulation of oxidative stress by removal of H_2O_2. All the above alternative functions of cyt *c* depends on its peroxidase-like activity [1]. However, the peroxidase-like activity of cyt *c* in its native and non-native hexacoordinated conformational states is still puzzling since in order for the H_2O_2 to be consumed it needs to interact with the heme iron [2]. While some authors proposed that cyt *c* peroxidase-like activity has to be activated by H_2O_2-induced covalent modifications [3], several other reports clearly demonstrated that an increased peroxidase-like activity of cyt *c* induced by point mutation [4] or as the result of interaction with cardiolipin containing vesicles [5] was not accompanied by significant conformational change of cyt *c* and its heme region remained in the native-like state. The apparent absence of conformational change suggests that the increased peroxidase-like activity is intermediated by transiently populated pentacoordinated state of the heme iron likely due to increased dynamics of the heme region as a result of reversible unfolding of the least stable foldons of cyt *c*. This suggestion was supported by demonstration of the binding of small ligands, such as cyanide [6] to the heme iron.

In our work, we show that peroxidase-like activity, measured by guaiacol oxidation and the ferrous oxidation in xylenol orange methods, correlates with the accessibility of the heme iron, which was assessed from the association rate constant of cyanide binding to cyt *c*. Our results suggest that dynamics equilibrium among the denaturant-induced non-native coordination states of cyt *c*, very likely due to reversible unfolding of the least stable foldons, is pre-requisite for enhanced peroxidase-like activity of cyt *c* in its compact state. Dynamics replacement of the native sixth coordination bond of methionine-80 by other ligands such as lysines (72, 73, and 79) and partially also by histidines (26 and 33) provides an efficient way how to increase peroxidase-like activity of cyt *c* without significant conformational change at physiological conditions.

Acknowledgement

This work was supported by Slovak Research and Development Agency and Ministry of education, research, and sport under the contracts No. APVV-15-0069 and VEGA 2/0009/17, respectively.

References

[1] L. J. Deterding, D. P. Barr, R. P. Mason and K. B. Tomer, Characterization of cytochrome c free radical reactions with peptides by mass spectrometry, J. Biol. Chem. 273 (1998) 12863-12869.

[2] B. Valderrama, M. Ayala and R. Vazquez-Duhalt, Suicide inactivation of peroxidases and the challenge of engineering more robust enzymes, Chem. Biol. 9 (2002) 555-565.

[3] V. Yin, G. S. Shaw and L. Konermann, Cytochrome c as a peroxidase: Activation of the precatalytic native state by H(2)O(2)-induced covalent modifications, J. Am. Chem. Soc. 139 (2017) 15701-15709.

[4] B. S. Rajagopal, A. N. Edzuma, M. A. Hough, K. L. I. M. Blundell, V. E. Kagan, A. A. Kapralov, L. A. Fraser, J. N. Butt, G. G. Silkstone, M. T. Wilson, D. A. Svistunenko and J. A. R. Worrall, The hydrogen-peroxide-induced radical behaviour in human cytochrome c-phospholipid complexes: implications for the enhanced pro-apoptotic activity of the G41S mutant, Biochem. J. 456 (2013) 441-452.

[5] A. Mandal, C. L. Hoop, M. DeLucia, R. Kodali, V. E. Kagan, J. Ahn and P. C. van der Wel, Structural changes and proapoptotic peroxidase activity of cardiolipin-bound mitochondrial cytochrome c, Biophys. J. 109 (2015) 1873-1884.

[6] R. Varhač, N. Tomášková, M. Fabián and E. Sedlák, Kinetics of cyanide binding as a probe of local stability/flexibility of cytochrome c, Biophys. Chem. 144 (2009) 21-26.

The ionic liquids as modulators of insulin amyloid aggregation

V. Vaník[1], Z. Bednáriková[1], G. Fabriciová[2], A. Antošová[1], Z. Gažová[1] and D. Fedunová[1]

[1] *Department of Biophysics, Institute of Experimental Physics, Slovak Academy of Sciences, Watsonova 47, 040 01 Košice, Slovakia*

[2] *Department of Biophysics, Faculty of Science, University of Pavol Jozef Šafárik, Jesenná 5, 040 01 Košice, Slovakia, e-mail: fedunova@saske.sk*

Amyloid aggregation is a well-known phenomenon connected to amyloid-related diseases (Alzheimer's, diabetes type II, etc.). Recently, amyloid aggregates were also found to hold great potential to be used as biomaterials due to their physico-chemical properties. Their unique features include high mechanical stiffness, resistance against enzymatic degradation and chemical denaturation, or self-assembly into ordered fibrillar structures. The important step for the utilization and fabrication of amyloid-based biomaterials is finding strategies to control the outcome of the amyloid aggregation process. One of the useful tools for regulation of amyloid fibril formation, namely structural and morphological characteristics of fibrils, is the variation of the solvent properties.

Ionic liquids (ILs) represent a class of novel solvents composed solely of ions, containing an organic cation and an organic or inorganic anion. A large number of ion combinations allow us to tune their physico-chemical properties (density, viscosity, melting point, polarity, water-miscibility, etc.) for a particular purpose [1].

In this work, we have studied the effect of two groups of imidazolium-based ILs on the kinetics of insulin fibril formation and morphology of amyloid fibrils using thioflavin T fluorescence assay, circular dichroism, FTIR and Raman spectroscopy, calorimetry and atomic force microscopy. The first group of ILs consisted of 1-ethyl-3-methylimidazolium cation and chaotropic or kosmotropic anions of Hofmeister series. We have found that the kinetics of insulin fibrillization in the presence of studied ILs follows the nucleation-dependent model characterized by the sigmoidal kinetic curve. The lag-time and half-time of aggregation were shortened compared to conditions without ILs. The extent of the effect depended on ILs concentration and correlated with reverse Hofmeister series, suggesting specific ion interactions with protein surface. The morphology of obtained fibrils was quantified by image analysis processing. The fibril morphology varied with the concentration and type of anion without any correlation to the Hofmeister series. ILs consisting of chloride anion and imidazolium cations with n-alkyl substituents (n = 2, 4, 6, 8, 10) were studied to test the effect of cation hydrophobicity on the amyloid fibrillization kinetics and morphology of aggregates. Our data suggest that the kinetics of insulin amyloid fibrillization can be inhibited or promoted by selected cations according to cation hydrophobicity and concentration. The ILs with the longest side-chain-containing cation (the most hydrophobic one) inhibited the amyloid fibrillization of insulin in a wide concentration interval (10 – 1 000 mM). On the contrary, the ILs with the shortest hydrophobic cation accelerated the kinetics of insulin amyloid fibrillization. The remaining ILs inhibited or promoted insulin fibrillization based on their concentration pointing out the importance of hydrophobic interaction and the length of the aliphatic chain.

The obtained results contribute to a better understanding of the processes responsible for the formation of structurally and morphologically defined fibrils.

Acknowledgment

This work was supported by the research grants from the Slovak Grant Agency VEGA No. 2/0030/18 and 2/0145/17, Slovak Academy of Sciences Grant scheme for PhD. students DoktoGrant APP0004, Slovak Research and Development Agency APVV-18-0284 and Structural Funds ITMS 313011T533 (DIAGNAD).

References

[1] C. Lange, G. Patil and R. Rudolph, Protein Sci. 14 (2005), 2693–2701

Increasing of GPCR solubility by directed protein evolution approach

M. Berta[1],V. Dzurillová[1], E. Sedlák[2]

[1]*Department of Biophysics, Faculty of Science, P. J. Šafárik University in Košice, Košice, Slovakia*
[2]*Center for Interdisciplinary Biosciences, Technology and Innovation Park, P.J. Šafárik University, Jesenná 5, Košice, Slovakia*
e-mail: Martin.Berta@student.upjs.sk

G-protein coupled receptors (GPCRs) are important cell surface receptors that mediate the cellular responses to endogenous signaling molecules. The importance of GPCR can be demonstrated in numerous diseases that are directly related to the disturbed GPCR signaling. Thus, GPCRs are major target for the pharmaceutical industry - more than 40% of all drugs available today act on a GPCR. Effective drug design and functional characterization of these receptors strongly depend on high-resolution structural information. The main problem in effort of crystallization and solving structure of GPCRs is associated with low solubility of membrane proteins. In principle, this obstacle can be overcome by improving solubility of the receptors, or in the extreme case by converting the receptors from "membrane-soluble" into water-soluble form.

In the presented research, we attempted to convert κ-opioid receptor, member of GPCR family, to a water-soluble form. The main strategy to reach the goal was redesigning the membrane surface of a GPCR by changing the hydrophobic amino acids of the protein/lipid interface with suitable polar or charged residues. The goal is toproduce a molecule that is able to fold and function in aqueous solution. It is highly improbable that the desired result can be reached in a single step by rational design. Instead, we have chosen a highly interdisciplinary approach of *in vitro* protein evolution.

For evolving GPCR we applied the method of ribosome display, that has beenrecently established in our laboratory. As a selection criterium we chose proper binding to its physiological ligand- dynorphin. The method of ribosome display proved to be powerful and efficient method for such complex modification of protein structure. From the κ-opioid receptor library we were able to select binders with specific affinity for dynorphin. The selected binders are variants of κ-opioid receptor and were purified without using a detergent. However, so far the selected analogues form water-soluble oligomers (from penta- to octa-mers). Despite the robustness of this selection method, we were not able to evolve water-soluble functional κ-opioid receptor, which would form monomeric or dimeric functional unit. We believe that optimizing of selection step and involvement of rational design in final steps of increasing solubility of the receptor might lead to preparation of water-soluble analogue of monomeric and/or dimeric structure of the receptor.

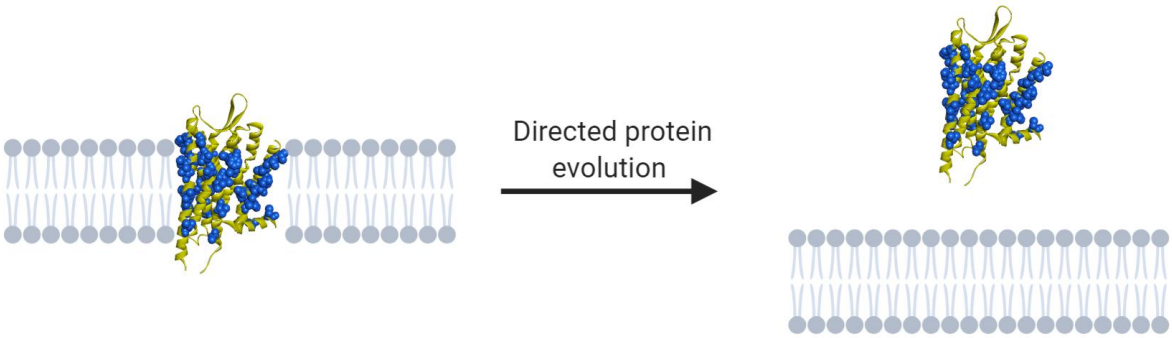

Fig. 1. Schematic description of the project main goal

Acknowledgments
We would like to thank to prof. AndreasPlückthun (Universit of Zürich) for continuing supportand provided plasmids and materials for our research. Thisworkwassupported by grants of Slovak grant agency APVV-15-0069 and VVGS-pf-2019-1058.

Index of Authors

K

L

M

N

P

R

S

T

V

W

Y

Z

List of Participants

1.	Antošová Andrea	Institute of Experimental Physics SAS, Košice
2.	Baglaeva Iuliia	Institute of Experimental Endocrinology, Biomedical Research Center SAS, Bratislava
3.	Bánó Gregor	Faculty of Science, Pavol Jozef Šafárik University, Košice
4.	Bednáriková Zuzana	Institute of Experimental Physics SAS, Košice
5.	Boško Ondrej	Jessenius Faculty of Medicine, Comenius University, Martin
6.	Cagalinec Michal	Institute of Experimental Endocrinology, Biomedical Research Center SAS, Bratislava
7.	Cehlár Ondrej	Institute of Neuroimmunology SAS, Bratislava
8.	Chorvát Dušan	International Laser Centre , Bratislava
9.	Dulanská Silvia	Institute of Medical Physics, Biophysics, Informatics and Telemedicine, Comenius University, Bratislava
10.	Džubinská Daniela	Faculty of Mathematics, Physics and Informatics, Comenius University, Bratislava
11.	Džupponová Veronika	Faculty of Science, Pavol Jozef Šafárik University, Košice
12.	Dzurillová Veronika	Institute of Physical Sciences, Faculty of Science, Pavol Jozef Šafárik University, Košice
13.	Fedunová Diana	Institute of Experimental Physics SAS, Košice
14.	Gaburjáková Marta	Institute of Molecular Physiology and Genetics, Centre of Biosciences SAS, Bratislava
15.	Gaburjáková Jana	Institute of Molecular Physiology and Genetics, Centre of Biosciences SAS, Bratislava
16.	Gala Michal	Faculty of Science, Pavol Jozef Šafárik University, Košice
17.	Gančár Miroslav	Institute of Experimental Physics, SAS, Košice
18.	Garaiova Zuzana	Faculty of Mathematics, Physics and Informatics, Comenius University, Bratislava
19.	Garčárová Ivana	Institute of Experimental Physics, SAS, Košice
20.	Gašparik Norbert	CEITEC Masaryk University, Brno
21.	Gažová Zuzana	Institute od Experimental Physics SAS, Košice
22.	Hianik Tibor	Faculty of Mathematics, Physics and Informatics, Comenius University, Bratislava
23.	Hovan Andrej	Faculty of Science, Pavol Jozef Šafárik University, Košice

24.	Huntošová Veronika	Center for Interdisciplinary Biosciences, TIP, Pavol Jozef Šafárik University, Kosice
25.	Húšťava Stefan	Faculty of Natural Sciences, UCM, Trnava
26.	Iaparov Bogdan	Institute of Experimental Endocrinology, Biomedical Research Center SAS, Bratislava
27.	Ilavská Lucia	Faculty of Mathematics, Physics and Informatics, Comenius University, Bratislava
28.	Jacko Juraj	Faculty of Mathematics, Physics and Informatics, Comenius University, Bratislava
29.	Jakuš Ján	Jessenius Faculty of Medicine, Comenius University, Martin
30.	Jancura Daniel	Faculty of Science, Pavol Jozef Šafárik University, Košice
31.	Jurašeková Zuzana	Faculty of Science, Pavol Jozef Šafárik University, Košice
32.	Jutková Annamária	University of Veterinary Medicine and Pharmacy, Košice
33.	Klbik Ivan	Faculty of Mathematics, Physics and Informatics, Comenius University, Bratislava
34.	Kopáni Martin	Institute of Medical Physics, Biophysics, Informatics and Telemedicine, Comenius University, Bratislava
35.	Kozeleková Aneta	CEITEC Masaryk University, Brno
36.	Lacinová Ľubica	Center of Biosciences SAS and Faculty of Natural Sciences, UCM, Bratislava
37.	Marček Chorvátová Alzbeta	International Laser Center Bratislava and Faculty of Natural Sciences, UCM, Trnava
38.	Martvoň Lukáš	Jessenius Faculty of Medicine, Comenius University, Martin
39.	Míšek Jakub	Jessenius Faculty of Medicine, Comenius University, Martin
40.	Miškovský Pavol	Faculty of Science, Pavol Jozef Šafárik University, Košice
41.	Morvová Jr. Marcela	Faculty of Mathematics, Physics and Informatics, Comenius University, Bratislava
42.	Poliaček Ivan	Jessenius Faculty of Medicine, Comenius University, Martin
43.	Sedlák Erik	Faculty of Science, Pavol Jozef Šafárik University, Košice
44.	Šipošová Katarína	Institute of Experimental Physics SAS, Košice
45.	Škrabana Rostislav	Institute of Neuroimmunology SAS, Bratislava
46.	Spodniaková Barbora	Institute of Experimental Physics SAS, Košice
47.	Strejčková Alena	University of Veterinary Medicine and Pharmacy, Košice
48.	Štroffeková Katarína	Faculty of Science, Pavol Jozef Šafárik University, Košice

49.	Šubjaková Veronika	Faculty of Mathematics, Physics and Informatics, Comenius University, Bratislava
50.	Šutý Šimon	Faculty of Mathematics, Physics and Informatics, Comenius University, Bratislava
51.	Talafova Veronika	Faculty of Science, Pavol Jozef Šafárik University, Košice
52.	Tomášková Nataša	Faculty of Science, Pavol Jozef Šafárik University, Košice
53.	Vaník Vladimír	Institute of Experimental Physics SAS, Košice
54.	Veterník Marcel	Jessenius Faculty of Medicine, Comenius University, Martin
55.	Waczulíková Iveta	Faculty of Mathematics, Physics and Informatics, Comenius University, Bratislava
56.	Zahradník Ivan	Institute of Experimental Endocrinology, Biomedical Research Center SAS, Bratislava
57.	Zahradníková Alexandra	Institute of Experimental Endocrinology, Biomedical Research Center SAS, Bratislava
58.	Zahradnikova jr. Alexandra	Institute of Experimental Endocrinology, Biomedical Research Center SAS, Bratislava
59.	Žoldák Gabriel	Center for Interdisciplinary Biosciences, TIP, Pavol Jozef Šafárik University, Košice

Book of Contributions. 9th Slovak Biophysical Symposium,
September 16 - 18, 2020, Trnava, Slovakia

Editors: Alžbeta Marček Chorvátová, Miroslav Michalka
Reviewers: Diana Fedunová, Ľubica Lacinová, Gabriel Žoldák
Published: International Laser Centre, Bratislava, Slovakia

Number of pages: 90

ISBN: 978-80-973719-0-6
EAN: 9788097371906